Summer 9-1-2014

Dynamic Responses at the Barrier Epithelium

Katherine Beebe
Washington University in St. Louis

WASHINGTON UNIVERSITY IN ST. LOUIS

Division of Biology & Biomedical Sciences

Developmental, Regenerative and Stem Cell Biology

Dissertation Examination Committee:
Craig A. Micchelli, Chair
Stephen L. Johnson
Stephen K. Kornfeld
James B. Skeath
Thaddeus S. Stappenbeck

Dynamic Responses at the Barrier Epithelium

by

Katherine Beebe

A dissertation presented to the
Graduate School of Arts and Sciences
of Washington University in
partial fulfillment of the
requirements for the degree
of Doctor of Philosophy

August 2014

St. Louis, Missouri

TABLE OF CONTENTS

List of Figures and Tables ……v

List of Abbreviations ……vii

Publications arising from this thesis ……viii

Acknowledgments ……ix

Abstract ……x

Chapter 1: Introduction

1.1 The GI barrier and its lumenal environment ……2

1.2 The adult *Drosophila* midgut as an experimental system ……3

1.2.1 The ISC lineage and midgut renewal ……4

1.2.2 The diffuse endocrine system ……5

1.3 Morphological and molecular markers of cell types in the adult *Drosophila* midgut……6

1.4 Genetic tools ……7

1.5 Summary of thesis chapters ……8

1.6 References ……10

Chapter 2: JAK/STAT signaling coordinates stem cell proliferation and multilineage differentiation in the *Drosophila* intestinal stem cell lineage

2.1 Summary ……13

2.2 Introduction ……13

2.3 Experimental Procedures ……15

2.4 Results ……20

2.4.1 JAK/STAT signaling is dynamically regulated in the midgut …… 20

2.4.2 JAK/STAT signaling is required in the ISC lineage …… 22

2.4.3 JAK/STAT signaling is required for differentiation in the ISC lineage ……23

2.4.4 Dl is sufficient to specify EC cell fate ……24

2.4.5 JAK/STAT is epistatic to Dl/N signaling in multi-lineage differentiation ……25

2.4.6 Little evidence that JAK/STAT signaling is required for ISC self-renewal …….. 26

2.4.7 The JAK/STAT pathway promotes ISC proliferation ……..…. 27

2.5 Discussion ……..……..……28

2.6 Figures ……..……32

2.7 Supplementary material ……..……..……..46

2.8 References .....……..57

Chapter 3: *Adenomatous polyposis coli* regulates *Drosophila* intestinal stem cell proliferation

3.1 Summary ……..……61

3.2 Introduction ……..……..……..……61

3.3 Experimental Procedures ……..……62

3.4 Results ……..……..……67

3.4.1 *Apc* regulates adult midgut homeostasis ……..……67

3.4.2 *Apc* is required in ISC lineages to maintain homeostasis ……..……67

3.4.3 *Apc* loss does not affect ISC self-renewal ……..……69

3.4.4 ISCs lacking *Apc* generate the differentiated cells of the lineage ……..……69

3.4.5 *Apc* is required in ISCs to regulate proliferation ……..……..…70

3.4.6 Wnt signaling regulates homeostasis in ISC lineages ……..……...71

3.4.7 *Apc* hyperplasia is suppressed by reductions in Wnt signaling ……..……..72

3.5 Discussion ……..……...73

3.6 Figures ……..……..…77

3.7 Supplementary material ……..……..…90

3.8 References .....……..……..97

Chapter 4: Enteroendocrine cells dynamically regulate the pro-secretory transcription factor Dimmed in response to the enteric pathogen *Pseudomonas entomophila*

4.1 Summary ……..……..……...…102

4.2 Introduction .....……..……...…102

4.3 Results 103

4.3.1 Mature enteroendocrine cells induce Dimm in response to *Pe* infection 103

4.3.2 Dimm induction in enteroendocrine cells is transient and systemic 105

4.3.3 Dimm induction in enteroendocrine cells is sensitive 106

4.3.4 Enteroendocrine cells express Dimm target genes in a *dimm*-dependent manner 106

4.3.5 *dimm* is required for changes in AstA expression following *Pe* infection 107

4.3.6 Dimm is a host factor that protects adult *Drosophila* against *Pe* infection 108

4.4 Discussion 108

4.5 Experimental Procedures 111

4.6 Acknowledgements 113

4.7 Figures 114

4.8 Supplementary material 121

4.9 References 124

Chapter 5: Summary and future directions

5.1 A screen to identify novel regulators of ISC proliferation 128

5.2 Characterization of the prosecretory response of enteroendocrine cells.....129

5.2.1 Transcriptional induction of Dimm.....129

5.2.2 Specificity of Dimm induction 129

5.2.3 Identification of the upstream mechanism of Dimm induction 130

5.2.4 Identification of downstream physiological consequences of Dimm induction 131

5.3 Figures 132

5.4 Tables 135

5.5 References 136

***Curriculum vitae* 137**

List of Figures and Tables

Chapter 2: JAK/STAT signaling coordinates stem cell proliferation and multilineage differentiation in the *Drosophila* intestinal stem cell lineage

Figure 2.1 The adult Drosophila midgut is maintained by a population of multipotent intestinal stem cells (ISCs) …….. 32

Figure 2.2 JAK/STAT signaling is dynamically regulated in midgut ISCs and EBs ……..33

Figure 2.3 JAK/STAT signaling is required in the ISC lineage ……..35

Figure 2.4 *stat92E* is required for multi-lineage differentiation ……37

Figure 2.5 *stat92E* is epistatic to Dl/N signaling for EC specification ……39

Figure 2.6 *stat92E* is epistatic to Dl/N signaling for EE specification ……41

Figure 2.7 JAK/STAT is not required for ISC self-renewal ……42

Figure 2.8 JAK/STAT activation promotes ISC proliferation ……44

Figure S2.1 JAK/STAT signaling is dynamically regulated in midgut ……46

Figure S2.2 Non-autonomous effects of $stat92E^{85C9}$ clones ……..48

Figure S2.3 ISCs are present in the absence of JAK/STAT signaling ……..49

Figure S2.4 Delta expression is sufficient to promote the EC cell fate ……..51

Figure S2.5 $stat92E^{06346}$ and $stat92E^{85C9}$ have similar phenotypes in the ISC lineage…..53

Figure S2.6 JAK/STAT is not absolutely required for self-renewal ……...55

Figure S2.7 A model for the role of JAK/STAT in the *Drosophila* intestinal stem cell lineage ……56

Chapter 3: *Adenomatous polyposis coli* regulates *Drosophila* intestinal stem cell proliferation

Figure 3.1 The adult *Drosophila* midgut is maintained by a population of multi-potent intestinal stem cells (ISCs) ……..……77

Figure 3.2 *Apc* is required to maintain adult midgut homeostasis ……..78

Figure 3.3 Loss of *Apc* in the midgut leads to hyperplasia and multi-layering ……..79

Figure 3.4 Loss of *Apc* in ISCs leads to an increase in clone size ……81

Figure 3.5 Cell fate in the ISC lineage is correctly specified in the absence of *Apc* 83

Figure 3.6 *Apc* is required in ISCs to regulate proliferation ……85

Figure 3.7 *Apc* hyperplasia is suppressed by reducing Wnt signaling ……...87

Figure 3.8 Wnt regulation of midgut ISCs ……89

Figure S3.1 The standard quantitative method used in analyzing mosaic midguts ……90

Figure S3.2 *Apc* loss leads to increased Dl levels ……92

Figure S3.3 Loss of *Apc* in ISCs enhances hyperplasia and multi-layering of the N^{RNAi} phenotype ……93

Figure S3.4 Quantification of clone size and mitotic index in N^{RNAi}, *Apc* lineages ……94

Figure S3.5 Wnt activation in the ISC lineage leads to an increase in clone size ……...96

Chapter 4: A prosecretory response of adult *Drosophila* enteroendocrine cells to the pathogenic bacteria *Pseudomonas entomophila*

Figure 4.1 Adult enteroendocrine cells induce Dimm in response to the bacterial pathogen *Pe* ……114

Figure 4.2 Dimm is transiently induced and is sensitive to sublethal doses of *Pe* ……116

Figure 4.3 *dimm* is necessary for target gene expression and peptide regulation in enteroendocrine cells ……118

Figure 4.4 Dimm is a host factor that protects against *Pe* infection ……120

Figure S4.1 Anti-Dimm staining is absent in *dimm* mutants ……121

Figure S4.2 Ablation of *esg* cells does not induce Dimm under baseline conditions ……122

Figure S4.3 Dose sensitivity of wild type *Canton-S* survival following exposure to *Pe* ……123

Chapter 5: Summary and future directions

Figure 5.1 An RNAi based genetic screen to identify repressors of ISC proliferation ……132

Figure 5.2 Validation of the RNAi phenotype and mutant analysis ……133

Figure 5.2 DIMM induction in EEs occurs in response to specific stimuli ……134

Table 5.1 A pathway based screen to identify upstream regulators of Dimm ……135

List of Abbreviations

AP: anterior posterior

Apc: Adenomatous polyposis coli

*Apc*1: *Apc*-like; CG1451

*Apc*2: *Apc* homolog 2; CG6193

AstA: Allatostatin A; CG13633

Dimm: dimmed; CG8667

Dl: Delta; CG3619

Dome: Domeless; CG14226

Hop: Hopscotcht, JAK-like; CG1594

EB: enteroblast

EC: enterocyte

EGF: epidermal growth factor

EGFR: EGF receptor; CG10079

EE: enteroendocrine cell

Esg: Escargot; CG3758

FLP: Flippase

FRT: Flippase recongnition target

Gal4: a yeast transcriptional activator

Gal80: a yeast transcriptional suppressor

GBE: Grh protein binding element

GFP: Green Fluorescent Protein

GOI: gene-of-interest

IL6: interleukin 6

InR: insulin-like receptor; CG18402

ISC: intestinal stem cell

JAK/STAT: Janus Kinase/Signal Transducer and Activator of Transcription

lof: loss-of-function

MARCM: mosaic analysis with a repressible cell marker system

N: Notch; CG3936

NPF: Neuropeptide F; CG10342

pHH3: phospho-histone H3

Phm: Peptidylglycine-alpha-hydroxylating monooxygenase; CG3832

Pros: Prospero; CG17228

RNAi: RNA interference

RSP: Regulated Secretory Pathway

s.e.m: standard error of the mean

Socs: Socs36E, Suppressor of cytokine signaling at 36E; CG15154

Stat92E: Signal-transducer and activator of transcription protein at 92E; CG4257

Su(H): Suppressor of Hairless; CG3497

TARGET: temporal and regional gene expression targeting system

Tk: Tachykinin; CG14734

UAS: upstream activation sequence

Upd1: Unpaired 1, outstretched; CG33542

Upd2: Unpaired 2; CG5988

Upd3: Unpaired 3; CG33542

Publications arising from this thesis

1. **Katherine Beebe, Wen-Chih Lee, Craig A. Micchelli.** (2010). JAK/STAT signaling coordinates stem cell proliferation and multilineage differentiation in the Drosophila intestinal stem cell lineage. *Dev Biol* **338**, 28-37. ……..… Chapter 3

   The content of this publication is reproduced in Chapter 2 under the author rights permission granted by *Elsevier/Developmental Biology*.

2. **Wen-Chih Lee, Katherine Beebe, Lisa Sudmeier, Craig A. Micchelli.** (2009). Adenomatous polyposis coli regulates *Drosophila* intestinal stem cell proliferation. *Development* **136**, 2255-2264. ……. Chapter 2

   The content of this publication is reproduced in Chapter 3 under the author rights permission granted by *Development*.

ACKNOWLEDGMENTS

First, with thanks to my advisor and mentor Dr. Craig Micchelli. Craig, thank you for giving me the opportunity to grow as a scientist and to develop a personal investment and confidence in the scientific process. Thanks also to colleagues and friends of the Micchelli lab. Marie, you are an amazing friend and scientist, thank you for all the support you gave me along the way. Mos, I learned so much from you and your approach to science, you are one of the best researchers I know. Thank you for all the support as a trusted friend. Ryan, you lifted me up on days when I was down. Thank you for your friendship and all of the hard work you provide to support the lab.

I am ever grateful to the network of scientists and supportive people at Washington University. Thank you to the Spencer T. Olin Fellowship for Women for financial support of my graduate work, and the network of wonderful people as well. Thank you to the department and program, especially Stacy Kiel and Sally Vogt. I would like to thank my thesis committee, Drs. Stephen Johnson, Kerry Kornfeld, James Skeath, and Thaddeus Stappenbeck, for their valuable input throughout my graduate studies. In particular, thank you Kerry and Jim for your calm insight and support. Dr. Raphael Kopan, I am grateful for your valuable input throughout my thesis development and my development as a scientist. Thank you to Drs. Paul Taghert and Dongkook Park. Your generosity, patience and insight throughout our work together is deeply appreciated.

To my friends and family - Carin and Dad, thank you for always being there, cheering me on. Maria, thank you for helping me finish the last phase of thesis work, Sophie is the luckiest sister in the world. Sophie, your laughter and light puts everything in its right perspective. Emel, thank you for enjoying graduate school together. Leti, Pedro, Eloisa, Diego!, Vincenzo, and the UMSL crew – we made it! Thank you for your friendship and all of the fun times of this era. To the Martinez/Hernandez clan and the Beebe/Starr clan – I love you endlessly, you are each a beautiful presence in this world. Thank you especially to my grandfather Frank Starr, who read my first manuscript and responded with insightful questions. And finally, to Javier - you are the best partner anyone could wish for in this life. You help me find my own voice and enjoy this journey together.

ABSTRACT OF THE DISSERTATION

Dynamic Responses at the Barrier Epithelium

by

Katherine Beebe

Doctor of Philosophy in Biology and Biomedical Sciences

Developmental, Regenerative and Stem Cell Biology

Washington University in St. Louis, 2014

Assistant Professor Craig A. Micchelli, Chair

A fundamental question in biology is how cellular systems sense and respond to their environment. The environment is a changing parameter, and cellular life has evolved a multitude of interesting and adaptive ways to sense and respond to external changes. The GI tract is a particularly interesting tissue in which to examine this question. One of few barrier epithelia, the intestine is exposed to both the unique environment of the lumen and the internal environment of the organism. Cells of the intestine simultaneously function as barrier, digestive organ, and sensory organ. Additionally, in many metazoan animals these functions occur in the context of active stem cell based turnover. Although substantial progress has been made in the identification of the genetic and molecular pathways that regulate these different processes, the manner in which function is responsive to changes in the environment remains incompletely understood.

In this dissertation, we used the adult *Drosophila* midgut as a model system to investigate two aspects of intestinal homeostasis in response to environmental change. Chapters 2 and 3 address the regulation of intestinal stem cell based renewal as a coordinated and phenotypically plastic system. In *Drosophila*, as in mammals, the adult intestinal epithelium is maintained by self-renewing and multipotent stem cells. A critical aspect of the success of adult stem cell renewing systems is the balance and regulation of proliferation, self-renewal, and differentiation. In Chapter 2 we demonstrate the requirement for JAK/STAT signal transduction in the ISC

lineage for multilineage differentiation. Work concurrent with ours was important in demonstrating the induction of JAK/STAT pathway ligands in response to intestinal stressors including enteric pathogens. Thus, JAK/STAT is an important pathway that coordinates proliferation and mulitlineage differentiation during epithelial renewal. In Chapter 3, we characterized the *Apc* loss of function phenotype in the ISC lineage. *Apc* is a repressor of Wnt signalling in mammals and *Drosophila*. *Apc* loss of function mutations had been shown to be a causative mutation associated with colon cancers in humans, however the intrinsic requirement of *Apc* in the ISC lineage itself had not been tested. We report that *Apc* is necessary within the lineage to repress ISC proliferation. This finding is important in establishing the groundwork for future investigation of the responsivity of hyperplastic lineages to changes in the inflammatory and nutritional environment.

Chapter 4 characterizes a novel response of the enteroendocrine system to pathogenic challenge. Enteroendocrine cells are professional secretory cells with the capacity to signal through various peptide hormones. These hormones regulate important aspects of local and organismal physiology. We discovered and characterized a prosecretory response of the mature enteroendocrine population to the pathogenic bacteria *Pseudomonas entomophila.* Specifically, the prosecretory bHLH transcription factor Dimmed is induced in a manner that is transient, sensitive to low doses and required for expression of the important peptide processing enzyme *phm*.

Taken together, these studies provide mechanistic insight into our understanding of renewal and enteroendocrine function as regulated and responsive processes. It remains an interesting question the extent to which these pathways are mechanistically integrated or operate independently from one another.

Chapter 1

Introduction

A fundamental question in biology is how cellular systems sense and respond to their environment. The environment is a changing parameter, and cellular life has evolved a multitude of interesting and adaptive ways to sense and respond to external changes. The gastrointestinal (GI) tract is a particularly interesting tissue in which to examine this question. One of few barrier epithelia, the intestine is exposed to both the unique environment of the lumen and the internal environment of the organism. Cells of the intestine simultaneously function as barrier, digestive organ, and sensory organ. Additionally, in many metazoan animals these functions occur in the context of active stem cell based turnover. Significant advances have been made in characterizing the lumenal environment and responses of intestinal functions to environmental stimuli. In some cases the molecular regulation of these responses is partially characterized. There are many unanswered questions however, and the molecular basis and regulation of phenotypic plasticity in the GI tract is currently an active area of investigative research.

1.1 The GI barrier and its lumenal environment

Metazoan animals have some tissues in direct contact with the external environment, and some that are not. Cells of the barrier epithelia are those in direct contact with the external world. These barrier epithelia include the skin, lung and intestine. The GI epithelium is unique in its high turnover activity as well as its contact with the lumenal space. With specific exposure to ingested materials, support of bacterial communities, and extreme regionalization, the lumenal space represents a specialized and extreme ecosystem on planet earth. This ecosystem presents many physiochemical stimuli to the host. For example, physical and nutritional stimulants include physical extension following ingestion of a large meal or presence of glucose and free fatty acids. Non-nutrient materials can be ingested as well, some of which present potential damage to the organism. These include toxic plant chemicals, viruses, fungi, parasitic animals and pathogenic bacterial species. Other non-nutrient materials may aid the host in digestion and function, such as commensal bacterial species or chemicals involved in taste receptor signaling (Brestoff and Artis, 2013; Furness et al., 2013).

Exposure of intestinal cells to lumenal signals is influenced in part by the morphology of the epithelium as well as its secretory products. The intestinal epithelium is a cellular monolayer that resides on a basement membrane. As a monolayer, all cells have the potential for direct contact with lumenal

contents. However, in many organisms this contact is influenced by the physical structure of the intestinal epithelium. In addition to large scale folding, the epithelium has evolved to generate additional surface area through cellular microvilli and, in some organisms, crypt of Lieberkühn (crypt) and villus structures. These invaginations and protrusions create increased surface area of exposure, an estimated 100m^2 of cellular-lumenal surface area for example in the human small intestine (Ferraris et al., 1989). Such structures also function to restrict signals presented to cells and create microenvironments of lumenal space. For example the cryptic space is thought to be free of bacteria under baseline homeostatic conditions, whereas the villus tips of the small intestine have increased exposure to commensal bacteria (Pelaseyed et al., 2014). The GI tract is a highly regional organ, and exposure to lumenal stimuli varies along the anterior to posterior axis. For example, commensal bacterial populations vary longitudinally along the GI tract with the stomach being almost sterile and the colon supporting an estimated density of 10^{11}-10^{12} cells/ml, the highest density recorded for any microbial habitat (Ley et al., 2006). Finally, it is important to note that exposure of the epithelium to lumenal contents is influenced by biochemical factors secreted from intestinal cells that serve important protective functions. Secretion of gastric acid in the stomach is one example. Important also are the secretions of different types of mucins and undigestable complex carbohydrates that form the mucus layer. The mucus layer functions to restrict access of bacteria and digestive products to cells of the host, thus protecting the epithelial cell from self-digestion and bacterial infection (Pelaseyed et al., 2014). Taken together, there are many potential stimuli and microenvironments that define the lumenal space.

1.2 The adult *Drosophila* midgut as an experimental system

The adult *Drosophila* midgut is proving to be a powerful genetic model system for the study of various aspects of GI biology. This is in large part due to the combination of a stem cell based renewing but relatively simple epithelium with the experimental strengths of *Drosophila* more generally; including high genetic tractability, a relatively simple genome in comparison to mammals, and fast life cycle. The midgut is a simplified but sufficiently complex barrier epithelium with many similarities to its mammalian counterpart. Both intestinal systems share a common developmental endodermal origin (de Santa Barbara et al., 2003; Immergluck et al., 1990). Additionally, both intestinal systems display high

regionality along the anterior posterior (AP) axis (For example, Buchon et al., 2013). Both tissue systems consist of differentiated absorptive and secretory cell types. In *Drosophila* these cell types display diversity along the AP axis but generally are classified into absorptive enterocytes (ECs) and secretory enteroendocrine cells (EEs). Lastly, both the mammalian and *Drosophila* intestinal epithelia rely on a population of self-renewing and multipotent intestinal stem cells for an active renewal and turnover of the epithelium (Micchelli and Perrimon, 2006; Ohlstein and Spradling, 2006).

Structurally, the midgut is relatively simple and allows analysis along the entire AP length in a given specimen. The cellular monolayer is situated on a basal membrane and does not have the crypt or villus structures found in mammals. As in mammals, however, the effective absorptive surface area is increased through extensive microvilli of differentiated enterocytes. The epithelium is pseudostratified with nuclei at different positions and generally all cells make contact with the basement membrane. Surrounding this epithelium is a network of circumferential and longitudinal visceral muscle. The foregut and midgut connect at a substructure of the midgut called the proventriculus, a specialized tissue that generates the peritrophic matrix. Made of chitins and glycoproteins and a structure for association of mucins, this matrix forms a tube within the luminal space and, similar to the mucus layer of the mammalian intestine, has both digestive and barrier functions (Kuraishi et al., 2011; Syed et al., 2008).

1.2.1 The ISC lineage and midgut renewal

Studies thus far have characterized various roles for conserved signaling pathways in the regulation of stem cell based renewal. For example, Notch (N), Wnt, JAK/STAT, EGFR, InR, and Hippo signaling pathways. Specifically, N signaling is necessary for cell fate specification of ECs and creates asymmetric division of the ISC and its enteroblast (EB) daughter. Wnt signaling is both necessary and sufficient to regulate proliferation and is also necessary for stem cell maintenance. ISC proliferation is also regulated by JAK/STAT and EGF signaling pathways. Specifically, a model has emerged in which stressed ECs produce Unpaired (Upd) cytokines of the JAK/STAT pathway that act directly and indirectly on the ISC lineage to promote proliferation and differentiation of daughter cells. Upd cytokines are somewhat homologous to IL6 in mammals and represent a similarity in this system with mammalian regulation of ISC proliferation as inflammatory cytokines (Jiang et al., 2009).

In addition to a pathway analysis of ISC lineage properties, investigators have developed and characterized a number of protocols to alter the lumenal environment of the GI tract. For example, strains of bacteria originally isolated from *Drosophila* can be cultured and exposed to experimental cohorts. These bacteria stimulate, to varying degrees, the immune and proliferative response of the midgut epithelium. For example, the pathogenic bacteria *Pseudomonas entomophila* (*Pe*) triggers an oxidative burst in the midgut that stimulates the secretion of Upd ligands and activation of JNK signaling in ECs (Buchon et al., 2009). Upd ligands, in turn, promote EGF ligand secretion from the muscle, and subsequent EGFR based proliferation of the ISC. Although this is a simplified summary of what is understood regarding the complex cellular processes that occur during infection based renewal, it is to emphasize that conserved transcriptional pathways regulate ISC lineage homeostasis in the response to stress. This response is coordinated in time and occurs through non-autonomous niche signaling. Taken together the *Drosophila* gut is an increasingly established model system to study the response of stem cells to environmental stimuli.

1.2.2 The diffuse endocrine system

In addition to the digestive, renewal, and barrier functions, the GI epithelium is also large and diverse endocrine organ. Endocrine cells are functionally specialized in the process of sensing and responding to stimuli. In both *Drosophila* and mammals, endocrine cells use the regulated secretory pathway (RSP) to accumulate and store large amounts of peptide signal in vesicles that can be released into the local and long-range circulatory environment to regulate a variety of physiological responses (Vazquez-Martinez et al., 2012).

Drosophila and mammalian enteroendocrine systems hold many similarities. Both display regional expression of a diversity of peptide hormones in longitudinally distinct regions along the gut (Veenstra et al., 2008) (Helander and Fandriks, 2012). In both systems, EEs are present at a relatively low frequency but have potent effects on local and long-range physiological processes (Gunawardene et al., 2011). In mammals for example, EE peptides regulate local processes such as acid production, intestinal peristalsis, epithelial secretions, and gastric emptying. Long range responses include regulation of appetite/satiety and pancreatic insulin secretion (Furness et al., 2013). Peptide release can be stimulated

by various lumenal stimuli. Examples of stimuli to which EEs respond include nutrients, mechanical distension, HCl, bacterially produced SCFAs, NO, and CO^2 (Helander and Fandriks, 2012).

The extent to which EEs respond to bacterial stimuli has been the focus of a limited number of studies in mammals. In mammalian EEs, Toll like receptors (TLRs) of the innate immune system are expressed in particular subtypes in culture conditions, and transcriptional responses have been shown to be activated in EEs in response to bacterial exposure (Bogunovic et al., 2007; Palazzo et al., 2007; Selleri et al., 2008). In an effort to understand the hypergastrinemia observed in patients with *H. pylori,* Beales *et al*. investigated the ability of cytokines and bacterial products to stimulate gastrin release in isolated enteroendocrine G cells of the mammalian stomach (Beales et al., 1997; Beales and Calam, 2000; Beales et al., 1996). In these studies, *H. pylori* sonicate, significantly potentiated gastrin release to over 5 fold that of cytokine stimulated gastrin release alone. This effect was not replicated by LPS or *E. coli* sonicate and was shown to be a regulated release of peptide not due to cell death. Thus, at least in cultured G cells, the amount of peptide released is flexible, and is enhanced by specific bacterial stimuli. However, the mechanism for this increased secretory response has not been identified. In *Drosophila*, a response of the diffuse endocrine system to environmental stress had not been explicitly reported or investigated. Additionally, in studies examining pathway regulation of the ISC lineage, reporters for N, Wnt, JAK/STAT, or EGF were not localized to the mature EEs, leaving open the question of their involvement in the gut response to infection and stress.

1.3 Morphological and molecular markers of cell types in the adult *Drosophila* midgut

The epithelium of the adult *Drosophila* midgut is composed of four general cell types, which can be identified on the basis of morphology and molecular markers. The adult intestinal stem cell (ISC) is of relatively small morphology, is diploid and is associated with the basement membrane. It is identified on the basis of expression of escargot (*esg*), a snail/slug type transcription factor, and Delta, a ligand of the Notch signaling pathway. Additionally, the ISC is negative for reporters of Notch signal transduction such as a reporter using multimerized binding sites for the transcription factor Supressor of Hairless (Su(H)-LacZ). The enteroblast (EB) is an undifferentiated daughter cell and can be identified on the basis of small morphology, Notch signal transduction (Su(H)-LacZ positive) and the absence of Delta expression.

In addition to these progenitor cell types, there are two formal classes of differentiated cells that comprise the midgut epithelium; the enterocyte (EC) and the enteroendocrine cell (EE). Both are general categories which encompass different subtypes on the basis of distinct morphologies, functions and genes expressed. ECs are generally large cells with polyploid nuclei. EEs are secretory cells that express a variety of different neuroendocrine peptides. On average, the relative proportions of the different cell types in the adult gut under baseline conditions are (2) ISCs: (1) EB: (9.3) ECs: (2) EEs. However these proportions do vary within regions (Sudmeier and Micchelli, unpublished data).

1.4 Genetic tools

One important aspect of what makes the adult *Drosophila* midgut an effective model system to study GI biology is the power of *Drosophila* genetics more generally. Genetic tools developed in *Drosophila* allow manipulation of gene expression with temporal and spacial control. Additionally, generation of marked lineages are particularly useful for the study of adult stem cell biology and the manipulation of gene expression within lineages. Below, I outline the genetic tools utilized in this dissertation that allowed characterization of the ISC lineage and testing of gene function.

The Gal4/UAS system, derived from a yeast transcriptional promoter system, is the basis of much of the gene expression manipulations utilized in *Drosophila*. Gal4, a yeast transcription factor, specifically activates the Upstream Activation Sequence (UAS) promoter. In *Drosophila*, this system is utilized whereby the Gal4 promoter sequence is under control of an experimentally specified promoter of interest, or in some cases inserted into an endogenous locus of the fly genome (Brand and Perrimon, 1993). Expression of Gal4 protein then activates transcription of a coding sequence under regulatory control of the UAS promoter. For example, *esg*Gal4, UAS-GFP drives expression of green fluorescent protein (GFP) in cells with endogenous transcriptional activation of the *escargot (esg)* promoter.

The temporal and regional gene expression targeting (TARGET) system utilizes the Gal4/UAS system with temporal regulation (McGuire et al., 2004). In this system, the yeast system is utilized again, in which the Gal80 protein, an inhibitor of the Gal4/UAS interaction, is expressed to block the UAS based transcription. Because a temperature sensitive form of the Gal80 protein is utilized ($Gal80^{TS}$), Gal4/UAS gene expression is blocked at 18C where $Gal80^{TS}$ is functional, and Gal4/UAS gene expression is

allowed at 29C where the Gal80^{TS} protein is not functional. For example, *esg*Gal4, UAS-GFP, *tub*Gal80^{TS} drives expression of GFP in *esg* expressing cells at 29C, however at 18C GAL80^{TS} is functional and expressed in *tubulin* expressing cells in which it inhibits Gal4/UAS interaction and thus GFP expression will be blocked.

Lastly, lineage analysis in this dissertation is performed through use of the MARCM system. This system allows positive marking of mitotic cells and can be combined with UAS based expression of a transgene of interest as well as loss of heterozygousity in marked lineages (Lee and Luo, 1999). Recombination during mitosis allows heritable separation of the GAL4 and GAL80 elements and the marking of a lineage with a marker such as GFP. This system can be employed to understand gene function as a variety of mutant alleles have been recombined onto chromosomes with an FRT site, thus allowing segregation of mutant alleles in daughter cells and generating a mosaic tissue.

1.5 Summary of thesis chapters

Chapters 2 and 3 of this dissertation contribute to our understanding of the regulated process of stem cell based renewal of the midgut epithelium and the establishment of the *Drosophila* ISC system as a model system relevant to human health and disease. Specifically, Chapter 2 examines the role of the JAK/STAT pathway in the ISC lineage. We characterized a requirement for JAK/STAT signal transduction as a competency factor for multilineage differentiation of both EEs and ECs. Additionally, we characterized the variable expression of Upd ligands in ECs and the sufficiency of Upd to promote proliferation. Lastly, our results are consistent with the EGF-niche signaling model in that we found that JAK/STAT signal transduction was not autonomously necessary within the ISC lineage for normal rates of proliferation.

Chapter 3 tests the intestinal stem cell lineage requirement for *Apc*. *Apc* is a repressor of Wnt signaling in *Drosophila* and mammals, and is highly associated with colon cancer in humans, however the precise mechanism of the proliferative phenotype had not been determined. This work demonstrates that *Apc*1 and *Apc*2 are required in the ISC lineage to repress proliferative output. Our findings are consistent with a concurrent publication in mammals examining the targeted *Apc* loss of function phenotype in the LGR5+ lineage (Barker et al., 2009).

In Chapter 4 I address the sensory organ biology of the GI tract through the study of the mature enteroendocrine population and its response to exogenous challenge. Specifically, I characterize a pro-secretory response of the enteroendocrine population to pathogenic bacterium *Pseudomonas entomophila*. This finding demonstrates that aspects of the RSP in mature EEs are transiently and sensitively responsive to infection.

Lastly, in Chapter 5 I summarize the thesis work and outline future directions of interest.

1.6 References

Barker, N., Ridgway, R.A., van Es, J.H., van de Wetering, M., Begthel, H., van den Born, M., Danenberg, E., Clarke, A.R., Sansom, O.J., and Clevers, H. (2009). Crypt stem cells as the cells-of-origin of intestinal cancer. Nature *457*, 608-611.

Beales, I., Blaser, M.J., Srinivasan, S., Calam, J., Perez-Perez, G.I., Yamada, T., Scheiman, J., Post, L., and Del Valle, J. (1997). Effect of Helicobacter pylori products and recombinant cytokines on gastrin release from cultured canine G cells. Gastroenterology *113*, 465-471.

Beales, I.L., and Calam, J. (2000). Helicobacter pylori increases gastrin release from cultured canine antral G-cells. European journal of gastroenterology & hepatology *12*, 641-644.

Beales, I.L., Post, L., Calam, J., Yamada, T., and Delvalle, J. (1996). Tumour necrosis factor alpha stimulates gastrin release from canine and human antral G cells: possible mechanism of the Helicobacter pylori-gastrin link. European journal of clinical investigation *26*, 609-611.

Bogunovic, M., Dave, S.H., Tilstra, J.S., Chang, D.T., Harpaz, N., Xiong, H., Mayer, L.F., and Plevy, S.E. (2007). Enteroendocrine cells express functional Toll-like receptors. American journal of physiology Gastrointestinal and liver physiology *292*, G1770-1783.

Brand, A.H., and Perrimon, N. (1993). Targeted gene expression as a means of altering cell fates and generating dominant phenotypes. Development *118*, 401-415.

Brestoff, J.R., and Artis, D. (2013). Commensal bacteria at the interface of host metabolism and the immune system. Nature immunology *14*, 676-684.

Buchon, N., Broderick, N.A., Chakrabarti, S., and Lemaitre, B. (2009). Invasive and indigenous microbiota impact intestinal stem cell activity through multiple pathways in Drosophila. Genes & development *23*, 2333-2344.

Buchon, N., Osman, D., David, F.P., Fang, H.Y., Boquete, J.P., Deplancke, B., and Lemaitre, B. (2013). Morphological and molecular characterization of adult midgut compartmentalization in Drosophila. Cell reports *3*, 1725-1738.

de Santa Barbara, P., van den Brink, G.R., and Roberts, D.J. (2003). Development and differentiation of the intestinal epithelium. Cellular and molecular life sciences : CMLS *60*, 1322-1332.

Ferraris, R.P., Lee, P.P., and Diamond, J.M. (1989). Origin of regional and species differences in intestinal glucose uptake. The American journal of physiology *257*, G689-697.

Furness, J.B., Rivera, L.R., Cho, H.J., Bravo, D.M., and Callaghan, B. (2013). The gut as a sensory organ. Nature reviews Gastroenterology & hepatology *10*, 729-740.

Gunawardene, A.R., Corfe, B.M., and Staton, C.A. (2011). Classification and functions of enteroendocrine cells of the lower gastrointestinal tract. International journal of experimental pathology *92*, 219-231.

Helander, H.F., and Fandriks, L. (2012). The enteroendocrine "letter cells" - time for a new nomenclature? Scandinavian journal of gastroenterology *47*, 3-12.

Immergluck, K., Lawrence, P.A., and Bienz, M. (1990). Induction across germ layers in Drosophila mediated by a genetic cascade. Cell *62*, 261-268.

Jiang, H., Patel, P.H., Kohlmaier, A., Grenley, M.O., McEwen, D.G., and Edgar, B.A. (2009). Cytokine/Jak/Stat signaling mediates regeneration and homeostasis in the Drosophila midgut. Cell *137*, 1343-1355.

Kuraishi, T., Binggeli, O., Opota, O., Buchon, N., and Lemaitre, B. (2011). Genetic evidence for a protective role of the peritrophic matrix against intestinal bacterial infection in Drosophila melanogaster. Proceedings of the National Academy of Sciences of the United States of America *108*, 15966-15971.

Lee, T., and Luo, L. (1999). Mosaic analysis with a repressible cell marker for studies of gene function in neuronal morphogenesis. Neuron *22*, 451-461.

Ley, R.E., Peterson, D.A., and Gordon, J.I. (2006). Ecological and evolutionary forces shaping microbial diversity in the human intestine. Cell *124*, 837-848.

McGuire, S.E., Mao, Z., and Davis, R.L. (2004). Spatiotemporal gene expression targeting with the TARGET and gene-switch systems in Drosophila. Science's STKE : signal transduction knowledge environment *2004*, pl6.

Micchelli, C.A., and Perrimon, N. (2006). Evidence that stem cells reside in the adult Drosophila midgut epithelium. Nature *439*, 475-479.

Ohlstein, B., and Spradling, A. (2006). The adult Drosophila posterior midgut is maintained by pluripotent stem cells. Nature *439*, 470-474.

Palazzo, M., Balsari, A., Rossini, A., Selleri, S., Calcaterra, C., Gariboldi, S., Zanobbio, L., Arnaboldi, F., Shirai, Y.F., Serrao, G.*, et al.* (2007). Activation of enteroendocrine cells via TLRs induces hormone, chemokine, and defensin secretion. Journal of immunology *178*, 4296-4303.

Pelaseyed, T., Bergstrom, J.H., Gustafsson, J.K., Ermund, A., Birchenough, G.M., Schutte, A., van der Post, S., Svensson, F., Rodriguez-Pineiro, A.M., Nystrom, E.E.*, et al.* (2014). The mucus and mucins of the goblet cells and enterocytes provide the first defense line of the gastrointestinal tract and interact with the immune system. Immunological reviews *260*, 8-20.

Selleri, S., Palazzo, M., Deola, S., Wang, E., Balsari, A., Marincola, F.M., and Rumio, C. (2008). Induction of pro-inflammatory programs in enteroendocrine cells by the Toll-like receptor agonists flagellin and bacterial LPS. International immunology *20*, 961-970.

Syed, Z.A., Hard, T., Uv, A., and van Dijk-Hard, I.F. (2008). A potential role for Drosophila mucins in development and physiology. PloS one *3*, e3041.

Vazquez-Martinez, R., Diaz-Ruiz, A., Almabouada, F., Rabanal-Ruiz, Y., Gracia-Navarro, F., and Malagon, M.M. (2012). Revisiting the regulated secretory pathway: from frogs to human. General and comparative endocrinology *175*, 1-9.

Veenstra, J.A., Agricola, H.J., and Sellami, A. (2008). Regulatory peptides in fruit fly midgut. Cell and tissue research *334*, 499-516.

Chapter 2

JAK/STAT signaling coordinates stem cell proliferation and multilineage differentiation in the *Drosophila* intestinal stem cell lineage

The research work in Chapter 2 is published in Developmental Biology. 2010 Feb;338(1):28-37. Katherine Beebe is the first author of this publication.

2.1 Summary

Adult stem cells are the most primitive cells of a lineage and are distinguished by the properties of self-renewal and multi-potency. Coordinated control of stem cell proliferation and multi-lineage differentiation is essential to ensure a steady output of differentiated daughter cells necessary to maintain tissue homeostasis. However, little is known about the signals that coordinate stem cell proliferation and daughter cell differentiation. Here we investigate the role of the conserved JAK/STAT signaling pathway in the *Drosophila* intestinal stem cell (ISC) lineage. We show first, that JAK/STAT signaling is normally active in both ISCs and their newly formed daughters, but not in terminally differentiated enteroendocrine (ee) cells or enterocyte (EC) cells. Second, analysis of ISC lineages shows that JAK/STAT signaling is necessary but not sufficient for daughter cell differentiation, indicating that competence to undergo multi-lineage differentiation depends upon JAK/STAT. Finally, our analysis reveals JAK/STAT signaling to be a potent regulator of ISC proliferation, but not ISC self-renewal. On the basis of these findings, we suggest a model in which JAK/STAT signaling coordinates the processes of stem cell proliferation with the competence of daughter cells to undergo multi-lineage differentiation, ensuring a robust cellular output in the lineage.

2.2 Introduction

Adult stem cell populations are present in a variety of tissues and function throughout the lifetime of an organism to maintain homeostasis. The dual characteristics of self-renewal and multipotency make stem cells ideally suited for this central role. In a variety of tissue systems, adult stem cells have been shown to reside in specialized microenvironments called niches, which regulate stem cell behavior at baseline homeostasis and dynamically respond to changing environmental stimuli by modulating lineage output (reviewed in(Jones and Wagers, 2008)). The coordinated control of stem cell proliferation and multi-lineage differentiation is essential to ensure a steady output of differentiated daughter cells at baseline homeostasis and in response to changing environmental conditions. However, little is currently known about the factors that coordinate these processes.

The ability to identify, mark and manipulate individual stem cell lineages has made *Drosophila* an excellent model system with which to dissect stem cell regulation. In the adult *Drosophila* midgut, for

example, the stem cell compartment is comprised of individual intestinal stem cells (ISCs) that are dispersed throughout the entirety of the tissue (Fig. S2.1A-D; (Micchelli and Perrimon, 2006; Ohlstein and Spradling, 2006)). ISCs have a pyramidal morphology and are located in an epithelial niche distant from the midgut lumen and adjacent to both the basement membrane and surrounding visceral musculature of the midgut. ISCs are multipotent and give rise to a lineage that consists of two types of differentiated daughters, the enteroendocrine (ee) cells and the enterocyte (EC) cells. Together, these cell populations form a cellular monolayer lining the length of adult midgut.

The *Ja*nus *K*inase/*S*ignal *T*ransducer and *A*ctivator of *T*ranscription (JAK/STAT) pathway is a conserved signal transduction pathway that has been implicated in a number of distinct developmental and disease processes (reviewed in (Arbouzova and Zeidler, 2006)). In *Drosophila*, the JAK/STAT pathway utilizes a set of core signaling components: a transmembrane receptor encoded by *domeless* (*dome*), a single JAK tyrosine kinase encoded by *hopscotch* (*hop*), the transcription factor *stat92E*, and *unpaired* (*upd*), as well as two related ligands encoded by *upd2*, *upd3*. Binding of Upd ligands to the Dome receptor leads to activation of Hop, a receptor-associated kinase, which has at least two substrates, Hop and Dome. Cytoplasmic Stat92E can bind to phosphorylated Dome/Hop complexes via SH2 domains. Once bound to the Dome/Hop complex, Stat molecules are also phosphorylated and form Stat dimers, which translocate to the nucleus and activate downstream transcriptional targets.

Phenotypic analysis in *Drosophila* has revealed that the JAK/STAT signaling pathway is a versatile regulator of stem cell populations and their cell lineages (reviewed in (Fuller and Spradling, 2007; Gregory et al., 2008)). Evidence suggests that JAK/STAT is necessary for the maintenance of germline and somatic stem cells and functions as a powerful signal promoting stem cell proliferation (Decotto and Spradling, 2005; Kiger et al., 2001; Singh et al., 2007; Tulina and Matunis, 2001). JAK/STAT signaling is also required in the ovary for subsequent differentiation and maintenance of specific cell types (Baksa et al., 2002; Ghiglione et al., 2002; McGregor et al., 2002; Silver et al., 2005). Recent studies in the adult midgut indicate that JAK/STAT signaling is a central mediator of adaptive homeostasis following a variety of experimental challenges including bacterial infection, directed cell ablation or stress signaling (Buchon et al., 2009; Cronin et al., 2009; Jiang et al., 2009). Collectively, these studies support a model in which JAK/STAT ligands are induced in response to challenge and stimulate ISC activity.

In this study, we investigate the role of the JAK/STAT pathway within the ISC lineage under conditions of baseline homeostasis. We show that JAK/STAT signaling is normally active in both ISCs and their newly formed daughters, but not in terminally differentiated enteroendocrine (ee) cells or enterocyte (EC) cells. We also show that cell autonomous loss of JAK/STAT signaling from individual ISC lineages results in a failure of EE and EC cell fate specification. Previous studies indicate that Notch signaling is a critical regulator of cell fate in the ISC lineage (Micchelli and Perrimon, 2006; Ohlstein and Spradling, 2006; Ohlstein and Spradling, 2007). Genetic analysis demonstrates that the transcription factor, *stat92E,* is epistatic to Delta/Notch (Dl/N) signaling in cell fate specification, suggesting that the JAK/STAT pathway functions downstream or in parallel to Dl/N signaling in newly formed ISC daughters. Finally, our analysis shows that JAK/STAT signaling is a potent regulator of ISC proliferation; tests revealed little evidence that JAK/STAT is required for ISC self-renewal. Thus, JAK/STAT signaling has dual, yet separable requirements in the undifferentiated cells of the ISC lineage. On the basis of these findings, we suggest a model in which JAK/STAT signaling coordinates the processes of stem cell proliferation with the competence of daughter cells to undergo multi-lineage differentiation.

2.3 Experimental Procedures

2.3.1 *Drosophila* strains and culture

w; 10xSTAT92E-GFP and *w; 10xSTAT92E-GFP^{destablized}* (transcriptional reporters of JAK/STAT activity; (Bach et al., 2007)). *upd1-Gal4* (Tsai and Sun, 2004). *w; upd3-Gal4* (Agaisse et al., 2003). *stat92E^{F}* (temperature sensitive allele; (Baksa et al., 2002)). *w; FRT^{82B} stat92E^{85C9} / TM6B-GFP* (missense mutation generated by EMS; (Silver and Montell, 2001)). *FRT^{82B} stat92E^{06346} / TM3* (also called *stat92E^{P1681}*, null allele; (Hou et al., 1996)). *hop^{C111} FRT^{19A} / FM7* (null allele; (Binari and Perrimon, 1994)). *y, w; UAS-hop^{Tum} / Cyo-GFP* (activated form of *hop*; (Harrison et al., 1995)). *w; UAS-Upd / Cyo-GFP* (Harrison et al., 1998). *w; UAS-N^{ECN}*(A dominant negative form of N; (Rebay et al., 1993)). *w, N^{55e11} FRT^{19A} / FM7* (null allele; (Kidd et al., 1986)). *ry^{506}, p[GBE + Su(H) m8, ry+, lacZ]* (*Su(H)GBE-lacZ;* (Furriols and Bray, 2001)). *w; UAS-N^{intra} / Cyo* (Struhl et al., 1993). *ry^{506}, Dl^{05151}*(*Dl-lacZ;* (Röttgen et al., 1998)). *w; UAS-Dl.H* (Jönsson and Knust, 1996). *vkg-GFP* (*collagen IV-GFP* protein trap; (Morin et al., 2001)). *w, tub-GAL80, hsFLP FRT^{19A}; UAS-lacZ^{nuc}, UAS-mCD8GFP; tub-Gal4* (Bello et al., 2003). *y, w,*

UAS-GFP, hsFLP; tubGal4, FRT^{82B} tub-Gal80 / TM6B (Lee and Luo, 1999). *w; FRT^{19A}* and *w; FRT^{82B} hsπM* (these stocks were used as a wild-type control in the mosaic analysis performed in this study; (Xu and Rubin, 1993)). *w; esg-Gal4 / Cyo* (Goto and Hayashi, 1999). *w; esg-Gal4, UAS-GFP* (Micchelli and Perrimon, 2006). *w; esg-Gal4, UAS-GFP, tub-Gal80^{TS}* (Micchelli and Perrimon, 2006). *y, w*; *esg^{K606} / Cyo* (*esg-lacZ;* (Samakovlis et al., 1996)). *y, w, hsFLP: AyGal4, UAS-GFP* (Flip-out clones; (Ito et al., 1997)). Crosses were cultured on standard dextrose media and transferred to fresh food supplemented with yeast paste every 1-2 days during the experimental period. Crosses were reared at 18, 25, or 29 °C, in passively illuminated and humidified incubators. In this study adult female flies of the following genotypes were analyzed:

Figure 2.1:

w; esg-Gal4, UAS-GFP

vkg-GFP / *esg^{K606}*

Figure 2.2 and S2.1:

y, w / w; esg^{K606} / 10xSTAT92E-GFP.

w / +; 10xSTAT92E-GFP / +; ry^{506}, Dl^{05151} / +.

w; 10xSTAT92E-GFP.

w / +; 10xSTAT92E-GFP^{D} / +.

w / +; 10XSTAT92E GFP^{D} / +; ry^{506}, p[GBE + Su(H) m8, ry+, lacZ] / +.

w / y, w, UAS-mCD8GFP; upd1-Gal4 / esg^{K606}.

w; upd3-Gal4, UAS-GFP.

Figure 2.3, S2.2, S2.3, S2.5, and S2.6:

stat92E^{F} / *FRT^{82B} stat92E^{06346}*

y, w, hsFLP, UAS-GFP / w; +; FRT^{82B} hsπM / tub-Gal4, FRT^{82B} tub-Gal80.

y, w, hsFLP, UAS-GFP / w; +; FRT^{82B} stat92E^{85C9} / tub-Gal4, FRT^{82B} tub-Gal80.

w, tub-Gal80, hsFLP FRT^{19A} / hop^{C111} FRT^{19A}; UAS-lacZ^{nuc}, UAS-mCD8GFP / +; tub-Gal4 / +.

y, w, hsFLP, UAS-GFP/+; +; FRT^{82B} stat92E^{06346} / tub-Gal4, FRT^{82B} tub-Gal80.

y, w, hsFLP, UAS-GFP / +; UAS-Dl / +; FRT^{82B} stat92E^{06346} / tub-Gal4, FRT^{82B} tub-Gal80.

y, w, hsFLP, UAS-GFP / w, UAS-N^{RNAi}; +; FRT^{82B} stat92E^{06346} / tub-Gal4, FRT^{82B} tub-Gal80.

Figure 2.4:

y, w, hsFLP, UAS-GFP / w; esg^{K606} / +; FRT^{82B} hsπM / tub-Gal4, FRT^{82B} tub-Gal80.

y, w, hsFLP, UAS-GFP / w; esg^{K606} / +; FRT^{82B} stat92E^{85C9} / tub-Gal4, FRT^{82B} tub-Gal80.

y, w, hsFLP, UAS-GFP / w; +; FRT^{82B} stat92E^{85C9} / tub-Gal4, FRT^{82B} tub-Gal80.

Figure 2.5 and S2.4:

y, w, hsFLP, UAS-GFP / w; +; FRT^{82B} hsπM / tub-Gal4, FRT^{82B} tub-Gal80.

y, w, hsFLP, UAS-GFP / w; UAS-Dl / +; FRT^{82B} hsπM / tub-Gal4, FRT^{82B} tub-Gal80.

y, w, hsFLP, UAS-GFP / w; UAS-Dl / +; FRT^{82B} stat92E^{85C9} / tub-Gal4, FRT^{82B} tub-Gal80.

y, w, hsFLP, UAS-GFP / w; UAS-N^{intra} / +; FRT^{82B} hsπM / tub-Gal4, FRT^{82B} tub-Gal80.

y, w, hsFLP, UAS-GFP / w; UAS-N^{intra} / +; FRT^{82B} stat92E^{85C9} / tub-Gal4, FRT^{82B} tub-Gal80.

ry^{506}, p[GBE+Su(H)m8,ry+, lacZ]

Figure 2.6:

w, tub-GAL80, hsFLP FRT^{19A} / N^{55e11} FRT^{19A}; UAS-lacZ^{nuc}, UAS-mCD8GFP / +; tub-GAL4 / +.

y, w, hsFLP, UAS-GFP / w, UAS-N^{RNAi}; +; FRT^{82B} hsπM / tub-Gal4, FRT^{82B} tub-Gal80.

y, w, hsFLP, UAS-GFP / w, UAS-N^{RNAi}; +; FRT^{82B} stat92E^{85C9} / tub-Gal4, FRT^{82B} tub-Gal80.

Figure 2.7:

y, w, hsFLP, UAS-GFP / w; +; FRT^{82B} hsπM / tub-Gal4, FRT^{82B} tub-Gal80.

w, tub-Gal80, hsFLP FRT^{19A} / hop^{C111} FRT^{19A}; UAS-lacZ^{nuc}, UAS-mCD8GFP / +; tub-Gal4 / +.

y, w, hsFLP, UAS-GFP / w; +; FRT^{82B} stat92E^{85C9} / tub-Gal4, FRT^{82B} tub-Gal80.

Figure 2.8:

w; esg-Gal4, UAS-GFP, tub-Gal80^{TS} / +.

w; esg-Gal4, UAS-GFP, tub-Gal80^{TS} / UAS-upd.

w; esg-Gal4, UAS-GFP, tub-Gal80^{TS} / +; UAS-N^{ECN} / +.

w; esg-Gal4, UAS-GFP, tub-Gal80^{TS} / UAS-upd; UAS-N^{ECN} / +.

y, w, hsFLP / w; AyGal4, UAS-GFP / UAS-upd.

y, w, hsFLP, UAS-GFP / y, w; UAS-hop^{Tum} / +; FRT^{82B} hsπM / tub-Gal4, FRT^{82B} tub-Gal80.

2.3.2 Mosaic analysis

Positively marked ISC lineages were generated using the MARCM system. MARCM clones were induced by placing experimental fly vials in a 37 °C water bath for 35-45 min. Induction protocols consisted of 2-3 heat pulses within a 24-h period and were performed within the first 5-10 days of adulthood. Expression of *UAS-upd* using the Flip-out technique was performed by subjecting experimental flies to a single 30 min heat shock within the first 5-10 days of adulthood (Fig. 2.8C,D).

2.3.3 Temperature shift experiments

Two different temperature shift analyses were performed in this study (Fig. 2.3A,B and Fig. 2.8A,B). In both cases, we established and cultured crosses at 18 °C until collection of F1 progeny. In the *stat92E*^{TS} analysis (Fig. 2.3A,B), we divided F1 progeny into two equal pools, maintaining controls at 18 °C and shifting the experimental group to 29 °C for 14 days. For the series of experiments shown in Fig. 2.8A and B, all F1 adult progeny were aged 4-7 days at 18 °C and were then shifted to 29 °C for 48 h prior to dissection.

2.3.4 Histology

Adult flies were dissected in 1x PBS (Sigma, USA). The gastrointestinal tract was removed and fixed in a final solution of 0.5x PBS (Sigma, USA) and 4% electron microscopy grade formaldehyde (Polysciences, USA) for a minimum of 30 min. Samples were washed in 1x PBS + 0.1% Triton-X100 (PBST) for 2 h, then incubated with primary antibodies overnight. Samples were washed in PBST for 2 h then incubated with secondary antibodies for 3 h. Finally, samples were washed in PBST overnight. Mounting media containing DAPI (Vectashield, USA) was added and samples were allowed to clear for 1 h prior to mounting. All steps were completed at 4 °C with no mechanical agitation.

2.3.5 BrdU incorporation experiments

Flies were aged for 4 weeks on standard media following clone induction and then transferred to BrdU media for 1 week. BrdU was administered *ad libitum* in *Drosophila* food media (200ul of 6 mg/ml BrdU in 20% sucrose per fresh vial). Dissected samples were fixed for 30 min at room temperature and then washed for 30 min at room temperature. DNA was denatured by applying a 2.2N solution of HCl to

samples for 30 min at room temperature followed by neutralization in Borax (100 mM) for 5 min and a final 30 min PBST wash. Samples were then stained as described above.

2.3.6 Antisera

Primary antibodies: Chicken anti-GFP (Abcam, USA) used at a dilution of 1:10,000; rabbit anti-β-Gal (Cappel, USA), 1:2000; mouse anti-β-Gal (Developmental Studies Hybridoma Bank; DSHB), 1:100; mouse anti-Pros (DSHB) 1:100; mouse anti-Dl (DSHB), 1:100; mouse anti-BrdU, 1:100; rabbit anti-Pdm-1 (gift of W. Chia (Yeo et al., 1995)),1:1000; rabbit anti-pHH3 (Upstate), 1:1000.

Secondary antibodies: Goat anti-chicken Alexa 488 (Molecular Probes, USA) used at a dilution of 1:2000; goat anti-mouse Alexa 568 (Molecular Probes, USA), 1:2000; goat anti-mouse Alexa 633 (Molecular Probes, USA), 1:2000; goat anti-rabbit Alexa 488 (Molecular Probes, USA), 1:2000; goat anti-rabbit Alexa 568 (Molecular Probes, USA), 1:2000.

Mounting media: Vectashield + DAPI mounting media (Vector, USA).

2.3.7 Microscopy and imaging

Samples were examined on a Leica DM5000 upright fluorescent microscope. Confocal images were collected using a Leica TCS SP5 confocal microscope system. Images were processed for brightness and contrast and assembled in Photoshop CS (Adobe, USA).

2.3.8 Measurements, cell counts and statistical analysis

Maximum nuclear diameter was measured in both anterior and posterior midgut frames at 40x magnification (A2.5 and P2.5; see (Lee et al., 2009) for additional information on midgut nomenclature) using the Leica Application Suite (LAS; Fig. 2.3E). We scored the number of $Pros^{+}$ or $Pdm1^{+}$ cells in both anterior and posterior midgut frames 5 days following clone induction (Fig. 2.4, Fig. 2.5 and Fig. 2.6). The number of GFP^{+} cells per frame was quantified in both the anterior and posterior midgut at 5, 10 and 20 days following clone induction (Fig. 2.7G and Supplemental Fig. S2.5E). In the experiments described above, we counted cells on the top surface of the midgut and excluded cells along the side and bottom surfaces. Combined data for anterior and posterior regions are displayed (Fig. 2.3, Fig. 2.7 and Supplemental Fig. S2.5E). To determine the number of dividing cells following UAS transgene activation, we counted the number of GFP^{+} $pHH3^{+}$ cells along the entire length of the midgut 48 h after temperature shift (Fig. 2.8B). The number of GFP^{-}, $Pros^{-}$ small cells was quantified in both anterior and posterior 40x frames and combined (Supplemental Figs. 2.5E,B). The number of GFP^{-}, $pHH3^{+}$ small cells was counted for the entire length of the midgut (Supplemental Fig. S2.2C). All *t*-tests were performed using Prism (GraphPad Software, USA); significance was tested at the 95% CI.

2.4 Results

2.4.1 *J*AK/STAT signaling is dynamically regulated in the midgut

JAK/STAT activation in the midgut was examined using a transcriptional reporter for pathway activation (Bach et al., 2007). The reporter, *10xSTAT92E-GFP*, is composed of multimerized Stat92E consensus binding sites fused to GFP, which is expressed in a manner that recapitulates the tissue specific distribution of Stat92E protein. Moreover, JAK/STAT signaling is both necessary and sufficient for

the activation of this reporter (Bach et al., 2007). Thus, *10xSTAT92E-GFP* functions as a high fidelity reporter for JAK/STAT activity *in vivo*.

Examination of the adult midgut revealed the presence of numerous *10xSTAT92E-GFP* positive cells with small nuclei distributed along the entire anterior-posterior axis of the tissue (52/52 midguts analyzed). Previous analysis has shown that *esg* marks both individual ISCs and their undifferentiated EB daughters, which can often be detected as pairs of cells or "doublets" in the midgut (Micchelli and Perrimon, 2006). Thus, *esg* distinguishes the undifferentiated cells of the ISC lineage from differentiated EE and EC cells. To determine the precise identity of the cells expressing the JAK/STAT reporter, we double labeled the midgut to reveal the distribution of *esg-lacZ* and the *10xSTAT92E-GFP* reporter. Double staining showed complete marker coexpression, suggesting that the JAK/STAT signal is transduced in both the ISC and EB (Fig. 2.2A). It has also been shown that elevated Dl protein levels mark a subset of midgut ISCs (Ohlstein and Spradling, 2007). Consistently, double staining of *Dl-lacZ* and *10xSTAT92E-GFP* also showed colocalization of these reporters in ISCs (Fig. 2.2B).

We next asked if JAK/STAT pathway activation could be detected in the differentiated cells of the ISC lineage. Staining for Pros protein, a marker for differentiated EE cells, revealed an inverse correlation with the *10xSTAT92E-GFP* reporter (Fig. 2.2C). Similarly, EC cells characterized by their large polyploid nuclei and positive staining for Pdm1 also did not detectably express *10xSTAT92E-GFP* (Fig. 2.2D). Taken together these expression studies suggest that JAK/STAT signaling is transduced primarily in the ISCs and EB cells.

The observation that *10xSTAT92E-GFP* is expressed at elevated levels in both the ISCs and EB cells raised the possibility that the EB signal detected is due to GFP perdurance. To investigate this possibility, we examined a more sensitive reporter of JAK/STAT activity, *10XSTAT92E-GFP*$^{destabilized(D)}$ (Bach et al., 2007). Previous analysis has suggested that *Su(H)GBE-lacZ* marks nascent EB cells (Micchelli and Perrimon, 2006; Ohlstein and Spradling, 2007); EBs can often be identified morphologically by the presence of a flared cytoplasmic "foot" (e.g. Fig. 2.2A). To determine if *10xSTAT92E-GFP*^{D} is detectable in EB cells we crossed the reporter into a genetic background containing *Su(H)GBE-lacZ*. Double labeling revealed that *10xSTAT92E-GFP*^{D} and *Su(H)GBE-lacZ* are both expressed at elevated levels in EB cells (Fig. 2.2E,F). Importantly, detectable levels of *10xSTAT92E-GFP*^{D} reporter could also be observed in

Su(H)GBE-lacZ cells adjacent to ISCs with no detectable expression (Fig. 2.2F, inset). These findings suggest that the JAK/STAT reporter is active in the EB cell.

In marked contrast to the stable reporter line, lower levels of expression and a great degree of heterogeneity existed in*10xSTAT92E-GFP*^{D} reporter. We observed regional differences along the anterioposterior axis of the midgut as well as differences among ISC/EB pairs (Supplemental Fig. S2.1A,B; 50/50 midguts analyzed). In ISC/EB pairs that both expressed the reporter, ISC expression levels were often detectably lower than in the EB (Supplemental Fig. 2.1C,D). These patterns of activity differed among individual midguts analyzed and were observed with two independent destabilized transgenic strains indicating that variation was not due to transgene insertion site. Consistent with these findings, examination of *upd1 and upd3* reporters revealed detectable levels of both JAK/STAT ligands distributed throughout the midgut, although the extent of expression varied widely even among age-matched samples (Supplemental Fig. S2.1E-H). Together, these observations suggest that at baseline homeostasis, JAK/STAT signaling is dynamically regulated in the midgut at both the regional and cellular level.

2.4.2 JAK/STAT signaling is required in the ISC lineage

Characterization of *10xSTAT92E-GFP* transcriptional reporters suggested that the JAK/STAT pathway might have a function in the midgut. To directly test the functional requirement of JAK/STAT, the effects of partially reducing JAK/STAT signaling were examined using a temperature sensitive, hypomorphic allelic combination of *stat92E*, *stat92E*^{F} */ stat92E*^{06346} (referred to subsequently as *stat*^{TS}). The distribution of cell nuclei in *stat*^{TS} adults was examined in DAPI stained samples following a 14-day shift to the non-permissive temperature. In contrast to unshifted controls, *stat*^{TS} adults exhibited an aberrant midgut organization characterized by the presence of distinct multicellular clusters most prominent in the posterior midgut (Fig. 2.3A,B; 6/8 midguts analyzed). Moreover, cells within the cluster typically displayed a small nuclear morphology unlike that of differentiated EC cells. Such clusters appeared to be the product of individual ISCs, although this could not be verified due to the absence of a genetic lineage marker.

To examine the consequence of reducing JAK/STAT signaling from individual ISC lineages we conducted a mosaic analysis of the *stat92E*. Positively marked ISC lineages were generated in the adult midgut using the MARCM system (Lee and Luo, 1999) and identified on the basis of GFP expression 5 days after induction (Fig. 2.3C-E). In contrast to wild-type cell lineages, ISCs lacking *stat92E* produced lineages consisting of smaller cells with the clones themselves often appearing fragmented (compare Fig. 2.3C,D). Measurements of nuclear diameter indicated that daughter cells failed to attain the maximal nuclear size detected in wild-type lineages (Fig. 2.3E). ISC lineages lacking *hop* produced a similar phenotype (Fig. 2.3F). Together, this analysis suggests that JAK/STAT signaling is required for normal differentiation in the ISC lineage.

In our mosaic analysis, we occasionally observed that the overall organization of the midgut epithelium was disrupted. For example, regions of increased small cell number could be detected in heterozygous tissue (e.g. GFP^- cells in Fig. 2.3D) raising the possibility that an increased number of small cells exist in the genetic background used to generate clones. To address this possibility we quantified the number of small cells in uninduced wild-type and $stat92E^{85C9}$ midguts used in our mosaic analysis however, no significant difference was observed (Supplemental Fig. S2.2A). A second possible explanation is that $stat92E^{85C9}$ clones can exert a non-autonomous effect on the surrounding tissue. To examine this possibility we quantified the number of both GFP^- small cells and $pHH3^+$ cells in induced wild-type and $stat92E^{85C9}$ midguts and observed a significant increase in each measure (Supplemental Fig. S2.2B,C). Thus, the variation in the midgut epithelium we observe is not a result of genetic background but is consistent with a non-autonomous effect of *stat92E* clone induction.

2.4.3 JAK/STAT signaling is required for differentiation in the ISC lineage

Clone morphology suggested that ISC lineages unable to transduce the JAK/STAT signal fail to undergo normal multi-lineage differentiation. To more rigorously analyze cell fate in JAK/STAT mutant lineages, we examined a panel of molecular markers. In wild-type lineages *esg* is expressed in ISCs and EBs, but not in either of the two differentiated cell types of the midgut, the EE or EC cells (Fig. 2.4A; (Micchelli and Perrimon, 2006)). Examination of *esg-lacZ* expression in $stat92E^{85C9}$ lineages revealed that almost every cell present was esg^+ (Fig. 2.4B; 18/18 midguts analyzed), suggesting that EE and EC cells

had not differentiated. To test this directly, we examined the expression of *prospero* (*pros*) a marker of the EE cell population. Pros positive cells were rarely detectable within *stat92E*^{85C9} mutant lineages (Fig. 2.4C,D; 47/47 midguts examined; wild-type, *n*=8; *stat92E*^{85C9}, *n*=8). Differentiated EC cells are distinguished by their large, polyploid nuclei and are often Pdm1^{+}. Inspection of *stat92E*^{85C9} lineages revealed a reduction or absence of Pdm1 staining (Fig. 2.4E,F; 21/21 midguts examined; wild-type, *n*=8; *stat92E*^{85C9}, *n*=8). Taken together, these observations suggest that *stat92E* is required for differentiation of both EE and EC cells.

Analysis of marker gene expression suggested that multi-lineage differentiation does not occur in the absence of *stat92E*; to determine if ISCs were present in lineages lacking JAK/STAT signaling we examined the distribution of Dl protein. As in the case of wild-type lineages, Dl protein could be detected, suggesting that ISCs are present in the absence of JAK/STAT, however the level of expression often appeared to be reduced.

2.4.4 Dl is sufficient to specify EC cell fate

Prior studies indicate that Dl/N signaling is critical to correctly specify cell fate within the ISC lineage (Supplemental Fig. S2.4A; (Micchelli and Perrimon, 2006; Ohlstein and Spradling, 2006)). Therefore, we next performed an epistasis analysis to determine the relationship between JAK/STAT and Dl/N signaling in the ISC lineage. We first examined the consequences of expressing a wild-type *Dl* transgene (*Dl*^{wt}) in ISC lineages and followed cell fate in the resultant lineage. Here, we employ the MARCM system to trace the lineages of individual ISCs expressing *Dl*^{wt} for 5 days following induction. To assay cell fate, Pdm1 and nuclear size were used to identify EC cells, while Pros was used to identify EE cells. Interestingly, even in wild-type controls ISC lineages could frequently be observed that consisted entirely of EC cells and lacked Pros^{+} cells (Supplemental Fig. S2.4B). This trend is most pronounced in the anterior midgut; in the posterior, the majority of wild-type clones contained one or more Pros^{+} cells in addition to ECs (Supplemental Fig. S2.4D). These observations suggest that there are significant regional differences affecting cell fate in the ISC lineage.

To quantify the effect of *Dl*^{wt} expression in ISC lineages we scored the number of Pros^{+} cells in the lineage. In contrast to wild-type, ISC lineages expressing *Dl*^{wt} resulted in a significant decrease in the

number of clones containing Pros^{+} cells within the lineage (Supplemental Figs. S2.4C,D; wild-type, *n*=12; *Dl*^{wt}, *n*=12). In addition, staining with the EC marker Pdm1 suggested that ISCs expressing *Dl*^{wt} produce lineages consisting almost entirely of ECs (Fig. 2.5A,B; Supplemental Fig. 2.4E). These effects on cell fate were also observed in *Dl*^{wt} expressing clones analyzed 10 days after induction, suggesting that the reduction in Pros^{+} cells was not simply due to a delay in EE cell differentiation (Supplemental Fig. S2.4F). We note that at later time points, ISCs expressing *Dl*^{wt} also produced large clones that appeared to contain many undifferentiated cells, as they were negative for both Pros and Pdm1 (Supplemental Fig. S2.4F). Such cells appeared to most closely resemble ectopic ISCs or EBs, raising the possibility that Dl has an additional role in regulating ISC proliferation. Taken together, these findings demonstrate that *Dl*^{wt} is sufficient to specify EC cell fate at the expense of EE cells and supports a model in which ISCs signal non-autonomously to nascent EB cells to specify the EC cell fate (Micchelli and Perrimon, 2006; Ohlstein and Spradling, 2007).

2.4.5 JAK/STAT is epistatic to Dl/N signaling in multilineage differentiation

To determine if *stat92E* is required for Dl-mediated EC cell fate specification we conducted a mosaic analysis of ISC lineages expressing *Dl*^{wt} but lacking *stat92E*^{85C9} function. In contrast to *Dl*^{wt} expressing lineages alone, *Dl*^{wt}, *stat92E*^{85C9} lineages appeared to lack differentiated EC cells based on the reduced number of Pdm1^{+} cells and were virtually indistinguishable from *stat92E*^{85C9}mutants (compare Fig. 2.5B,C and Fig. 2.4E). Similar results were also obtained by analyzing a second allele, *stat92E*^{06346} (Supplemental Fig. S2.5C).

A quantitative analysis was performed to determine the effect of *stat92E*^{85C9} loss on *Dl*^{wt} expressing lineages by comparing the number of Pdm1^{+} cells present in *Dl*^{wt} lineages with the number of Pdm1^{+} cells present in *Dl*^{wt}, *stat92E*^{85C9} lineages. This analysis revealed a significant decrease in the number of Pdm1^{+} GFP^{+} cells in *Dl*^{wt}, *stat92E*^{85C9} lineages compared to *Dl*^{wt} alone (Fig. 2.5D; *Dl*^{wt}, *n*=12; *Dl*^{wt}, *stat92E*^{85C9}, *n*=12). Consistent with this finding, we observe that differentiated ECs induced by cell autonomous N activation were also blocked by the loss of *stat92E* (Fig. 2.5E,F; 29/29 midguts analyzed). Thus, although *stat92E* is required in the ISC for normal levels of Dl expression (Supplemental Fig. S2.3),

our epistasis analysis shows that *stat92E* is also necessary for EC differentiation in the presence of Dl/N signaling.

We next sought to extend the epistasis analysis to determine the requirement for JAK/STAT in differentiation of EE cells. Previous analysis has demonstrated that ISC lineages lacking *N* generate two phenotypic classes, clones that appear to be comprised of ectopic ISCs and clones that appear to be comprised of ectopic EE cells (Fig. 2.6A; (Ohlstein and Spradling, 2006)). To test whether JAK/STAT signaling is required for EE differentiation, we asked if the production of $Pros^{+}$ EE cells present in N mutant lineages depends on the JAK/STAT signaling pathway. To test this requirement, genetic mosaics were created in which both N and *stat92E* functions were reduced. In contrast to N^{RNAi}, mosaic analysis of N^{RNAi}, $stat92E^{85C9}$ clones revealed a reduction in EE cells (Fig. 2.6B,C; 30/30 midguts examined). Similar results were obtained by analyzing a second hypomorphic allele, $stat92E^{06346}$ (Supplemental Fig. S2.5D).

A quantitative analysis was performed to determine the effect of $stat92E^{85C9}$ loss on N^{RNAi} expressing lineages. This analysis revealed a significant decrease in the number of $Pros^{+}$ GFP^{+} cells in N^{RNAi}, $stat92E^{85C9}$ lineages compared to N^{RNAi} alone (Fig. 2.6D; N^{RNAi}, n=8; N^{RNAi}, $stat92E^{85C9}$, n=8). Thus, the transcription factor encoded by *stat92E* is required downstream or in parallel to *N*, suggesting that *stat92E* is also required in EB cells for EE differentiation.

2.4.6 Little evidence that JAK/STAT signaling is required for ISC self-renewal

Analysis of the *10xSTAT92E-GFP* transcriptional reporters revealed detectable expression in ISCs (Fig. 2.2A,B), suggesting that JAK/STAT signaling might also have a function in the ISC. Studies of *Drosophila* germline stem cells first employed a genetic lineage-tracing assay to measure stem cell self-renewal (Margolis and Spradling, 1995). A pulse/chase design was used to determine the number of marked stem cell lineages retained in the midgut at defined times following induction. To determine if JAK/STAT signaling is required for ISC self-renewal we generated labeled ISCs lacking components of the JAK/STAT signaling pathway and analyzed the lineages at 5, 10, and 20 days after induction. In controls, wild-type lineages could be detected in the midgut throughout the chase interval. Similarly, in hop^{C111} and $stat92E^{85C9}$ mutants, marked lineages were detectable in the midgut 20 days after induction (Fig. 2.7A-F).

A quantitative analysis was performed to examine the effect of JAK/STAT loss on ISC self-renewal. As noted above, loss of JAK/STAT signaling often results in a distinct clonal morphology and the inability to unambiguously identify individual clones (e.g. Fig. 2.3D,F). As such, clone number is not a suitable measure of ISC number in the JAK/STAT mutants we examined. Therefore, to approximate the number of ISCs we scored the number of GFP^+ daughter cells in defined regions of each sample. Quantification of the pulse/chase studies showed that reductions in hop^{C111}, $stat92E^{85C9}$, or $stat92E^{06346}$ were associated with the retention of 67%, 22% or 31% of labeled cells, respectively, at 20 days after induction (*n*=12; Fig. 2.7G, Supplemental Fig. 2.5E). In addition, we observed that hop^{C111} and $stat92E^{85C9}$ lineages could be identified at late time points that stained positively for both pHH3 and BrdU, suggesting that JAK/STAT is not absolutely required for ISC proliferation (Fig. 2.7B,D,F and Supplemental Fig. S2.6D,E). We also note that hyperplastic *stat92E* clones could be detected at late time points suggesting that JAK/STAT may be a necessary modulator of ISC proliferation (Supplemental Fig. S2.6A-C). Taken together these data suggest that ISC self-renewal is not grossly disrupted in the absence of JAK/STAT signaling.

2.4.7 The JAK/STAT pathway promotes ISC proliferation

To determine if the levels of JAK/STAT signaling affect the ISC lineage, we examined the consequences of pathway activation in the midgut. Using conditional Gal4 induction in *esg+* cells (esg^{TS}), we first examined the effect of expressing the JAK/STAT ligand *upd* on the number of $pHH3^+$ cells 2 days after induction. Quantification revealed a significant increase in the number pHH3+ cells following *upd* expression, compared to both wild-type controls and the expression of a dominant negative form of *N* (*n*=18; Fig. 2.8A,B). The effect of *upd* expression on proliferation was enhanced by simultaneous expression of a dominant negative form of *N*, as would be predicted if Upd acts directly on ISCs to stimulate proliferation (*n*=18; Fig. 2.8B). Similar increases in $pHH3^+$ were obtained when *upd* was expressed using the Flip-out (F/O) technique (27/27 midguts examined; Fig. 2.8C). However, in addition to the increase in $pHH3^+$ cells, we also observed many cells that appeared to be in the process of delaminating from the midgut epithelium (Fig. 2.8D). Finally, using the MARCM system we generated ISC lineages expressing constitutively active hop^{Tum} (Harrison et al., 1995); such clones were rapidly lost from the midgut (7/7 midguts examined; Fig. 2.8E,F). Thus, activation of JAK/STAT signaling promotes ISC

proliferation in the midgut, although this response may depend on the precise level and cell types in which the pathway is activated

2.5 Discussion

2.5.1 Stem cells, JAK/STAT and self-renewal

A series of studies have addressed the requirement of JAK/STAT signaling for stem cell self-renewal in distinct *Drosophila* stem cell populations. For instance, male germline stem cells (GSCs) are arrayed in rosette like pattern around a focus of "hub" cells situated at the apical tip of the testis. Hub cells are a source of Upd ligand; GSCs lacking the ability to transduce the JAK/STAT signal are detectably reduced by 5 days and completely lost after 9 days. In contrast, misexpression of the Upd ligand increases the number of GSC like cells in the testis and mitigates GSC loss at the hub (Boyle et al., 2007; Kiger et al., 2001; Tulina and Matunis, 2001). Thus, JAK/STAT functions as a signal for GSC self-renewal. The rapid failure of stem cell self-renewal and concomitant depletion of the stem cell compartment following loss of JAK/STAT has subsequently been reported for female GSCs, cyst progenitor cells (CPCs), follicle stem cells (FSCs), and renal stem cells (RNSCs) (Decotto and Spradling, 2005; Kiger et al., 2001; Singh et al., 2007; Tulina and Matunis, 2001). Thus, the theme that has emerged is that JAK/STAT signaling is generally required for *Drosophila* stem cell self-renewal.

Our studies have revealed an exception to this generalization. Here, we examined the consequences of JAK/STAT loss in the midgut up to 20 days following induction (~40% of the fly lifetime), at which point marked ISC lineages were still detected. Consistently, BrdU and pHH3 staining suggested that ISCs were still capable of dividing up to 5 weeks in the absence of JAK/STAT signaling. Finally, very large *stat92E* clones could occasionally be detected in the midgut. Taken together, these findings are not consistent with a requirement for JAK/STAT in ISC self-renewal. We note that our studies differed from the aforementioned in one respect, experimental limitations prevented us from unambiguously identifying individual ISC lineages. Therefore the number of stem cell progeny at each time point was scored, to infer the presence of stem cells. While these experiments do not rule out a requirement for JAK/STAT in long term ISC maintenance, they provide little evidence that JAK/STAT signaling is required for ISC self-renewal.

2.5.2 JAK/STAT coordinates competence to undergo multi-lineage differentiation and ISC proliferation

Two lines of evidence support a role for JAK/STAT signaling in multi-lineage differentiation of ISC daughters. First, a synthetic JAK/STAT transcriptional reporter is expressed throughout the midgut; coexpression studies demonstrate that JAK/STAT signaling occurs in *Su(H)GBE-lacZ*$^{+}$ cells, a marker for undifferentiated EB daughter cells. In addition, we observe JAK/STAT reporter expression in daughters adjacent to ISCs, which have no detectable JAK/STAT reporter expression themselves, suggesting this is not due to GFP perdurance. Second, reductions or loss of the JAK/STAT signaling pathway in marked ISC lineages leads to morphologically aberrant clones with reduced nuclear diameter, and the production of cells that lack molecular markers of either differentiated EE or EC cell types. Given this requirement of JAK/STAT signaling for both EE and EC cell differentiation, we might predict that activation of the JAK/STAT pathway would not be sufficient to affect cell fate. Consistently, analysis of ISC lineages in which JAK/STAT signaling is constitutively active was found to have no discernible effect on fate. Thus, JAK/STAT signaling is necessary but not sufficient for cell fate specification of ISC daughters. As such, we conclude that JAK/STAT signaling is necessary to establish competence for EBs to undergo multi-lineage differentiation.

In addition to the requirement for JAK/STAT in ISC daughters, our studies demonstrate that JAK/STAT signaling is a potent regulator of ISC proliferation. First, co-labeling studies with transcriptional reporters indicated that JAK/STAT signaling is activated in cells that express ISC marker genes. Second, ectopic expression of Upd ligand resulted in a rapid increase in proliferation throughout the midgut. Third, the effect of Upd on proliferation was enhanced under conditions in which N signaling was simultaneously reduced, suggesting that *upd* is sufficient to directly stimulate ISC proliferation. Our analysis suggests that JAK/STAT signaling may also be necessary to regulate the ISC proliferation, perhaps via both canonical and non-canonical pathways (e.g. Fig. 2.7A,C,E; Supplemental Fig. S2.6A-C). Thus, JAK/STAT signaling has dual, yet separable roles in the ISCs and their immediate daughters. On the basis of these findings, we suggest a model in which JAK/STAT signaling coordinates the processes of stem cell proliferation with the competence of daughter cells to undergo multi-lineage differentiation, ensuring a rapid and

robust cellular output in the lineage (Supplemental Fig. S2.7). JAK/STAT mediated gaiting of proliferation and differentiation may be particularly important in the midgut where ISCs and their undifferentiated daughters are typically found in a poised, “doublet” configuration. These conclusions are in general agreement with recent reports (Jiang et al., 2009).

2.5.3 N and JAK/STAT signaling pathways interact to regulate the ISC lineage

We have conducted genetic epistasis experiments to determine the nature of the interaction between Dl/N signaling and the JAK/STAT signaling pathway in the ISC lineage. Our experiments show that while JAK/STAT is required for wild-type levels of Dl expression in the ISC, the requirement for JAK/STAT in EB differentiation is independent of Dl/N signaling. This observation suggests that JAK/STAT functions downstream or in parallel with Dl to establish competence of EBs to undergo differentiation. Recent studies, however, suggest a different relationship. Studies of midgut regeneration show that Dl ligand is strongly induced in ISCs following Upd ligand expression, directed epithelial cell ablation or bacterial infection (Buchon et al., 2009; Jiang et al., 2009). These studies suggest that under conditions of adaptive homeostasis, Upd ligands are produced in gut epithelial cells and activate Dl in ISCs to promote new cell production. Consistent with this model, we observe that expression of Dl leads to an increase in the size of ISC lineages, suggesting a potential role for Dl in promoting ISC proliferation. Thus, there is evidence that JAK/STAT signaling functions both upstream and downstream of Dl/N in the ISC lineage.

2.5.4 Regulation of Upd ligands at baseline and adaptive homeostasis

At baseline homeostasis, the most distinctive feature of Upd ligand expression that we observe is heterogeneity among age-matched samples. Prior studies show that Upd ligands are strongly induced following bacterial infection, directed cell ablation, or stress signaling (Buchon et al., 2009; Cronin et al., 2009; Jiang et al., 2009). It remains an open question as to whether Upd ligand expression and associated JAK/STAT activity that we report here is a direct manifestation of midgut stress, albeit to a lesser extent in unchallenged animals, or if there is a distinct regulation of Upd ligands under baseline homeostasis. Previous studies indicate that apoptosis and stress signaling are both detectable in the adult midgut at baseline homeostasis (Biteau et al., 2008; Ohlstein and Spradling, 2006). Studies of

antimicrobial peptide reporters, which serve as markers of infection, indicate a limited signal in the adult midgut (Tzou et al., 2000). Nonetheless, a degree of infection undetectable by such reporters under conditions of laboratory culture is possible. If activation of Upd ligands is exclusively regulated in response to exogenous factors this would provide an efficient means of coupling the ISC proliferative response to the magnitude, duration and location of the stimulus. However, in this view one might predict that the additive effects of locally generated stress in the midgut under normal circumstances would, over time, lead to a distortion of tissue architecture. On the other hand, if there is also a distinct regulation of Upd ligands under baseline homeostasis, this might contribute to a stereotyped mode of growth control and tissue homeostasis, in conjunction with other signals known to regulate ISC proliferation (Lee et al., 2009; Lin et al., 2008). Such models are not mutually exclusive. Future experiments, which clarify the precise mechanisms of Upd ligand regulation will provide important insights into the control of the ISC lineage under a broad range of biological conditions.

2.6 Figures

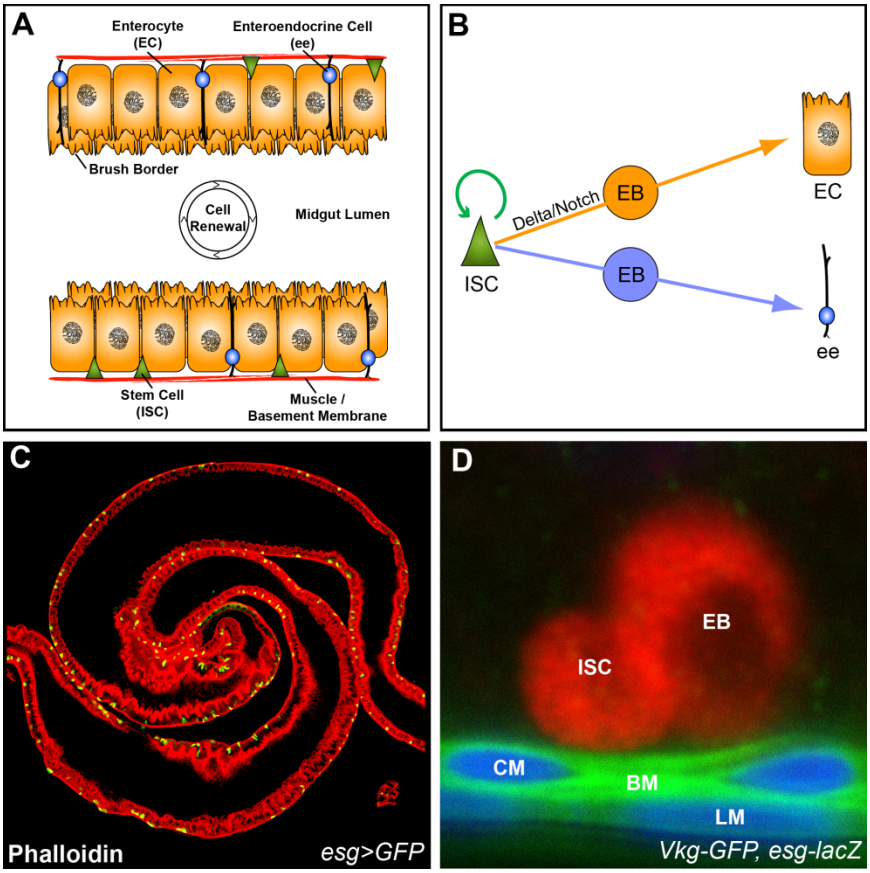

Figure 2.1: The adult *Drosophila* midgut is maintained by a population of multipotent intestinal stem cells (ISCs). (A) Diagram of the adult midgut in cross section. ISCs (green) occupy an epithelial niche adjacent to the basement membrane and the visceral muscle (red). ISCs give rise to two types of differentiated daughters, enteroendocrine (ee) cells (blue) and enterocytes (ECs; orange). (B) A model of ISC division; the ISC undergoes self-renewal and generates a daughter cell or enteroblast (EB), which can become either an EE or an EC cell. Specification of the EC cell fate requires *N* signaling. (C, D) All micrographs display superficial views of the midgut, except where indicated. (C) Low magnification view in cross section; *esg* > *GFP* (green) and phalloidin (red). (D) High magnification view of midgut in cross section showing a newly divided ISC; *vkg-GFP* (green), *esg-lacZ* (red) and phalloidin (blue). CM (circumferential muscle), LM (longitudinal muscle), BM (basement membrane).

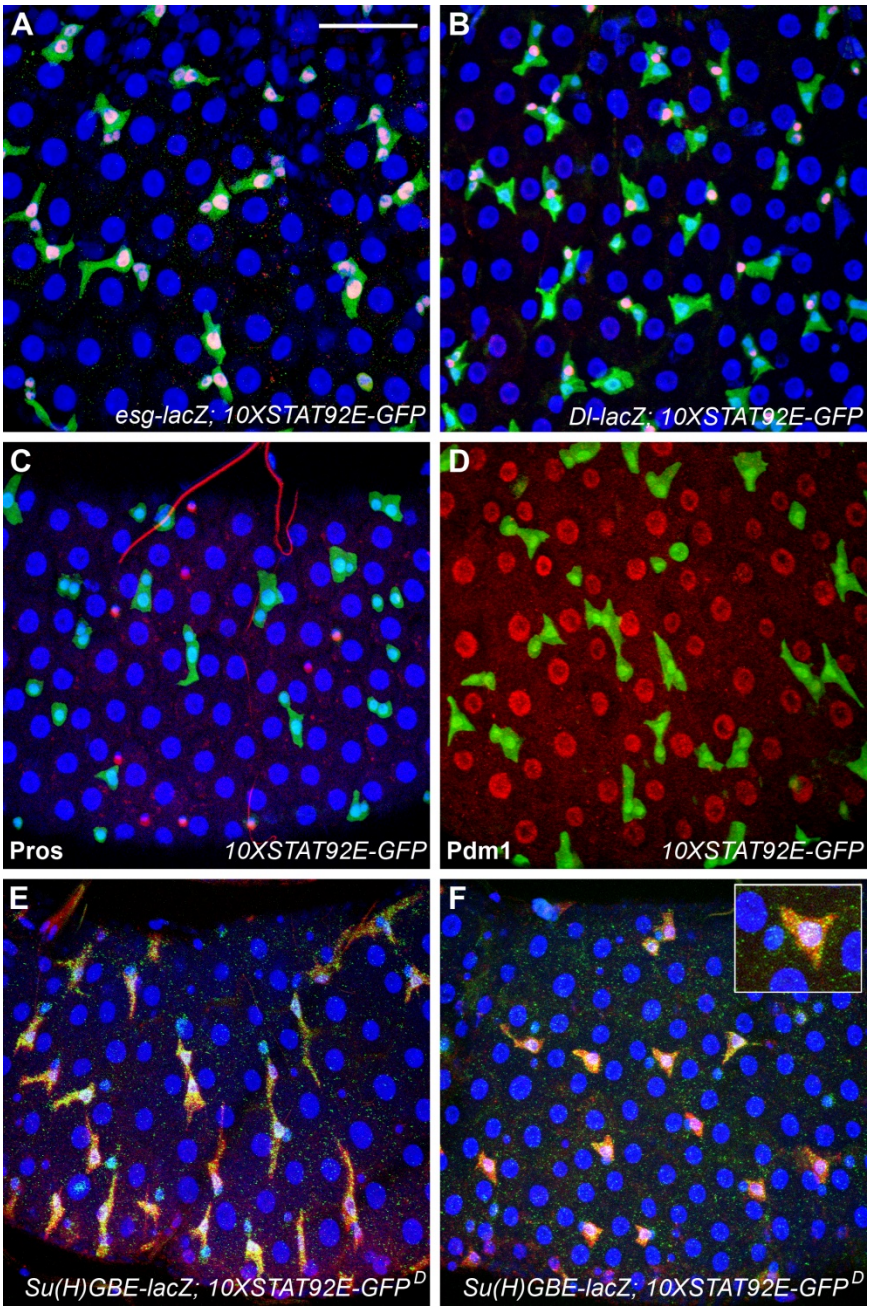

Figure 2.2: JAK/STAT signaling is dynamically regulated in midgut ISCs and EBs. (A-F) Characterizing transcriptional reporters of JAK/STAT activity in the midgut (green); nuclei are counterstained with DAPI (blue), except in D. (A-D) *10xSTAT92E-GFP* reporter with stable GFP. (A) ISC and EB cells (*esg-lacZ*; red) express the *10xSTAT92E-GFP* reporter. (B) ISCs (*Dl-lacZ*; red) express the *10xSTAT92E-GFP* reporter. (C) Differentiated EE cells are marked with anti-Pros (red). (D) Differentiated EC cells are marked with anti-Pdm1 (red). (E, F) *10xSTAT92E-GFP^{D}* reports expression of a destabilized

GFP. EB cells (*Su(H)GBE-lacZ*, red). (E) ISC and EB cells express the destabilized reporter. (F) EBs expressing the destabilized reporter adjacent to ISCs with no detectable expression. High magnification, insert. Scale bar: 50 μm.

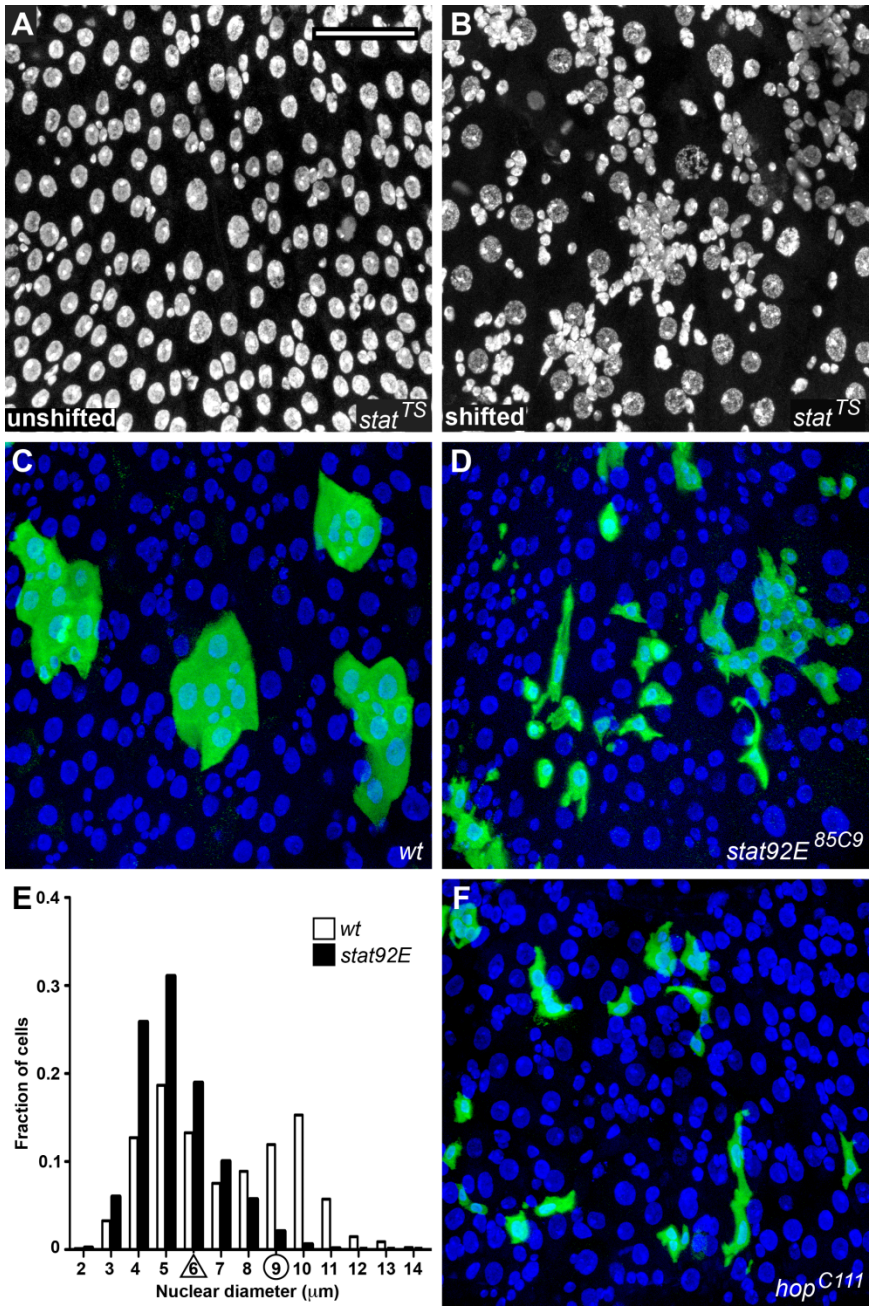

Figure 2.3: JAK/STAT signaling is required in the ISC lineage. (A, B) *stat92E* temperature shift analysis, nuclei (DAPI, grayscale). (A) *stat92E*^{TS}, unshifted controls. (B) *stat92E*^{TS}, shifted to non-permissive temperature for 14 days. Global reduction of *stat92E* leads to the formation of clusters of small cells in the midgut. (C-F) The MARCM system was used to positively identify ISC lineages with GFP 5 days after induction (anti-GFP, green; DAPI, blue). (C) Wild-type ISC lineages. (D) ISC lineages lacking *stat92E*. Loss of *stat92E* leads to generation of cells with abnormal clonal morphology and reduced

nuclear size. (E) Quantification of nuclear size. Histogram displays the distribution of nuclear size in wild-type (white) and *stat92E* lineages (black). *stat92E* mutant lineages fail to generate cells of the larger nuclear size classes. The average nuclear size of wild-type EB cells (*Su(H)GBE-lacZ*) is indicated by a triangle; the average nuclear size of wild-type EC cells (anti-Pdm1) is indicated by a circle. (F) ISC lineages lacking *hop* resemble those lacking *stat92E*. We note that many of the cells detected in *stat92E* and *hop* mutant lineages exhibited the cytoplasmic foot characteristic of EB cells. Scale bar: 50 μm.

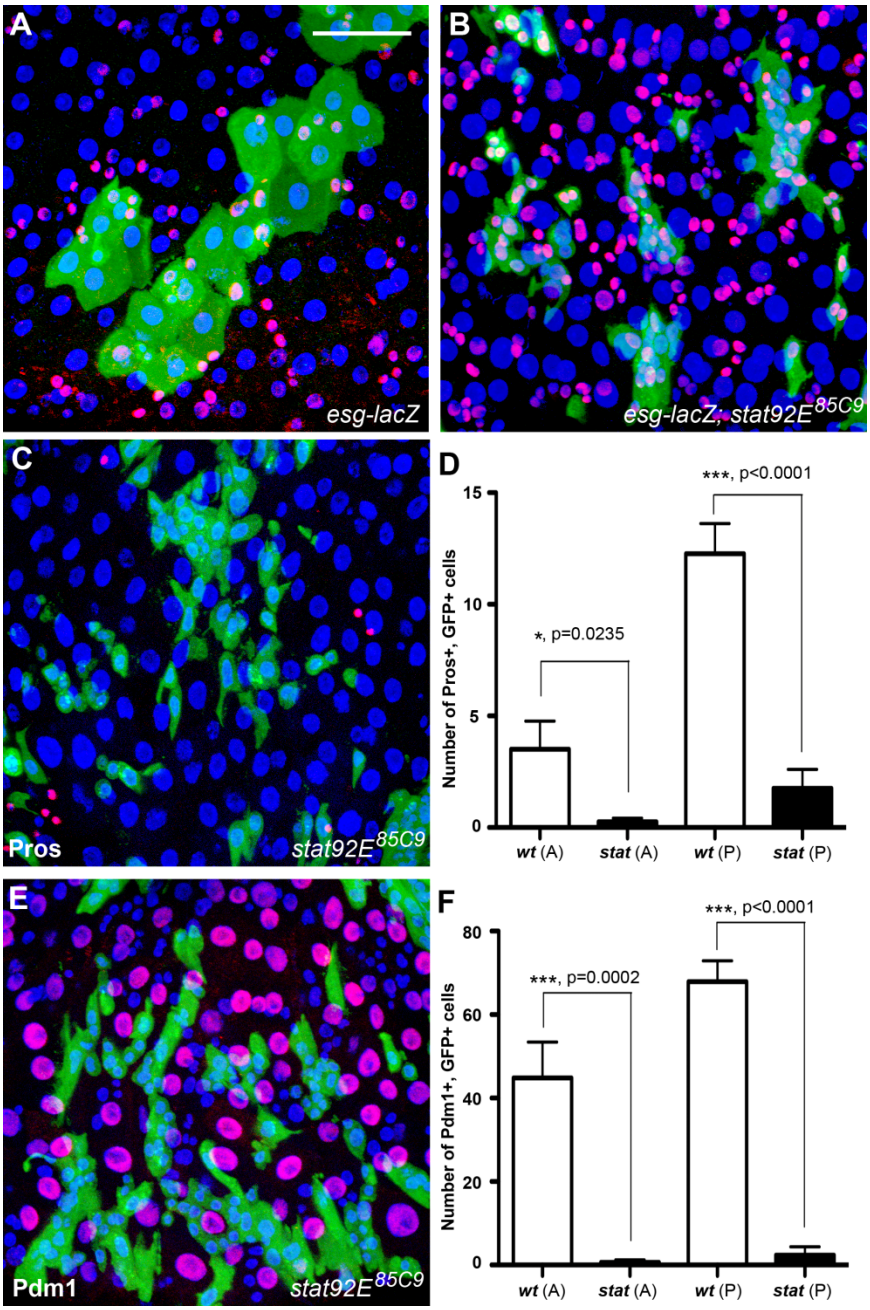

Figure 2.4: *stat92E* is required for multi-lineage differentiation. (A–F) The MARCM system was used to positively identify ISC lineages with GFP 5 days following induction. (anti-GFP, green; DAPI, blue). (A) Wild-type ISC lineages contain *esg-lacZ* positive and negative cells (anti-βgal, red). (B) ISC lineages lacking *stat92E* have an increased number of *esg-lacZ*$^{+}$ cells and a decreased number of *esg-lacZ*$^{-}$ cells (anti-βgal, red). (C, D) *stat92E*^{85C9} mutant lineages have a significantly reduced number of Pros^{+} cells in both the anterior (A) and posterior (P) midgut. (C) Representative micrograph. (D) Quantification (*n*=8;

anti-Pros, red). (E, F) *stat92E*^{85C9} mutant lineages have a significantly reduced number of Pdm1^{+} cells in both the anterior (A) and posterior (P) midgut. (E) Representative micrograph. (F) Quantification (*n*=8; anti-Pdm1, red). Error bars denote s.e.m. Scale bar: 50 μm.

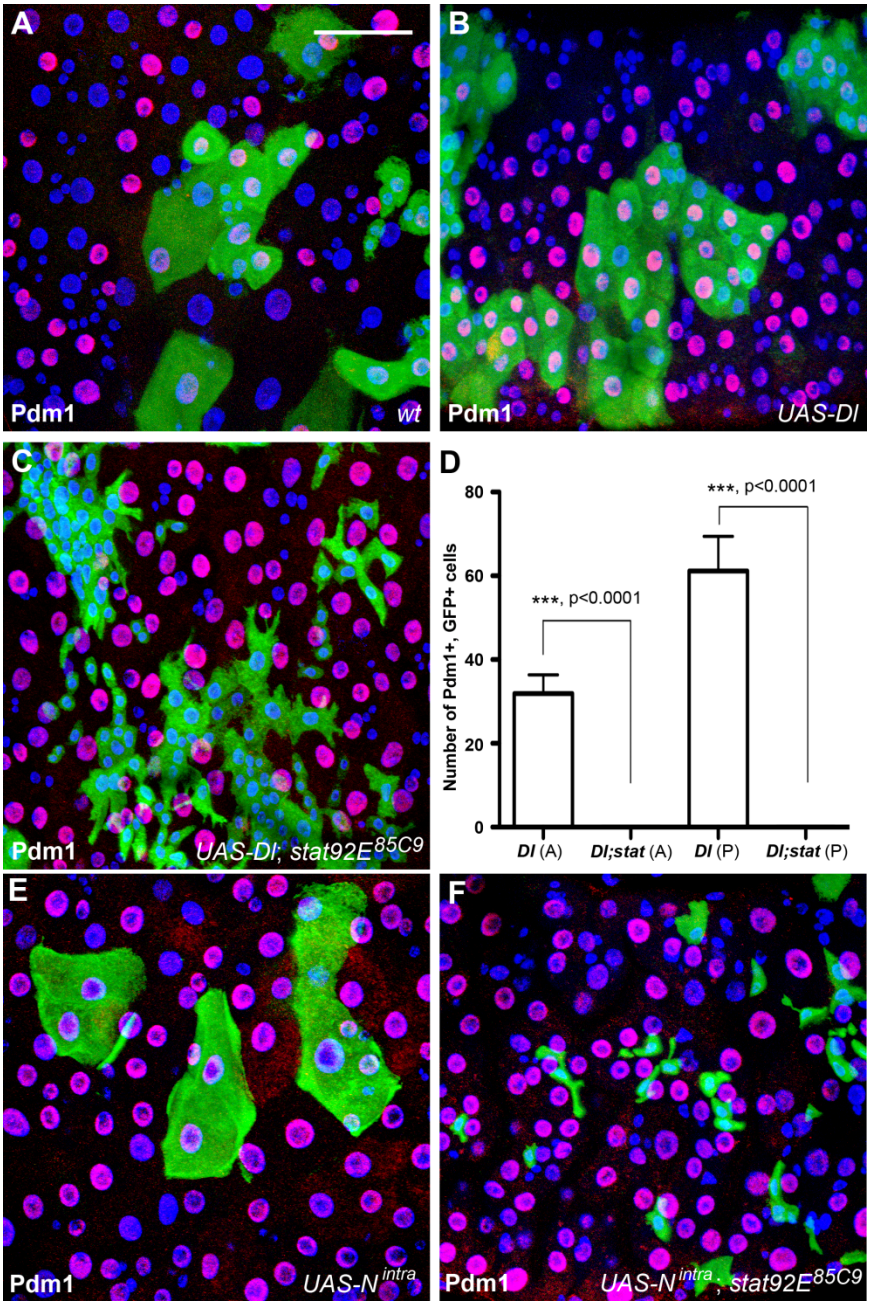

Figure 2.5: *stat92E* is epistatic to Dl/N signaling for EC specification. (A–F) The MARCM system was used to positively identify ISC cell lineages with GFP 5 days following induction (anti-GFP, green; DAPI, blue). (A) Wild-type ISC lineages generate EC cells distinguished by large cell morphology and are often Pdm1^{+} (anti-Pdm1, red). (B) ISC lineages expressing Dl^{wt} generate lineages enriched for EC cells (anti-Pdm1, red). (C) ISC lineages expressing Dl^{wt} and lacking *stat92E* display the $stat92E^{85C9}$phenotype. (D) Quantification of the number of Pdm1^{+} cells in Dl^{wt} and Dl^{wt}; $stat92E^{85C9}$ lineages in both the anterior (A) and posterior (P) midgut. (E) ISC lineages expressing N^{intra} generate ECs. (F) ISC lineages expressing

N^{intra} and lacking $stat92E^{85C9}$ display the $stat92E^{85C9}$phenotype. Error bars denote s.e.m. Scale bar: 50 μm.

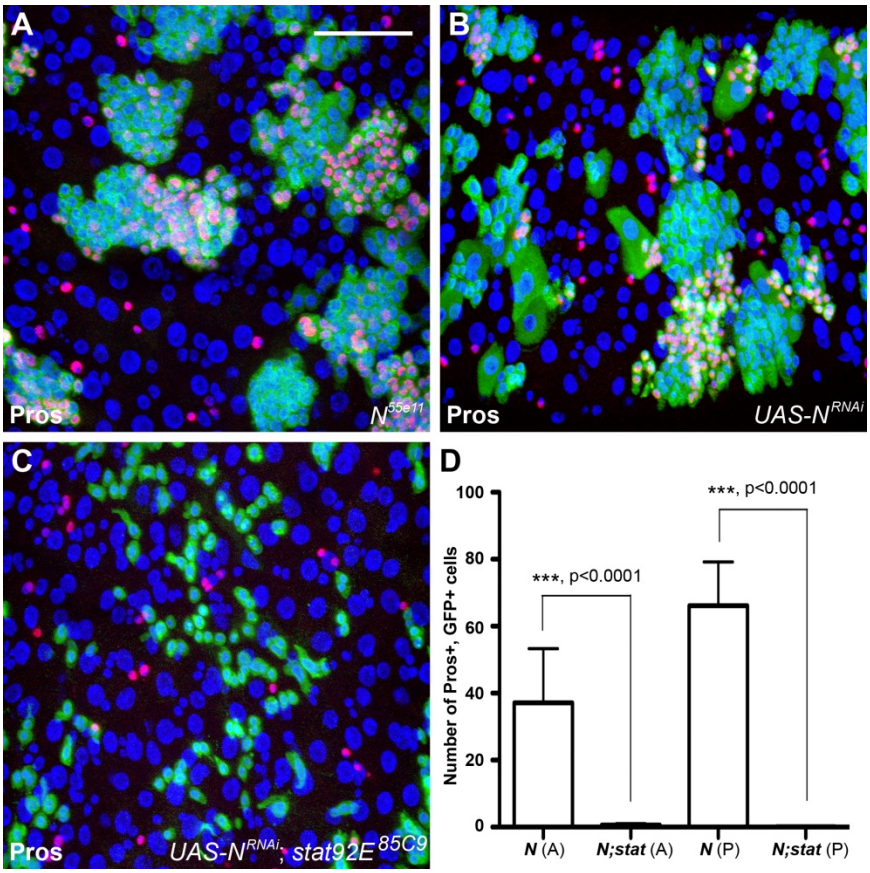

Figure 2.6: *stat92E* is epistatic to Dl/N signaling for EE specification. (A–D) The MARCM system was used to positively identify ISC lineages with GFP 5 days following induction (anti-GFP, green; anti-Pros, red; DAPI, blue). (A) ISC clones lacking *N* generate clusters of $Pros^{+}$ and $Pros^{-}$ cells. (B) ISC clones expressing N^{RNAi} generate clusters of $Pros^{+}$ and $Pros^{-}$ cells. Note the presence of some ECs at early time points due to residual N activity. (C) ISC lineages expressing N^{RNAi} and lacking $stat92E^{85C9}$ resulted in a loss of the $Pros^{+}$ cells. The occasional ECs observed in the N^{RNAi} lineages were not observed in N^{RNAi}, $stat92E^{85C9}$ lineages. (D) Quantification. The number of Pros+ cells in N^{RNAi}, $stat92E^{85C9}$ lineages is significantly reduced in both the anterior (A) and posterior (P) midgut (n=8). Error bars denote s.e.m. Scale bar: 50 μm.

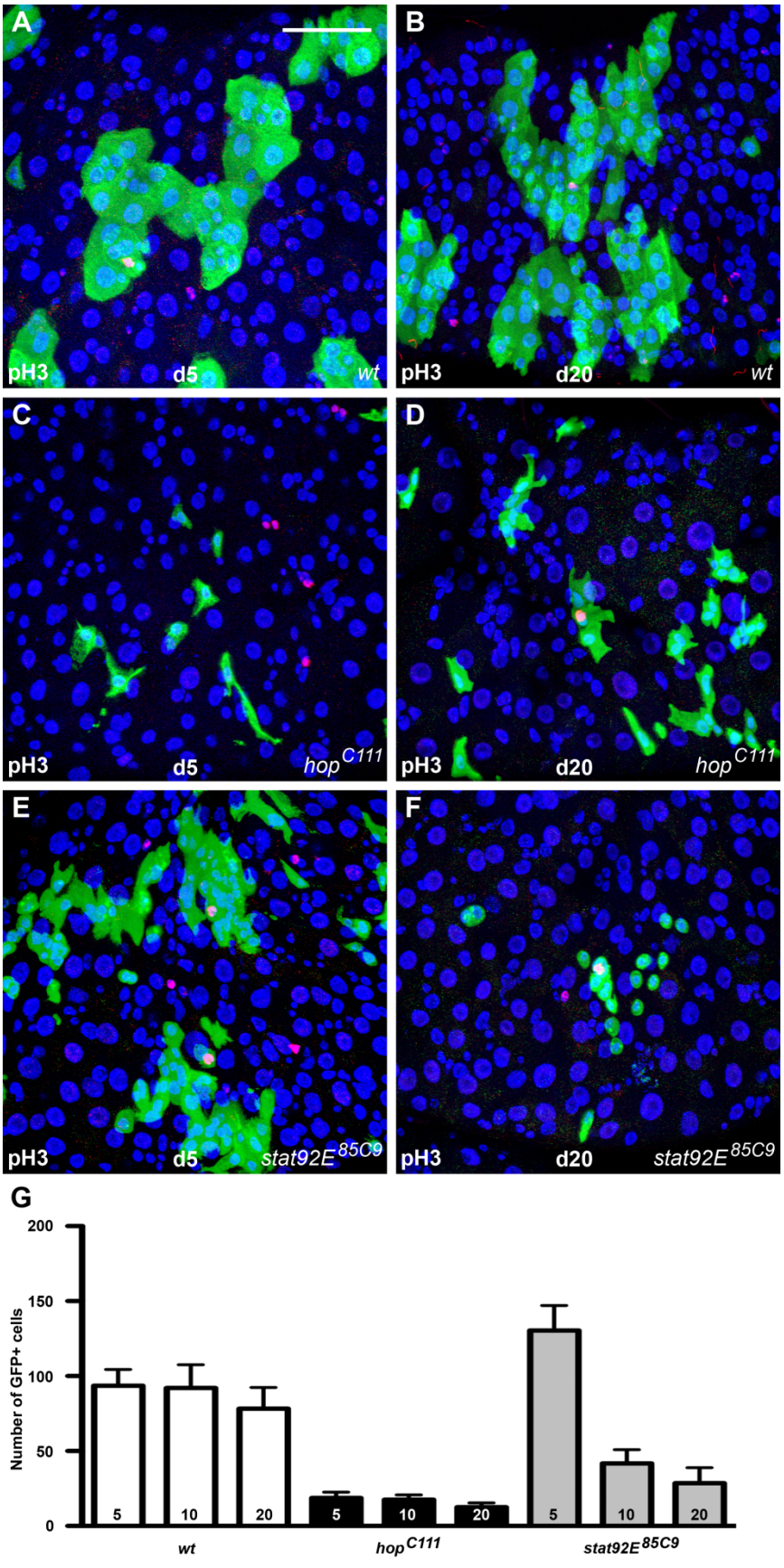
A
pH3
d5
wt
B
pH3
d20
wt
C
pH3
d5
hop C111
D
pH3
d20
hop C111
E
pH3
d5
stat92E 85C9
F
pH3
d20
stat92E 85C9
G
Number of GFP+ cells
200
150
100
50
0
5
10
20
5
10
20
5
10
20
wt
hop C111
stat92E 85C9

Figure 2.7: JAK/STAT is not required for ISC self-renewal. (A–G) The MARCM system was used to positively identify ISC lineages with GFP between 5 and 20 days after induction (anti-GFP, green; anti-pHH3, red; DAPI, blue). (A, C, E) 5 days after induction, (B, D, F) 20 days after induction. (A, B) Wild-type ISC lineages retain dividing ISCs. (C, D) ISC lineages lacking hop^{C111}. 20 days after induction hop^{C111} clones have detectable $pHH3^{+}$ expression. (B) ISC lineages lacking *stat92E*. 20 days after induction $stat92E^{85C9}$ clones have detectable $pHH3^{+}$ expression. (G) Wild-type, hop^{C111} and $stat92E^{85C9}$ mutant lineages are detectable in the midgut 20 days following induction. Error bars denote s.e.m. Scale bar: 50 μm.

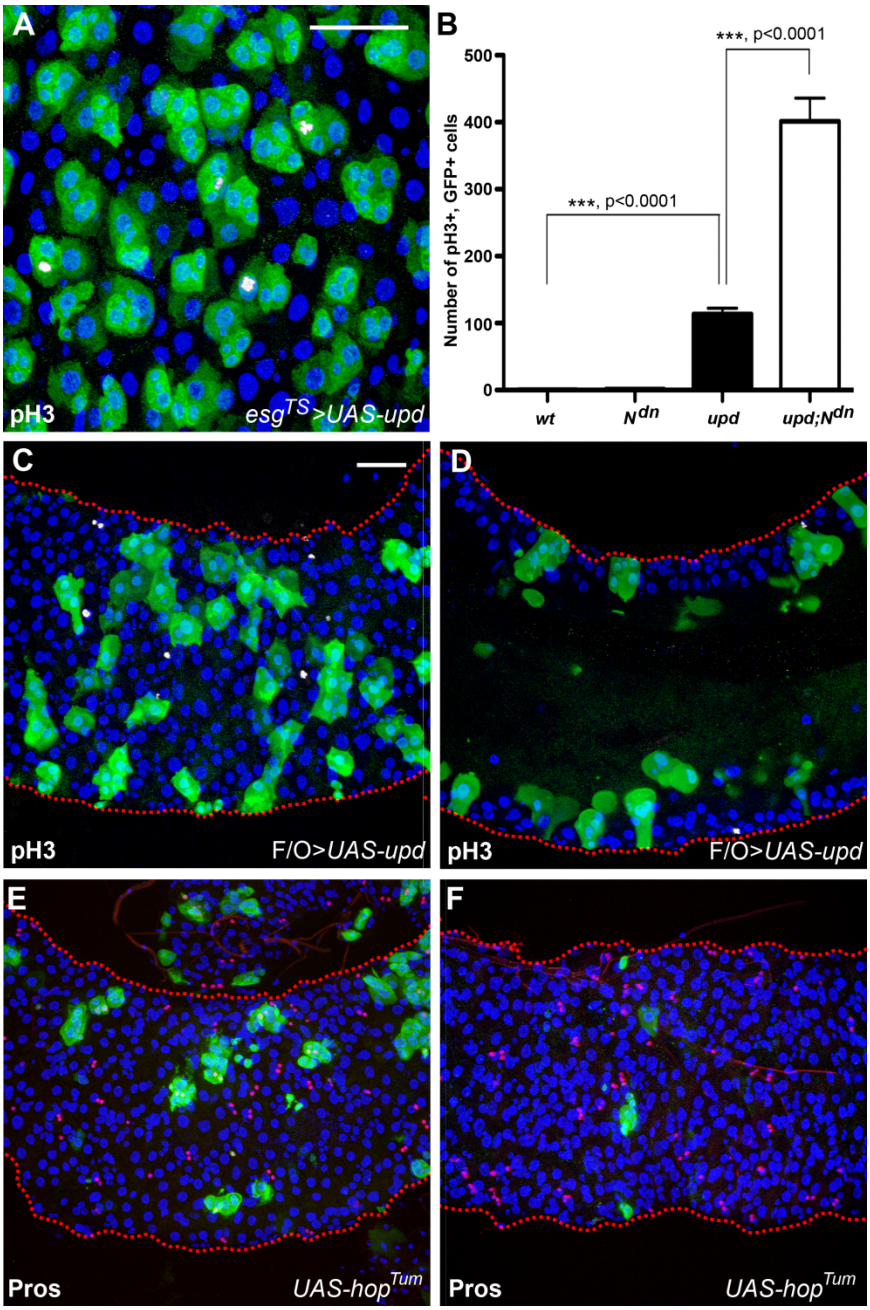

Figure 2.8: JAK/STAT activation promotes ISC proliferation. (A–D) Expression of *upd* leads to an increase in ISC proliferation. (A, B) Conditional expression of *upd* using the *esg-Gal4, UAS-GFP, tub-Gal80^{TS}* driver (anti-GFP, green; anti-pHH3, grayscale; DAPI, blue). (A) Expression of *upd* is sufficient to increase the number of pHH3+ cells 48 h after induction. (B) Quantification. Note that simultaneous reduction of N activity using a dominant negative construct leads to a further increase in pHH3^{+} cell number. (C, D) Expression of *upd* using the Flip-out (F/O) cassette (anti-GFP, green; anti-pHH3,

grayscale; DAPI, blue). (C) Cells marked in Flip-out experiments were associated with increased numbers of $pHH3^{+}$ cells. (D) Many marked cells rapidly delaminate from the midgut, as seen here in cross section. (E, F) ISC lineages expressing the activated form of *hop* (hop^{Tum}) are rapidly lost from the midgut (anti-GFP, green; anti-Pros, red; DAPI, blue). (E) hop^{Tum} lineages 5 days after induction. (F) hop^{Tum} lineages 10 days after induction. Error bars denote s.e.m. Scale bar: 50 μm.

2.7 Supplementary material

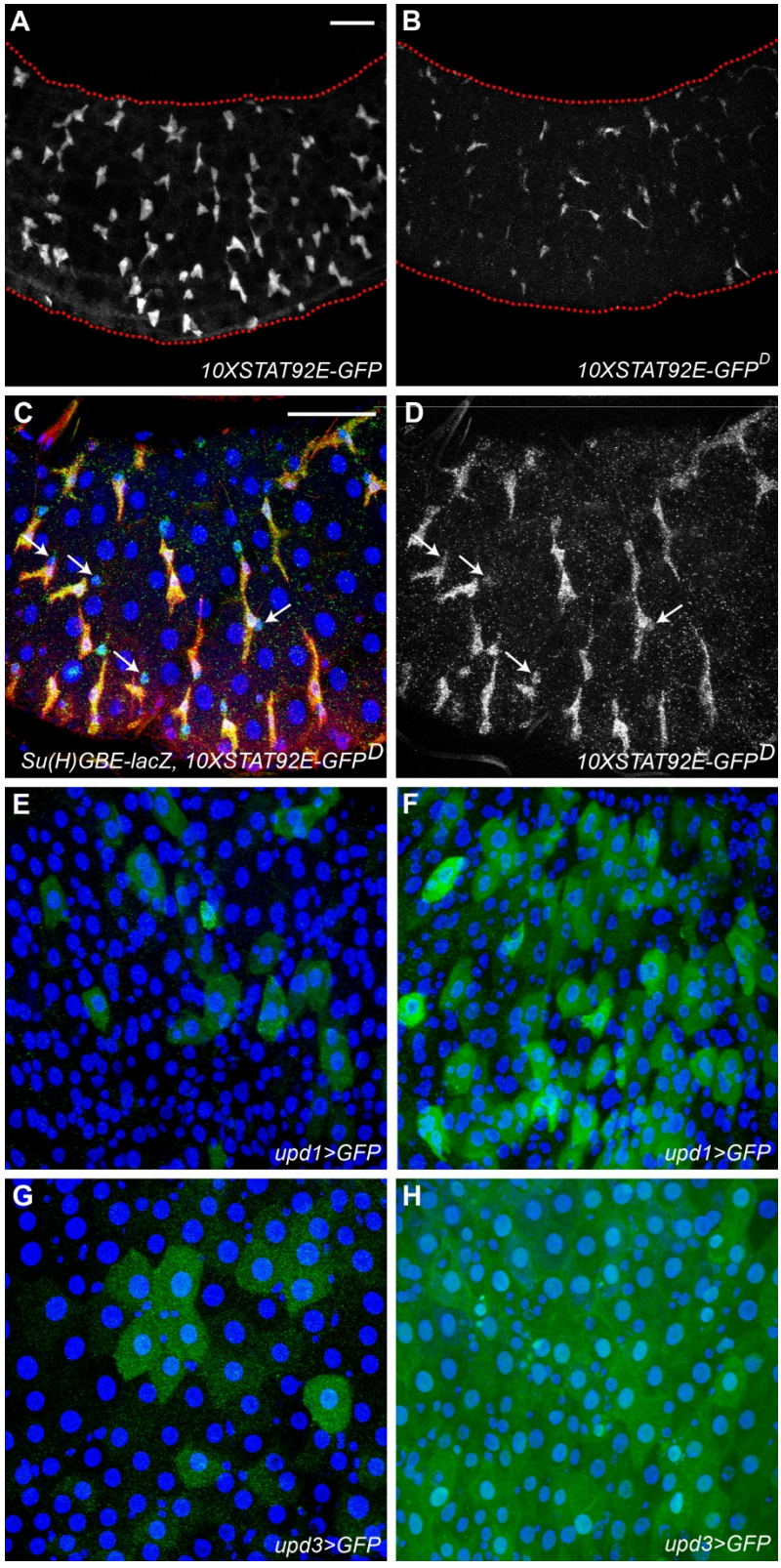

Supplemental Figure S2.1: JAK/STAT signaling is dynamically regulated in midgut. (A–D) Characterizing transcriptional reporters of JAK/STAT activity in the midgut. (A, B) A comparison of stable and destabilized JAK/STAT reporters (anti-GFP, grayscale). (A) The stabilized *10xSTAT92E-GFP* reporter was consistently found in pairs of small cells and at high levels throughout the length of the midgut. (B) The destabilized reporter, *10xSTAT92E-GFP*^{D}, demonstrated lower and more variable expression levels than the stabilized reporter. (C, D) ISCs have lower levels of destabilized reporter expression than EBs (*Su(H)GBE-lacZ*$^{+}$ cells). Arrows indicate ISCs with low GFP levels. (C) Merged (anti-GFP, green; anti-βgal, red; DAPI, blue). (D) Single channel showing *10xSTAT92E-GFP*^{D} (anti-GFP, grayscale). (E–H) Distribution of JAK/STAT ligands in the midgut (anti-GFP, green; DAPI, blue). (E, F) *upd1 > GFP*. The extent and distribution of reporter gene expression varied in the midgut. (G, H) *upd3 > GFP*. The extent and distribution of reporter gene expression varied in the midgut. Scale bar: 50 μm.

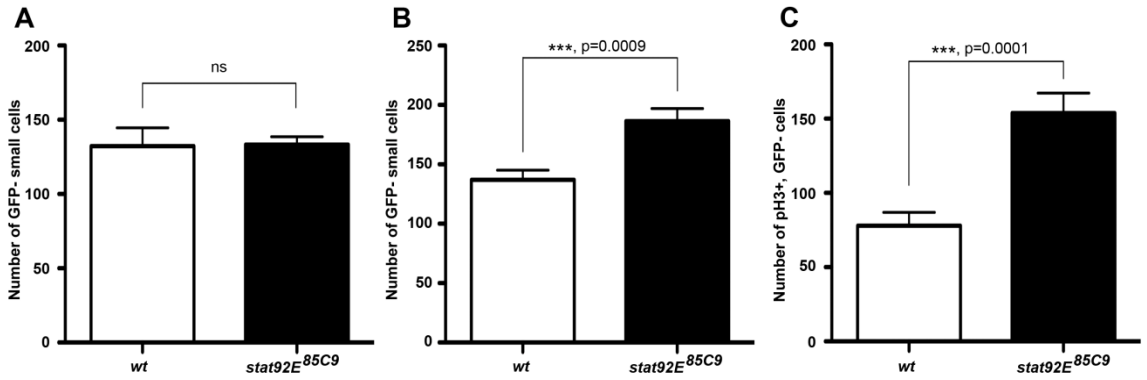

Supplemental Figure S2.2: Non-autonomous effects of *stat92E^{85C9}* clones. The MARCM system was used to positively identify wild-type and *stat92E^{85C9}* mutant lineages. (A) Uninduced. The number of GFP$^-$ small cells was scored; no difference between the two genetic backgrounds was detected in the absence of clone induction. (B) Induced. The number of GFP$^-$ small cells was scored; an increase was detected in *stat92E^{85C9}* mosaic animals. (C) Induced. The number of GFP$^-$, pHH3$^+$ cells was scored; an increase was detected in *stat92E^{85C9}* mosaic animals. Error bars denote s.e.m.

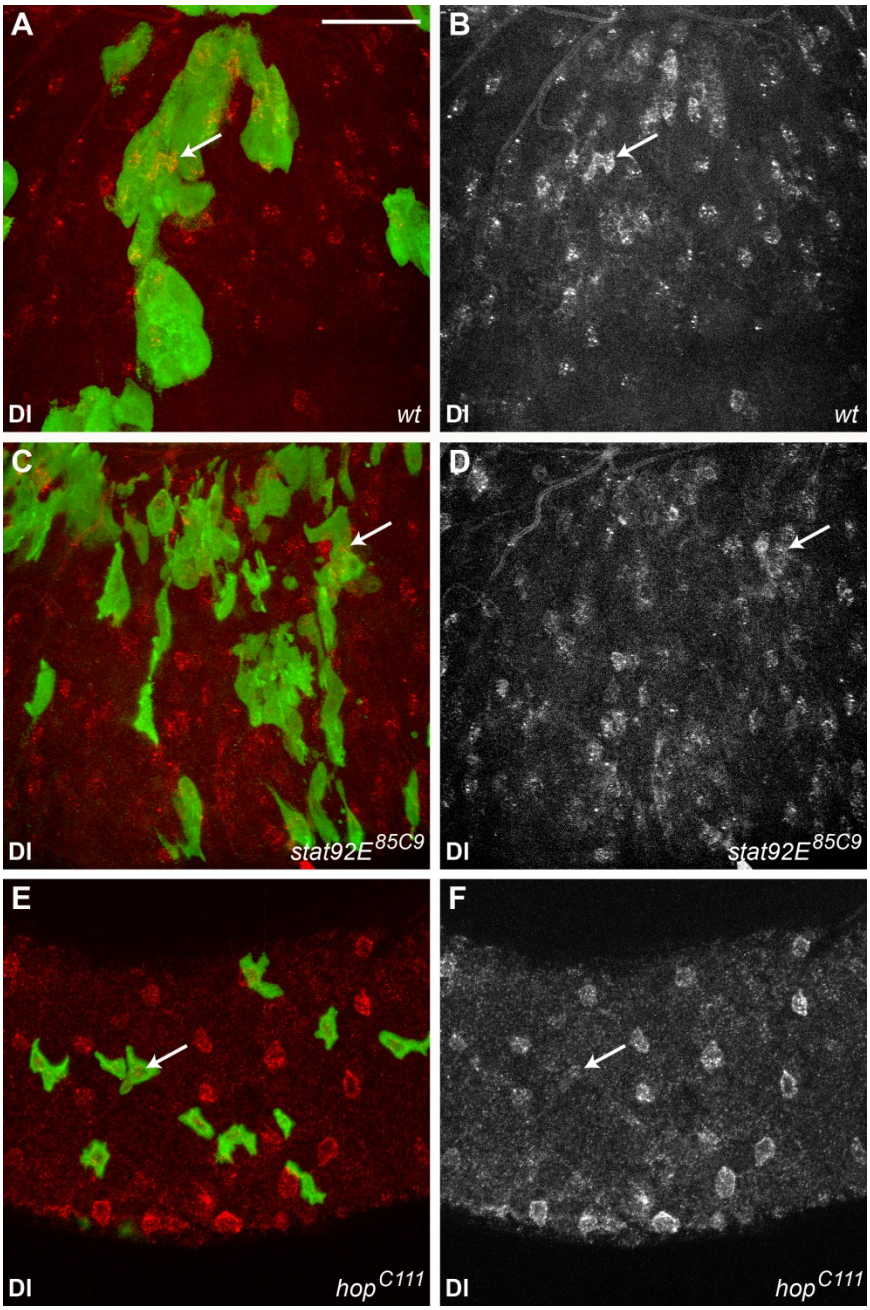

Supplemental Figure S2.3: ISCs are present in the absence of JAK/STAT signaling. (A, C, E) The MARCM system was used to positively identify ISC lineages with GFP (anti-GFP, green; anti-Dl, red; DAPI, blue). (A, B) Wild-type ISC lineages contain Dl^{+} cells. Arrow indicates cell with high Dl staining. (A) Merged. (B) Anti-Dl, grayscale. (C, D) Decreased levels of Dl can be detected in *stat92E*^{85C9} mutants. Arrow indicates cell with reduced Dl staining. (C) Merged. (D) Anti-Dl, grayscale. (E, F) Decreased levels

of Dl can be detected in *hop*^{C111} mutants. Arrow indicates cell with reduced Dl staining. (E) Merged. (F) Anti-Dl, grayscale. Scale bar: 50 μm.

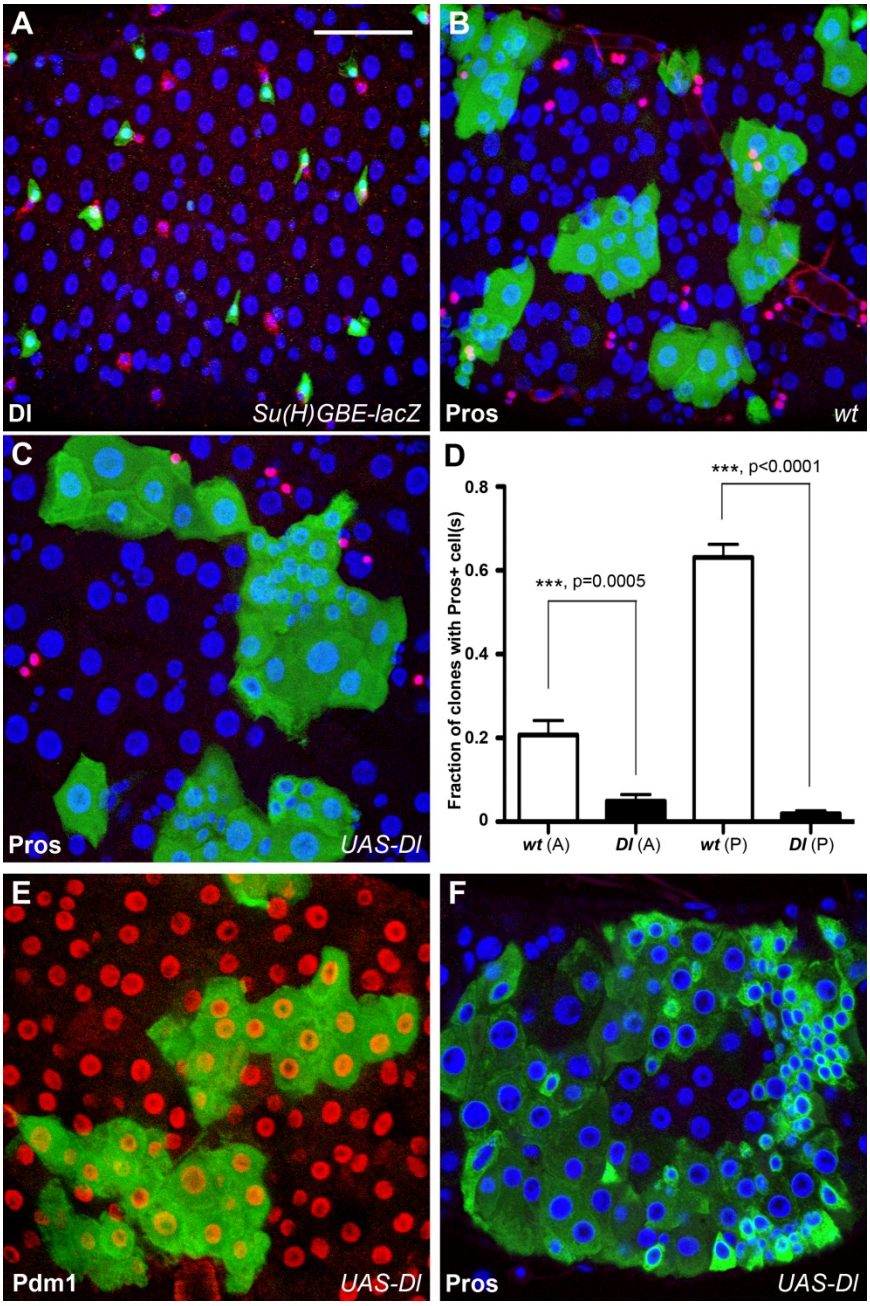

Supplemental Figure S2.4: Delta expression is sufficient to promote the EC cell fate. (A) Dl expressing ISCs can be detected adjacent to EBs transducing the N signal (*Su(H)GBE-lacZ*$^{+}$ cells; anti-βgal, green; anti-Dl, red; DAPI, blue). (B-F) The MARCM system was used to positively identify ISC lineages with GFP 5 days after induction, except F (anti-GFP-green; DAPI, blue). (B) Wild-type lineages often contain Pros^{+} cells. (C, D) Expression of *Dl* in ISC lineages resulted in a significant decrease of the Pros^{+} population (anti-Pros, red). (C) Representative image. (D) Quantification. (E) Expression of *Dl* in ISC lineages, produces cells with large nuclear size that are Pdm1^{+} (anti-Pdm1, red). (F) At later time

points (here 10 days after clone induction) expression of *Dl* in ISC lineages was often associated with an increased number of cells in comparison to wild-type lineages (anti-Pros, red). Error bars denote s.e.m. Scale bar: 50 μm.

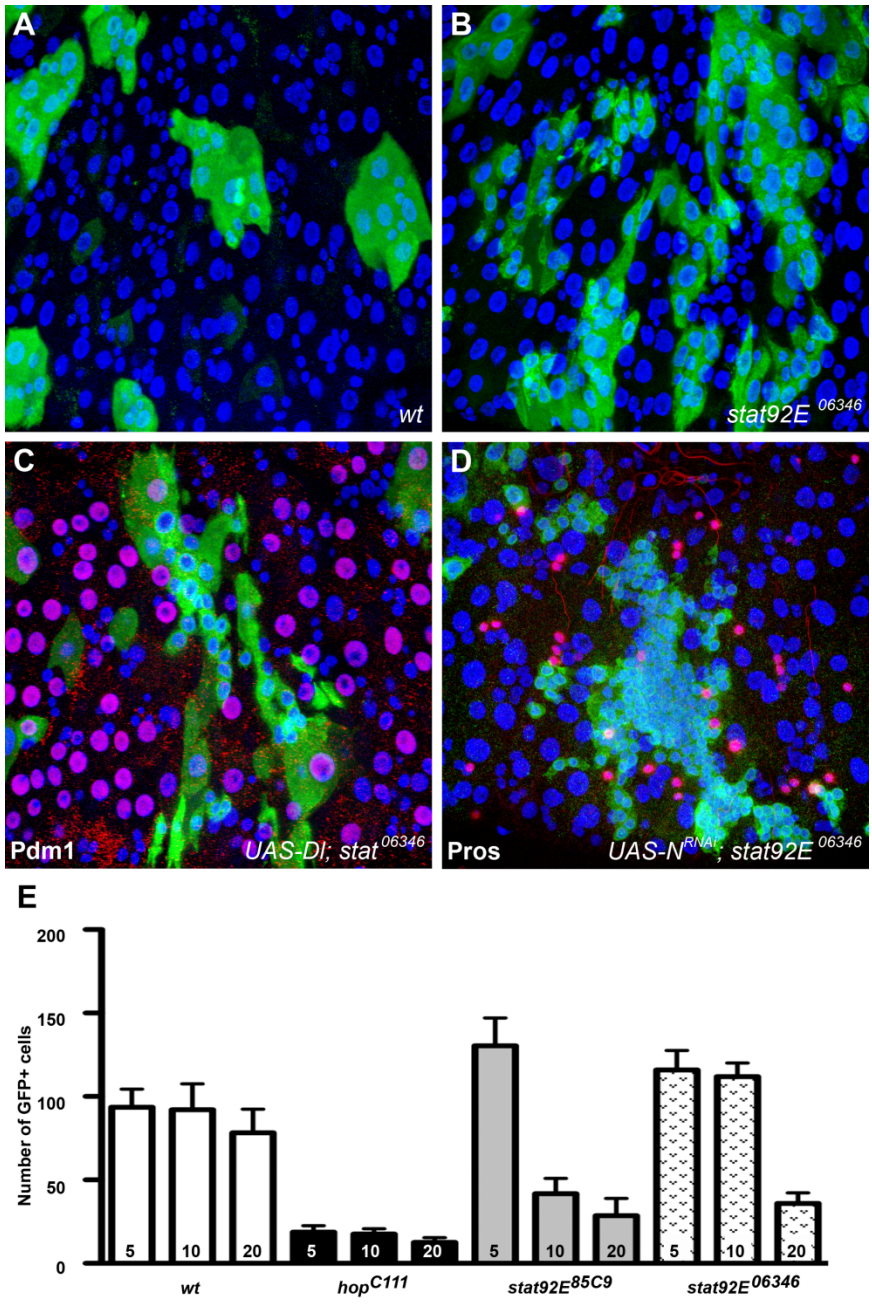

Supplemental Figure S2.5: *stat92E*^{06346} and *stat92E*^{85C9} have similar phenotypes in the ISC lineage. (A-D) The MARCM system was used to positively identify ISC lineages with GFP 5 days following induction (GFP, green; DAPI, blue). (A) Wild-type ISC lineages. (B) *stat92E*^{06346} mutant lineages. (C) *Dl*^{wt}, *stat92E*^{06346} lineages (anti-Pdm1, red). (D) *N*^{RNAi}, *stat92E*^{06346} lineages (anti-Pros, red). (E) GFP^{+} cells from *stat92E*^{06346} mutant lineages are still detectable 20 days following clone induction, *stat92E*^{06346} represented by dotted bars. Error bars denote s.e.m. Scale bar: 50 μm.

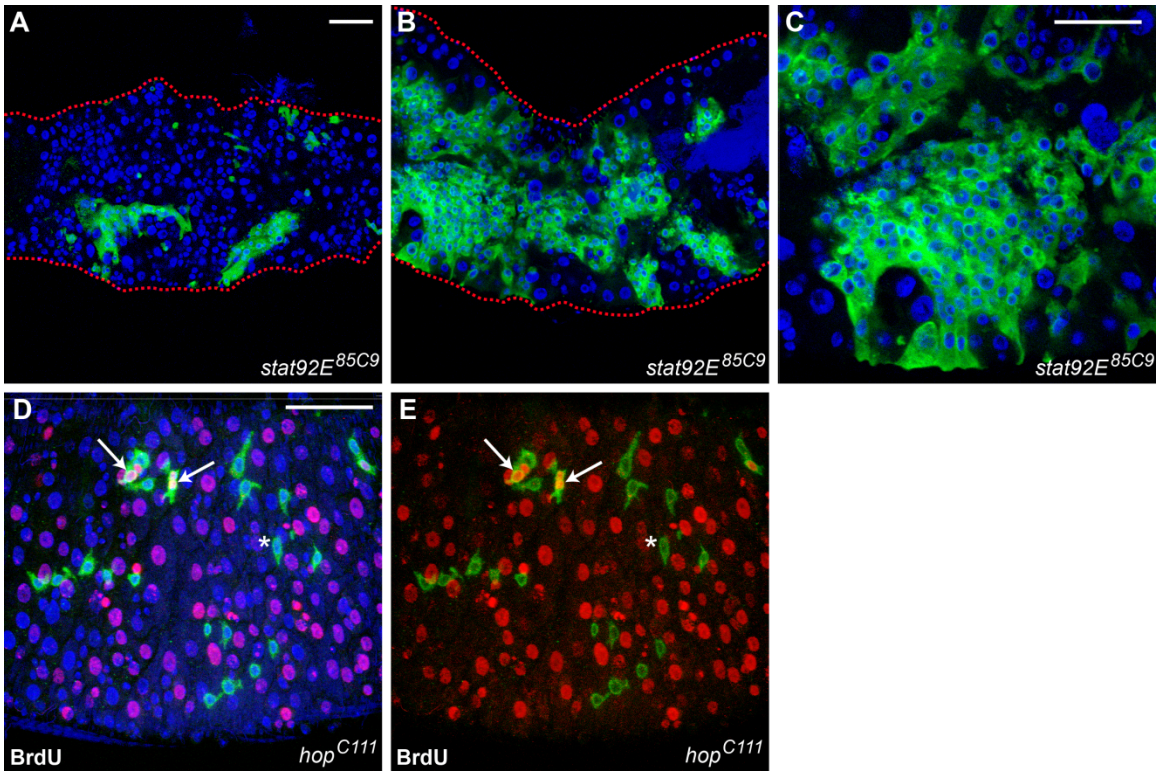

Supplemental Figure S2.6: JAK/STAT is not absolutely required for self-renewal. (A-E) The MARCM system was used to positively identify ISC lineages with GFP (anti-GFP, green; DAPI, blue). (A-C) 20-day *stat92E* clones occasionally display lineages that appear hyperplastic. Images showing superficial and cross sections of the midgut. (A) Superficial (B) Cross-section. Note that clone profile appears smaller in superficial sections (anti-GFP, green; DAPI, blue). (C) High magnification. (D, E) Cells in hop^{C111} mutant lineages could be observed to incorporate BrdU during the 5th week after clone induction (anti-GFP, green; anti-BrdU, red; DAPI, blue). (D) Merged. (E) Arrows indicate BrdU positive cells. Asterisk indicates an unlabeled cell. Scale bar: 50 μm.

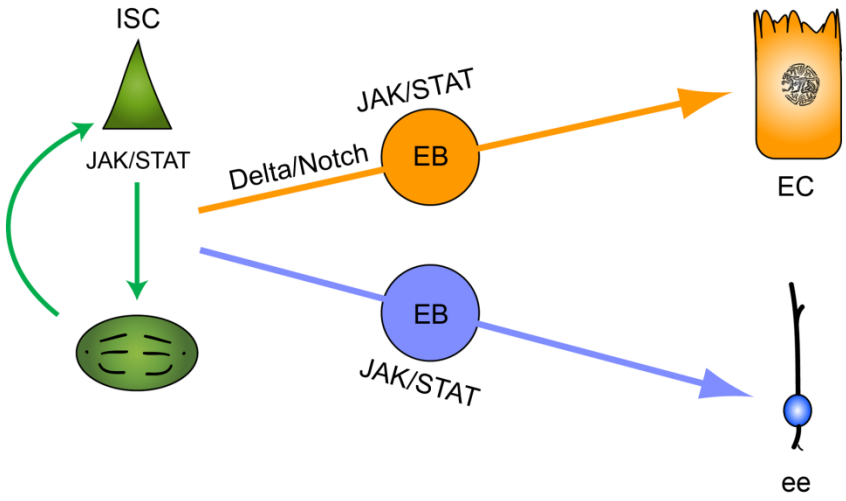

Supplemental Figure S2.7: A model for the role of JAK/STAT in the *Drosophila* intestinal stem cell lineage. JAK/STAT functions to coordinate stem cell proliferation and multi-lineage differentiation.

2.8 References

Agaisse, H., Petersen, U.M., Boutros, M., Mathey-Prevot, B., Perrimon, N. (2003). Signaling role of hemocytes in Drosophila JAK/STAT-dependent response to septic injury. Dev Cell. 5, 441-50.

Arbouzova, N.I. and Zeidler, M.P. (2006). JAK/STAT signalling in Drosophila: insights into conserved regulatory and cellular functions. Development. 133, 2605-16.

Bach, E.A., Ekas, L.A., Ayala-Camargo, A., Flaherty, M.S., Lee, H., Perrimon, N. and Baeg, G.H. (2007). GFP reporters detect the activation of the Drosophila JAK/STAT pathway in vivo. Gene Expr Patterns. 7, 323-31.

Baeg, G.H., Zhou, R. and Perrimon, N. (2005). Genome wide RNAi analysis of JAK/STAT signaling components in Drosophila. Genes Dev. 19, 1861-1870.

Baksa, K., Parke, T., Dobens, L.L. and Dearolf, C.R. (2002). The Drosophila STAT protein, Stat92E, Regulates Follicle Cell Differentiation during Oogenesis. Dev. Biol. 243, 166-175.

Bello, B.C., Hirth, F., and Gould, A.P. (2003). A pulse of the Drosophila Hox protein Abdominal-A schedules the end of neural proliferation via neuroblast apoptosis. Neuron, 37, 209-219.

Binari, R. and Perrimon, N. (1994). Stripe-specific regulation of pair-rule genes by hopscotch, a putative Jak family tyrosine kinase in Drosophila. Genes Dev. 8, 300-312.

Boyle, M., Wong, C., Rocha, M. and Jones, D.L. (2007). Decline in Self-Renewal Factors Contributes to Aging of the Stem Cell Niche in the Drosophila Testis. Cell Stem Cell 1, 470-478.

Buchon, N., Broderick, N.A., Poidevin, M., Pradervand, S. and Lemaitre, B. (2009). Drosophila Intestinal Response to Bacterial Infection: Activation of Host Defense and Stem Cell Proliferation. Cell Host Microbe 5, 200-211.

Cronin, S.J., Nehme, N.T., Limmer, S., Liegeois, S., Pospisilik, J.A., Schramek, D., Leibbrandt, A., Simoes, R.D., Gruber, S., Puc, U., Ebersberger, I., Zoranovic, T., Neely, G.G., von Haeseler, A., Ferrandon, D. and Penninger, J.M. (2009). Genome-wide RNAi Screen Identifies Genes Involved in Intestinal Pathogenic Bacterial Infection. Science 325, 340-343.

Deccota, E., and Spradling, A.C. (2005). The Drosophila Ovarian and Testis Stem Cell Niches: Similar Somatic Stem Cells and Signals. Dev. Cell 9, 501-510.

Fuller, M.T. and Spradling, A.C. (2007). Male and Female Drosophila Germline Stem Cells: Two Versions of Immortality. Science 316, 402-404.

Furriols, M. and Bray, S. (2001). A model Notch response element detects Suppressor of Hairless-dependent molecular switch. *Curr Biol.* 11, 60-64.

Ghiglione, C., Devergne, O., Georgenthum, E., Carballes, F., Medioni, C., Cerezo, D. and Noselli, S. (2002). The Drosophila cytokine receptor Domeless controls border cell migration and epithelial polarization during oogenesis. Development 129, 5437-5447.

Goto S, Hayashi S. (1999). Proximal to distal cell communication in the Drosophila leg provides a basis for an intercalary mechanism of limb patterning. Development 126, 3407-13.

Gregory, L., Came, P.J. and Brown, S. (2008). Stem cell regulation by JAK/STAT signaling in Drosophila. Semin Cell Dev Biol. 19, 407-413.

Harrison, D.A., Binari, R., Nahreini, T.S., Gilman, M. and Perrimon, N. (1995). Activation of a Drosophila Janus kinase (JAK) causes hematopoietic neoplasia and developmental defects. EMBO J. 14, 2857-65.

Harrison, D.A., McCoon, P.E., Binari, R., Gilman, M., Perrimon, N. (1998). Drosophila unpaired encodes a secreted protein that activates the JAK signaling pathway. Genes Dev. 12, 3252-63.

Hou, X.S., Melnick, M.B., Perrimon, N. (1996). Marelle acts downstream of the Drosophila HOP/JAK kinase and encodes a protein similar to the mammalian STATs. Cell 84, 411-419.

Ito, K., Awano, W., Suzuki, K., Hiromi, Y., Yamamoto, D. (1997). The Drosophila mushroom body is a quadruple structure of clonal units each of which contains a virtually identical set of neurones and glial cells. Development 124, 761-771.

Jiang, H., Patel, P.H., Kohlmaier, A., Grenley, M.O., McEwen, D.G. and Edgar, B.A. (2009). Cytokine/JAK/STAT Signaling Mediates Regeneration and Homeostasis in the Drosophila Midgut. Cell 137, 1343-1355.

Jones, D.L., and Wagers, A.J. (2008). No place like home: anatomy and function of the stem cell niche. Nat Rev Mol Cell Biol 9, 11-21.

Jonsson, F. and Knust, E. (1996). Distinct functions of the Drosophila genes Serrate and Delta revealed by ectopic expression during wing development. Dev. Genes Evol. 206(2): 91-101.

Kidd, S., Kelley, M.R., Young, M.W. (1986). Sequence of the notch locus of Drosophila melanogaster: relationship of the encoded protein to mammalian clotting and growth factors. Mol Cell Biol. 6, 3094-108.

Kiger, A.A., Jones, D.L., Schultz, C. Rogers, M.B. and Fuller, M.T. (2001). Stem Cell Self-Renewal Specified by JAK/STAT Activation in Response to a Support Cell Cue. Science 294, 2542-2545.

Lee, T and Luo, L. (1999). Mosaic Analysis with a Repressible Cell Marker for Studies of Gene Function in Neuronal Morphogenesis. Neuron 22, 451-461.

Lee, W.C., Beebe, K.B., Sudmeier, L. and Micchelli, C.A. (2009). *Adenomatous polyposis coli* regulates *Drosophila* intestinal stem cell proliferation. Development 136, 2255-2264.

Lin, G., Xu, N. and Xi, R. (2008). Paracrine Wingless signaling controls self-renewal of Drosophila intestinal stem cells. Nature 455, 310-312.

Margolis J., Spradling A. (1995). Identification and behavior of epithelial stem cells in the Drosophila ovary. Development 121, 3797-3807.

McGregor, J.R., Xi, R. and Harrison, D.A. (2002). JAK signaling is somatically required for follicle cell differentiation in Drosophila. Development 129, 705-717.

Micchelli, C.A. and Perrimon, N. (2006). Evidence that stem cells reside in the adult Drosophila midgut epithelium. Nature 439, 475-479.

Morin X, Daneman R, Zavortink M, Chia W. (2001). A protein trap strategy to detect GFP-tagged proteins expressed from their endogenous loci in Drosophila. Proc Natl Acad Sci U S A., 98, 15050-15055.

Müller, P., Kuttenkeuler, D., Gesellchen, V., Zeidler, M.P. and Boutros, M. (2005). Identification of JAK/STAT signaling components by genome wide RNA interference. Nature 436, 871-875.

Ohlstein, B. and Spradling, A. (2006). The adult Drosophila posterior midgut is maintained by pluripotent stem cells. Nature 439, 470-474.

Ohlstein, B. and Spradling, A. (2007). Multipotent Drosophila intestinal stem cells specify daughter cell fates by differential notch signaling. Science 315, 988-992.

Rebay, I., Fehon, R.G., Artavanis-Tsakonas, S. (1993). Specific truncations of Drosophila Notch define dominant activated and dominant negative forms of the receptor. Cell 74, 319-29.

Röttgen, G., Wagner, T., Hinz, U. (1998). A genetic screen for elements of the network that regulates neurogenesis in Drosophila. Mol Gen Genet. 257, 442-51.

Samakovlis, C., Manning, G., Steneberg, P., Hacohen, N., Cantera, R., Krasnow MA. (1996). Genetic control of epithelial tube fusion during Drosophila tracheal development. Development 122, 3531-6.

Silver, D.L. and Montell, D.J. (2001). Paracrine signaling through the JAK/STAT pathway activates invasive behavior of ovarian epithelial cells in Drosophila. Cell 107, 831-841.

Silver, D.L., Geisbrecht, E.R. and Montell, D.J. (2005). Requirement for JAK/STAT signaling throughout border cell migration in Drosophila. Development 132, 3483-3492.

Singh, S.R., Liu, W. and Hou, S.X. (2007). The Adult Drosophila Malpighian Tubules Are Maintained by Multipotent Stem Cells. Cell Stem Cell 1, 191-203.

Struhl, G., Fitzgerald, K., Greenwald, I. (1993). Intrinsic activity of the Lin-12 and Notch intracellular domains in vivo. Cell 74, 331-45.

Tulina, N. and Matunis, E. (2001). Control of Stem Cell Self-Renewal in Drosophila Spermatogenesis by JAK-STAT Signaling. Science 294, 2546-2549.

Xu, T. and Rubin, G.M. (1993). Analysis of genetic mosaics in developing and adult Drosophila tissues. Development 117, 1223-1237.

Yeo, S.L., Lloyd, A., Kozak, K., Dinh, A., Dick, T., Yang, X., Sakonju, S., Chia, W. (1995). On the functional overlap between two Drosophila POU homeo domain genes and the cell fate specification of a CNS neural precursor. Genes Dev 9, 1223-1236.

Chapter 3

Adenomatous polyposis coli regulates *Drosophila* intestinal stem cell proliferation

The research work in Chapter 3 is published in Development. 2009 Jul;136(13):2255-64. Katherine Beebe is the second author of this publication.

3.1 Summary

Adult stem cells define a cellular reserve with the unique capacity to replenish differentiated cells of a tissue throughout an organism's lifetime. Previous analysis has demonstrated that the adult *Drosophila* midgut is maintained by a population of multi-potent intestinal stem cells (ISCs) that resides in epithelial niches. *Adenomatous polyposis coli* (*Apc*), a tumor suppressor gene conserved in both invertebrates and vertebrates, is known to play a role in multiple developmental processes in *Drosophila*. Here, we examine the consequences of eliminating *Apc* function on adult midgut homeostasis. Our analysis shows that loss of *Apc* results in the disruption of midgut homeostasis and is associated with hyperplasia and multi-layering of the midgut epithelium. A mosaic analysis of marked ISC cell lineages demonstrates that *Apc* is required specifically in ISCs to regulate proliferation, but is not required for ISC self-renewal or the specification of cell fate within the lineage. Cell autonomous activation of Wnt signaling in the ISC lineage phenocopied *Apc* loss and *Apc* mutants were suppressed in an allele-specific manner by abrogating Wnt signaling, suggesting that the effects of *Apc* are mediated in part by the Wnt pathway. Together, these data underscore the essential requirement of *Apc* in exerting regulatory control over stem cell activity, as well as the consequences that disrupting this regulation can have on tissue homeostasis.

3.2 Introduction

Many adult tissues require the activity of tissue-specific stem cell populations to maintain homeostasis throughout the course of an organism's lifetime. The dual characteristics of self-renewal and multi-potency make stem cells ideally suited for this central role. Adult stem cells reside in specialized microenvironments called niches, which regulate stem cell behavior at baseline homeostasis and dynamically respond to changing environmental stimuli by modulating lineage output (reviewed in (Jones and Wagers, 2008)). Tight control of stem cell proliferation is essential to ensure that homeostatic balance is maintained; disruption of stem cell proliferation can lead to homeostatic imbalance, compromised wound healing, and disease. However, little is currently known about the factors that constrain stem cell proliferation.

The precise location and cellular architecture of the adult stem cell niche has been defined with high resolution in only a small number of tissues (reviewed in (Morrison and Spradling, 2008)). The ability to

identify, manipulate and mark individual stem cell lineages has made *Drosophila* an excellent model system with which to dissect stem cell regulation. For example, the adult *Drosophila* midgut contains approximately 1200 intestinal stem cells (ISCs) distributed along the anteroposterior (AP) axis of the organ (Fig. 2.1A,B) (Micchelli and Perrimon, 2006; Ohlstein and Spradling, 2006). ISCs have a pyramidal morphology and are located in an epithelial niche distant from the midgut lumen, adjacent to the basement membrane and the visceral musculature surrounding the midgut. ISCs are multi-potent and give rise to a lineage that consists of two types of differentiated daughters, the enteroendocrine (ee) cells and the enterocytes (ECs), which together form a cellular monolayer lining the length of the adult midgut.

Adenomatous polyposis coli (*Apc*) encodes an evolutionarily conserved protein, which was first identified by positional cloning as one of the genes commonly deleted in the hereditary colon cancer syndrome familial adenomatous polyposis (FAP) (Groden et al., 1991; Kinzler et al., 1991). Mutations in both copies of *Apc* are also detected in many spontaneous colorectal adenomas (Ichii et al., 1992; Miyoshi et al., 1992; Powell et al., 1992). As the majority of *Apc* mutations are loss of function, *Apc* is thought to function as a tumor suppressor gene. Early insight into the molecular function of *Apc* came from the identification of β-catenin, a Wnt pathway effector, as a binding partner for Apc (Rubinfeld et al., 1997; Su et al., 1993). The requirement for *Apc* in the Wnt signaling pathway is now well characterized and current models suggest that Apc together with Axin, Glycogen Synthase Kinase 3 and Casein Kinase 1 comprise a multi-protein β-catenin destruction complex. In the absence of Wnt ligands, the destruction complex phosphorylates β-catenin, targeting it for proteasomal degradation.

The *Drosophila* genome, like that of both mouse and human, contains two Apc family members, *Apc1* (also known as *Apc* – FlyBase) and *Apc2* (Ahmed et al., 1998; Hamada et al., 1999a; Hayashi et al., 1997; McCartney et al., 1999). Previous analysis in *Drosophila* has implicated *Apc* in a number of developmental processes, including cell survival, cell fate specification and proliferation. Yet, the role of *Apc* in maintaining adult *Drosophila* midgut homeostasis has not been examined. In this study, we investigate the consequences of eliminating *Apc* function on adult midgut homeostasis and ISC behavior.

3.3 Experimental Procedures

3.3.1 *Drosophila* strains and culture

Apc2^{C9} / TM6 Tb, Hu (*Apc2^{C9}* is a temperature-sensitive allele with a permissive temperature of 18°C and non-permissive temperature of 27°C; gift from B. McCartney, Carnegie Mellon University, Pittsburgh, PA, USA). *w; FRT^{82B} Apc2^{g10}, Apc1^{Q8} / TM6C* (*Apc2^{g10}* is null for Armadillo degradation but retains the ability to promote Wnt signaling in the eye; *Apc1^{Q8}* is a null allele; gift from B. McCartney). *w; FRT^{82B} Apc2^{33}, Apc1^{Q8} / TM6C* (*Apc2^{33}* is a strong hypomorph resulting from a deletion; gift from Y. Ahmed, Dartmouth College, Hanover, NH, USA). *w; FRT^{82B} Axins^{044230} / TM3 Sb* (*Axins^{044230}* is a loss-of-function allele; gift from Y. Ahmed). *y, w, UAS-GFP, hsFLP; tub-Gal4, FRT^{82B}, tub-Gal80 / TM6B* (gift from N. Perrimon, Harvard Medical School, Boston, MA, USA*). y, w; esg-Gal4 / Cyo* (gift from S. Hayashi, RIKEN, Kobe, Japan). *w, UAS-N^{RNAi}. UAS-GFP*. *y, w*; *esg^{K606} / Cyo* (*esg-lacZ*). *w; FRT^{82B} hsπM* (this stock was used as a wild-type control in the mosaic analysis performed in this study). *y, w, UAS-arm^{S10}* (activated arm). *y, w; UAS-pan.dTCFΔN4* (dominant-negative allele). Unless indicated, all strains were obtained from the Bloomington Stock Center. Crosses were cultured on standard dextrose media and were transferred to fresh food augmented with yeast paste every 1-2 days during the experimental period. Crosses were reared at 18, 25, or 29°C, in passively illuminated and humidified incubators. In this study, only adult female flies of the following genotypes were analyzed.

Figure 3.2:

+; esg^{K606} / +; FRT^{82B} Apc2^{g10}, Apc1^{Q8} / Apc2^{C9}.

+ / w; FRT^{82B} Apc2^{g10}, Apc1^{Q8} / Apc2^{C9}.

Figures 3.3, 3.4 and S3.2:

y, w, hsFLP, UAS-GFP / w; +; FRT^{82B} hsπM / tub-Gal4, FRT^{82B} tub-Gal80.

y, w, hsFLP, UAS-GFP / +; +; FRT^{82B} Apc2^{g10}, Apc1^{Q8} / tub-Gal4, FRT^{82B} tub-Gal80.

Figure 3.5:

y, w, hsFLP, UAS-GFP / w; esg^{K606} / +; FRT^{82B} hsπM / tub-Gal4, FRT^{82B} tub-Gal80.

y, w, hsFLP, UAS-GFP / +; esg^{K606} / +; FRT^{82B} Apc2^{g10}, Apc1^{Q8} / tub-Gal4, FRT^{82B} tub-Gal80.

y, w, hsFLP, UAS-GFP / +; +; FRT^{82B} Apc2^{g10}, Apc1^{Q8} / tub-Gal4, FRT^{82B} tub-Gal80

Figures 3.6, S3.3 and S3.4:

y, w, hsFLP, UAS-GFP / UAS-N^{RNAi}; +; FRT^{82B} hsπM / tub-Gal4, FRT^{82B} tub-Gal80.

y, w, hsFLP, UAS-GFP / UAS-N^{RNAi}; +; FRT^{82B} Apc2^{g10}, Apc1^{Q8} / tub-Gal4, FRT^{82B} tub-Gal80.

y, w, hsFLP, UAS-GFP / UAS-N^{RNAi}; esg^{K606} / +; FRT^{82B} hsπM / tub-Gal4, FRT^{82B} tub-Gal80.

y, w, hsFLP, UAS-GFP / UAS-N^{RNAi}; esg^{K606} / +; FRT^{82B} Apc2^{g10}, Apc1^{Q8} / tub-Gal4, FRT^{82B} tub-Gal80.

Figures 3.7 and S3.5:

y, w, hsFLP, UAS-GFP / w; +; FRT^{82B} hsπM / tub-Gal4, FRT^{82B} tub-Gal80.

y, w, hsFLP, UAS-GFP /w; UAS-pan.dTCFΔN4 / +; FRT^{82B} hsπM / tub-Gal4, FRT^{82B} tub-Gal80.

y, w, hsFLP, UAS-GFP / w; +; FRT^{82B} Axin^{s044230} / tub-Gal4, FRT^{82B} tub-Gal80.

y, w, hsFLP, UAS-GFP / w; UAS-pan.dTCFΔN4 / +; FRT^{82B} Axin^{s044230} / tub-Gal4, FRT^{82B} tub-Gal80.

y, w, hsFLP, UAS-GFP / w; +; FRT^{82B} Apc2^{33}, Apc1^{Q8} / tub-Gal4, FRT^{82B} tub-Gal80.

y, w, hsFLP, UAS-GFP / w; UAS-pan.dTCFΔN4 / +; FRT^{82B} Apc2^{33}, Apc1^{Q8} / tub-Gal4, FRT^{82B} tub-Gal80.

y, w, hsFLP, UAS-GFP / w; +; FRT^{82B} Apc2^{g10}, Apc1^{Q8} / tub-Gal4, FRT^{82B} tub-Gal80.

y, w, hsFLP, UAS-GFP / w; UAS-pan.dTCFΔN4 / +; FRT^{82B} Apc2^{g10}, Apc1^{Q8} / tub-Gal4, FRT^{82B} tub-Gal80.

y, w, hsFLP, UAS-GFP / UAS-arm^{S10}; +; FRT^{82B} hsπM / tub-Gal4, FRT^{82B} tub-Gal80.

3.3.2 Mosaic analysis

The MARCM system was used to generate marked ISC lineages or 'clones'. MARCM was used to produce both marked wild-type and mutant lineages; in addition, all manipulations involving the misexpression of UAS transgenes were also performed using the MARCM system to ensure that only ISC lineages were analyzed. To induce clones, experimental animals were subjected to a 37°C heat pulse for 35-45 minutes within the first week of adulthood. Induction protocols varied from one to three heat pulses within a 24-hour period, depending on the desired rate of mitotic recombination.

3.3.3 Temperature shift experiments

Crosses were established and cultured at 18°C until adulthood. F1 progeny were divided into two equal pools; controls were cultured at 18°C and the experimental group was shifted to 29°C for 10 days. BrdU was administered *ad libitum* in *Drosophila* food media (200 µl of 6 mg/ml BrdU in 20% sucrose per vial) for the 24-hour period immediately preceding the 10-day time point.

3.3.4 Histology

Adult flies were dissected in 1x PBS (Sigma, USA). The gastrointestinal tract was removed and fixed in a final solution of 0.5x PBS (Sigma, USA) and 4% electron microscopy grade formaldehyde (Polysciences, USA) for a minimum of 30 minutes. Samples were washed in 1x PBS with 0.1% Triton X-100 (PBST) for 2 hours and then incubated with primary antibodies overnight. Samples were washed in PBST for 2 hours and then incubated with secondary antibodies for 3 hours. Finally, samples were washed in PBST overnight. Mounting media containing DAPI (Vectashield, USA) was added and samples were allowed to clear for 1 hour prior to mounting. All steps were completed at 4°C, with no mechanical agitation.

3.3.5 Antisera

Primary antibodies: Chicken anti-GFP (Abcam, USA) used at a dilution of 1:10,000; rabbit anti-β-Gal (Cappel, USA), 1:2000; mouse anti-Pros (Developmental Studies Hybridoma Bank; DSHB), 1:100; mouse anti-Dl (DSHB), 1:10; mouse anti-BrdU (Becton Dickinson, USA), 1:100; rabbit anti-Pdm1 (gift of W. Chia (Yeo et al., 1995)), 1:1000; rabbit anti-Tachykinin (gift of D. Nässel (Siviter et al., 2000)), 1:1000.

Secondary antibodies: Goat anti-chicken Alexa 488 (Molecular Probes, USA) used at a dilution of 1:2000; goat anti-mouse Alexa 568 (Molecular Probes, USA), 1:2000; goat anti-mouse Alexa 633 (Molecular Probes, USA), 1:2000; goat anti-rabbit Alexa 568 (Molecular Probes, USA), 1:2000.

Dyes and mounting media: Alexa 594-conjugated Phalloidin (Molecular Probes, USA) diluted 1:500; Vectashield+DAPI mounting media (Vector, USA).

3.3.6 Microscopy and imaging

Samples were examined on a Leica DM5000 upright fluorescent microscope. Confocal images were collected using a Leica TCS SP5 confocal microscope system. Images were processed for brightness and contrast, and assembled in Photoshop CS (Adobe, USA).

3.3.7 Cell counts, measurements and statistical analysis

In the temperature-shift analyses, entire midguts were scored. $BrdU^+$ *esg-lacZ*$^+$ positive pairs of cells were scored as a single event; clusters of three cells were scored as two events. In those TS experiments lacking *esg-lacZ* only small $BrdU^+$ clusters were scored (Fig. 3.2D). Midgut area was determined by first acquiring digital images of the posterior midgut on a compound microscope; Leica application suite (LAS) software was then used to determine the area of the posterior region. Next, the maximal number of nuclear layers and maximal epithelial height was determined based on confocal micrographs taken from the same posterior midguts. Only those regions of the epithelium from the outer face of posterior midgut, which has a larger circumference, were analyzed to minimize secondary distortion of the epithelium due to the coiled morphology of the midgut (Fig. 3.3E,F). In our mosaic analysis, the number of cells per clone was scored in either anterior and/or posterior midgut frames 5 days following induction (Fig. 3.4A; see also Supplemental Fig. S3.1; Fig. 3.4D,F; Fig. 3.6G). Data from the anterior and posterior midgut are combined in Fig. 3.4D, but separated by region in Fig. 3.4F. Unless indicated, counts were collected from posterior frames. Clones within selected frames were defined as clusters of contiguous cells, as assessed at 40x magnification on compound or confocal microscopes. For a clone to be scored it had to lie completely in the field of view; clones that partially wrapped around the 'edge' of the midgut sample were excluded from the analysis to minimize counting inaccuracy. To determine the number of dividing cells per frame, GFP^+ $pHH3^+$ cells were counted from the middle frame of the posterior midgut 5 days after heatshock induction (Fig. 3.4E). To assay ISC self-renewal, the number of clones per entire midgut was scored 5 and 10 days following heat-shock induction (Fig. 3.4G). Mitotic index was calculated by dividing the number of $pHH3^+$ $pros^-$ small nuclei by the total number of $pros^-$ small nuclei from marked lineages in posterior midgut frames 5 days following induction (Fig. 3.6H; see also Supplemental Fig. S3.4). All *t*-tests were performed using Prism (GraphPad Software, USA).

3.4 Results

3.4.1 *Apc* regulates adult midgut homeostasis

Previous studies of *Apc* have demonstrated that functional redundancy exists between *Apc1* and *Apc2* in a number of *Drosophila* tissues, including the embryonic epidermis, the wing and eye imaginal discs, and the larval brain (Ahmed et al., 2002; Akong et al., 2002a; Akong et al., 2002b; McCartney et al., 2006). We therefore reasoned that simultaneous reduction of both *Apc1* and *Apc2* would be a direct means by which to initially assess the requirement for *Apc* in the adult midgut. To globally reduce *Apc* function in a conditional manner, we used a temperature-sensitive allelic combination and measured the extent of 5-bromo-2-deoxyuridine (BrdU) incorporation in the adult midgut (Fig. 3.2A-D). Here, we employed three well-characterized alleles of *Apc* to establish the temperature-sensitive genotype $Apc2^{g10}$, $Apc1^{Q8}/Apc2^{C9}$ [subsequently referred to as Apc^{TS} (Ahmed et al., 1998; McCartney et al., 2006). Unshifted control animals grown at the permissive temperature were compared with experimental animals shifted to the non-permissive temperature for 10 days during adulthood. In these experiments, we observed an increase in the number of $BrdU^+$ cells in experimental samples that often appeared as clusters of two to three small cells (Fig. 3.2A-C). Previous analysis has demonstrated that the transcriptional repressor encoded by *escargot* (*esg*) can be used to identify ISCs and their nascent daughters, called enteroblasts (EBs) (Fig. 3.2A,B) (Micchelli and Perrimon, 2006). To quantify the Apc^{TS} phenotype, we counted the number of small BrdU+ clusters in the midgut following a 24-hour BrdU pulse that immediately preceded the 10-day time point (BrdU administered *ad libitum* in food media). Global reduction in the levels of *Apc1* and *Apc2* resulted in a significant increase in the number of $BrdU^+$ small cell clusters (Fig. 3.2D; n=11). This analysis suggested that *Apc* is necessary for the maintenance of midgut homeostasis in the adult.

3.4.2 *Apc* is required in ISC lineages to maintain homeostasis

Although the TS analysis suggested a role for *Apc* in regulating midgut homeostasis, it did not directly establish a requirement for *Apc* in the midgut. To test the requirement for *Apc* specifically in the midgut, we next conducted a mosaic analysis of *Apc* double mutants ($Apc2^{g10}$, $Apc1^{Q8}$; subsequently referred to as *Apc* clones, except where indicated). Positively marked ISC lineages lacking *Apc* function were generated in the adult using the MARCM system (Lee and Luo, 1999) and identified on the basis of GFP

expression. At 20 days after induction, midguts containing *Apc* clones were associated with gross anatomical changes, including midgut hyperplasia and multi-layered cellular masses that distorted the luminal surface of the midgut (Fig. 3.3A-D). Plotting the maximal number of nuclear layers as a function of midgut area revealed an inverse correlation in *Apc* mosaics and an increase in each parameter compared with wild-type (Fig. 3.3E; wild-type, *n*=11; *Apc*, *n*=12). At 20 days after induction, it was often difficult to unambiguously identify individual marked *Apc* mutant lineages because of the changes in overall midgut morphology. However, by plotting the maximal number of nuclear layers as a function of maximal epithelial height, it was evident that up to five layers could be detected in mosaic *Apc* midguts (Fig. 3.3F; wild-type, *n*=11; *Apc*, *n*=12). Finally, in those cases in which individual clones could be definitively identified, *Apc* mutant lineages were found to produce multi-layered masses more frequently than were wild-type (*Apc*, 31.5%, *n*=181; wild-type, 1.3%, *n*=227).

The analysis of *Apc* clones was extended to determine the number of labeled cells in individual ISC lineages. As we observed little or no distortion of the midgut due to multi-layering at early time points, a 5-day post-induction time point was selected to quantify the number of cells per ISC clone. Cell counts were performed by scoring clones at two defined regions within each midgut analyzed (Fig. 3.4A; see Experimental Procedures and Supplemental Fig. S3.1 for experimental criteria). Mosaic analysis revealed a significant increase in the number of cells per clone in *Apc* lineages compared with in marked wild-type controls (Fig. 3.4B-D; *n*=76). This increase in clone size suggested that *Apc* loss leads to an increase in proliferation. Consistently, we observed that *Apc* mutant lineages were associated with a significant increase in the number of phosphohistone H3 positive ($pHH3^{+}$) cells when compared with wild-type cell lineages (Fig. 3.4E; wild-type, *n*=18; *Apc*, *n*=17).

An analysis of *Apc* clone size along the AP axis of the gastrointestinal tract was performed to determine whether the requirement for *Apc* was dependent on midgut region. This analysis revealed a significant increase in *Apc* clone size in both the anterior and posterior midgut compared with in wild-type controls (Fig. 3.4F). Although the trend towards increased clone sizes in ISCs lacking *Apc* was observed throughout the midgut, the average size of *Apc* clones was found to be greater in the posterior. Taken together, our mosaic analysis demonstrates that *Apc* is required in the ISC cell lineage throughout the midgut to maintain homeostasis.

3.4.3 *Apc* loss does not affect ISC self-renewal

One possible explanation for the hyperplasia associated with *Apc* loss is that *Apc* affects ISC self-renewal. Early studies of *Drosophila* germ line stem cells employed a lineage-tracing assay to measure stem cell self-renewal (Margolis and Spradling, 1995). A pulse/chase experiment was used to determine the number of marked stem cell lineages retained in the tissue at defined intervals following induction. To determine whether *Apc* loss affected ISC self-renewal in the midgut, we generated labeled ISCs and counted the number of marked ISC lineages per midgut at 5 and 10 days after induction. When the number of ISC lineages per gut lacking *Apc* was compared with wild-type, no significant differences were detected (Fig. 3.4G). These data show that *Apc* loss does not detectably affect the fidelity of ISC self-renewal.

3.4.4 ISCs lacking *Apc* generate the differentiated cells of the lineage

A second possible explanation for the hyperplasia associated with *Apc* loss is that *Apc* is required for differentiation in the ISC lineage. Inspection of *Apc* clone morphology initially suggested that cell fate in the lineage was correctly specified. To more rigorously analyze cell fate in *Apc* lineages, we examined a panel of molecular markers to label distinct cell types in the ISC lineage. The transcriptional repressor encoded by *esg* is expressed in ISCs and their undifferentiated EB daughters, but *esg* is not expressed in either of the two differentiated cell types of the midgut, the EE cells or the ECs (Fig. 3.5A) (Micchelli and Perrimon, 2006). Examination of *esg-lacZ* expression in *Apc* clones revealed the presence of both esg^{+} and esg^{-} cell populations (Fig. 3.5B). Similarly, elevated levels of Delta (Dl), which marks a subset of ISCs (Ohlstein and Spradling, 2007), were also detected in *Apc* clones (Fig. 3.5C). We note that in some instances levels of Dl appeared to be higher in certain ISC/EB pairs (Fig. 3.5C; see also Supplemental Fig. S3.2B). Thus, undifferentiated cells of the ISC lineage can be detected in the absence of *Apc*.

The presence of esg^{-} cell populations in *Apc* lineages suggested that EE cell and EC fates had been specified in the absence of *Apc*. To test this directly, we examined *Apc* lineages for the presence of EE cells and ECs using molecular markers. To determine whether EE cell fate is specified in lineages lacking *Apc*, we examined the expression of Prospero (Pros), a marker of the EE cell population (Micchelli and Perrimon, 2006; Ohlstein and Spradling, 2006). The presence of $pros^{+}$ cells was detected in *Apc* clones

(Fig. 3.5D), as observed in wild-type cell lineages (Micchelli and Perrimon, 2006; Ohlstein and Spradling, 2006). Similarly, examination of Tachykinin (Tk) expression, which marks a specific subset of EE cells (Ohlstein and Spradling, 2006), demonstrated that *Apc* is not necessary for this EE cell subtype (Fig. 3.5E). Finally, differentiated ECs are distinguished by their large, polyploid nuclei (Micchelli and Perrimon, 2006; Ohlstein and Spradling, 2006), and by the expression of Pdm1 (Nubbin - FlyBase). Inspection of *Apc* clones revealed the presence of large $Pdm1^{+}$ nuclei within mutant lineages (Fig. 3.5F). Taken together, this analysis demonstrates that ISCs lacking *Apc* are capable of producing both EE cell and EC fates.

3.4.5 *Apc* is required in ISCs to regulate proliferation

Our experiments show that a reduction or loss of *Apc* leads to ISC lineages of increased size, as well as an increase in the number of both S-phase and M-phase markers. Over time, this leads to hyperplasia and multi-layering of the midgut. Yet, no alteration in ISC self-renewal or cell fate specification was detected using lineage-tracing analysis. Collectively, these findings raised the possibility that *Apc* is required specifically in ISCs to regulate proliferation. Previous analyses demonstrated that targeted knockdown of Notch (N) in ISCs leads to an expansion of esg^{+} cell number in the midgut (Micchelli and Perrimon, 2006). Similarly, the generation of ISC lineages completely lacking *N* function leads to an expanded clonal population of undifferentiated cells (Ohlstein and Spradling, 2006). Thus, reduction of *N* function generates a population of ectopic cells that exhibit the characteristics of midgut ISCs.

If *Apc* functions specifically in ISCs to limit proliferation, then we predict that the loss of *Apc* should enhance the severity of the *N* loss-of-function phenotype. To directly test this possibility, we compared the number of cells per clone generated by ISCs lacking *N* with the number generated by ISCs lacking both *N* and *Apc*. Using the MARCM system, we created *Apc* mosaics that simultaneously expressed a N^{RNAi} transgene (Presente et al., 2002) (N^{RNAi}, $Apc2^{g10}$, $Apc1^{Q8}$; subsequently referred to as N^{RNAi}, *Apc* clones). At 10 days after induction, the cell proliferation and multi-layering observed in N^{RNAi}, *Apc* clones was often extensive (Fig. 3.6A-D; see also Supplemental Fig. S3.3), suggesting that *Apc* enhances the N^{RNAi} phenotype.

A quantitive analysis was performed to compare the number of ISCs generated in N^{RNAi}, *Apc* clones with the number of ISCs in marked N^{RNAi} lineages 5 days after induction (Fig. 3.6E-G; see also Supplemental Fig. S3.4A,B). As in previous experiments, a 5-day time point was selected for this analysis to minimize the distortion of clone size due to multi-layering. This comparison revealed a significant increase in the number of ISCs present in N^{RNAi}, *Apc* clones compared with in N^{RNAi} lineages alone (Fig. 3.6G; N^{RNAi}, *n*=116; N^{RNAi}, *Apc*, *n*=110; also compare with Fig. 3.4D for *Apc* alone). Thus, loss of *Apc* is sufficient to enhance the N^{RNAi} phenotype.

One explanation for the increased clone size in ISCs lacking both N^{RNAi} and *Apc* is that ISC proliferation has increased. If loss of *Apc* specifically affects stem cell proliferation, then we would expect to see an associated increase in the ISC mitotic index. Mitotic index was determined by counting the number of ISCs in M-phase as a function of the total number of ISCs (see Supplemental Fig. S3.4C,D). This analysis revealed a significant increase in the mitotic index of ISCs lacking both *N* and *Apc* compared with a lack of *N* alone (Fig. 3.6H; N^{RNAi}, *Apc*, *n*=16; N^{RNAi}, *n*=18). This finding, together with the increased size of N^{RNAi}, *Apc* mutant clones, demonstrates that the loss of *Apc* can affect ISC proliferation in the midgut independently of *N*-mediated cell fate specification.

3.4.6 Wnt signaling regulates homeostasis in ISC lineages

The requirement for Apc in the β-catenin destruction complex suggested that the Wnt signaling pathway might function to regulate the ISC lineage. To investigate this possibility, we first examined the effects of activating Wnt signaling on the size of marked ISC lineages. Wnt signaling was activated by generating mosaic animals expressing a constitutively active form of β-catenin, arm^{S10} (Pai et al., 1997). As in the case of *Apc* loss, arm^{S10} clones appeared abnormally large (see Supplemental Fig. S3.5A-C).

To quantify the *armS10* phenotype, we compared the number of cells labeled in ISC lineages expressing *armS10* to the number in marked wild-type lineages 5 days after induction. This analysis revealed a significant effect of arm^{S10} on ISC clone size compared with wild-type controls (see Supplemental Fig. S3.5D). A comparison of the *Apc* and arm^{S10} phenotypes revealed that in both cases there was a significant increase in clone size relative to wild-type. Nevertheless, the magnitude of the increase was greater following *Apc* loss than in the presence of arm^{S10}, as has been observed in other

contexts (e.g. (Hayden et al., 2007; Pai et al., 1997)) (see Supplemental Fig. S3.5D). Thus, Wnt pathway activation leads to an increase in the size of marked ISC lineages.

3.4.7 *Apc* hyperplasia is suppressed by reductions in Wnt signaling

The finding that constitutive Wnt activation resembled *Apc* loss raised the possibility that hyperplasia observed in ISC lineages lacking *Apc* resulted from Wnt activation. To test this directly, we examined the effect of blocking Wnt signaling in *Apc* mutants. In these studies, Wnt signaling was reduced by generating mosaic animals expressing a dominant-negative form of *pangolin* (*pan*), *pan*Δ*N*, a transcription factor necessary for Wnt signaling (Brunner et al., 1997; van de Wetering et al., 1997). Control experiments showed first that, in contrast to wild-type lineages, mosaic expression of *pan*Δ*N* resulted in reduced clone size 5 days after induction (Fig. 3.7A,B), as has previously been reported for the loss of other Wnt pathway components upstream of *pan* (Lin et al., 2008). Second, loss of a negative regulator in the Wnt pathway, *Axin* (Hamada et al., 1999b; Willert et al., 1999) phenocopied both *Apc* loss and arm^{S10} expression (Fig. 3.7C). Third, ISC lineages simultaneously expressing *pan*Δ*N* and lacking *Axin* led to complete suppression of the *Axin* loss-of-function phenotype (Fig. 3.7D). Together, these control experiments established that *pan*Δ*N* can suppress robust activation of the Wnt signaling pathway resulting from *Axin* loss.

We next investigated whether *pan*Δ*N* was sufficient to suppress the *Apc* double mutant phenotype. Simultaneous expression of *pan*Δ*N* in ISC lineages lacking $Apc2^{33}$ and $Apc1^{Q8}$ led to a complete suppression of *Apc* hyperplasia (Fig. 3.7E,F). However, simultaneous expression of *pan*Δ*N* in ISC lineages lacking $Apc2^{g10}$ and $Apc1^{Q8}$ resulted only in a partial suppression of the *Apc* phenotype (Fig. 3.7G,H). One potential explanation for these differences is that $Apc2^{g10}$, in contrast to $Apc2^{33}$, encodes a protein that retains an amino-terminal fragment, which has been shown to have an activating role in the Wnt signaling pathway (Takacs et al., 2008). Similarly truncated alleles of *Apc* are known to be associated with human adenomas (Albuquerque et al., 2002; Cheadle et al., 2002; Lamlum et al., 1999; Rowan et al., 2000). Taken together, our studies show that the abrogation of Wnt signaling in ISC lineages is sufficient to suppress the effect of *Apc* loss in an allele-specific manner.

3.5 Discussion

In the current study, we report that loss of *Apc* results in a disruption of midgut homeostasis and is associated with hyperplasia and multi-layering of the midgut epithelium. Our mosaic analyses show that *Apc* is required specifically in ISCs to regulate stem cell proliferation. By contrast, loss of *Apc* did not detectably affect self-renewal or cell fate specification in the ISC lineage. Activation of Wnt signaling in the ISC lineage phenocopied *Apc* loss and *Apc* mutants were suppressed in an allele-specific manner by abrogating Wnt signaling, suggesting that the effects of *Apc* are mediated in part by the Wnt pathway. The finding that Apc differentially affects ISC proliferation without obviously altering self-renewal or multi-potency highlights the ability of the stem cell to fine-tune lineage output to meet homeostatic need; loss of Apc appears to short-circuit this regulation, providing increased cellular output in the absence of true physiological demand for new cells.

Previous analysis of Wnt signaling in the midgut has led to the assertion that Wnt functions as the primary maintenance signal for ISCs; cell-autonomous loss of Wnt transduction components results in a failure of ISC maintenance, while ectopic expression of Wnt ligand leads to an increase in the number of Dl-expressing cells (Lin et al., 2008). These observations led to the following model: transduction of the Wnt signaling pathway in ISCs adjacent to a Wnt source maintains the stem cell population by preventing lineage differentiation. A central prediction of the model is that cell-autonomous activation of the Wnt signaling pathway in ISCs should lead to the production of daughter cells, which constitutively transduce the Wnt signal and, as such, remain undifferentiated. The predicted consequence of this manipulation is an expansion in the number of ISCs at the expense of differentiated cells within the lineage, as has been observed in the case of N loss (Micchelli and Perrimon, 2006; Ohlstein and Spradling, 2006; Ohlstein and Spradling, 2007). In this study, we directly tested this prediction by analyzing marked ISC lineages. Our experiments clearly demonstrate that in contrast to *N* loss, ISCs lacking Apc generate both differentiated cell types of the adult midgut: EE cells and ECs. Importantly, these findings suggest that ISCs and their daughters are not distinguished solely on the basis of Wnt signal transduction.

Several explanations could account for these apparent disparities. First, it is worth noting that although Dl might be a reliable marker for certain stem cells in wild-type midguts, this might not be the case in every mutant background examined. For example, a previous analysis in *Drosophila* has

demonstrated that Wnt activation is sufficient to stimulate high levels of Dl expression in a cell-autonomous manner (Micchelli et al., 1997). Thus, it is possible that Wnt pathway activation can uncouple Dl expression from stem cell identity, thereby diminishing the utility of Dl as a reliable stem cell marker. A second possible explanation is methodological; the use of genetic mosaic analyses to analyze individual ISC lineages, as in this study, might provide a different view of the Wnt pathway activation phenotype to that seen following the use of Gal4 driver lines. Third, it is possible that Wnt can affect stem cell maintenance upstream of Apc via a noncanonical pathway. For example, studies have demonstrated that Wnt signaling can act directly via dishevelled (dsh) to inhibit the N signaling pathway (Axelrod et al., 1996; Rulifson et al., 1996). Such effects might not be detected in the *Apc*, *Axin* or activated arm^{S10} ISC lineages analyzed here.

In this study, we have demonstrated an increase in the number of dividing cells following Apc loss, which is consistent with what has previously been reported for mutations that activate the Wnt pathway (Lin et al., 2008). And yet, as discussed above, the presence of differentiated cells within marked Apc mutant lineages strongly suggested that the increase in dividing cells could not be explained solely by a N-dependent change in cell fate within the ISC lineage as was proposed by Lin et al. Based on our analysis of Apc, we hypothesized that the increased proliferation following *Apc* loss reflects a cell-autonomous requirement for Apc specifically in ISCs. This view is further supported by the observation that *Apc* loss can lead to an increase in mitotic index when *N* and *Apc* are simultaneously removed from the ISC lineage. Thus, there is a requirement for Apc specifically in ISCs to regulate proliferation that is separable from N-dependent cell fate specification. Taken together, we conclude that a primary requirement for Apc in the ISC lineage is to autonomously restrict the proliferation of ISCs, and not to regulate the choice of cell fate.

On the basis of our findings we propose that ISC activity is regulated by the level of Wnt signal transduction (Fig. 3.8). In this model, Wnt functions as a permissive signal for ISC self-renewal, as we show that constitutive Wnt activation is not a sufficient criterion to convert all ISC progeny to stem cells, nor is activation sufficient to alter the fidelity of ISC self-renewal. Intermediate levels of Wnt define an adaptive homeostatic range, which permits the midgut to respond to environmental changes that the

organism encounters. ISCs transducing Wnt at levels outside this range appear refractory to homeostatic input, as low levels of Wnt are associated with ISC loss, whereas Wnt activation leads to hyperplasia.

Nevertheless, our data do not rule out additional roles for Apc in the ISC lineage. For example, it is possible that the hyperplasia observed in Apc mutants reflects the combined requirement of Apc to regulate proliferation both in the ISCs and in nascent EB daughters. Similarly, Apc might also play a role in regulating cell turnover in the midgut. Indeed, several of our observations support the view that Apc might, in fact, be required for EC differentiation. First, mosaic analysis of *Apc* shows that cells of the lineage contribute to the multi-layering phenotype, which suggests that mutant cells might have failed to properly establish appropriate adhesive contacts with the monolayer and/or the surrounding extracellular matrix (Fig. 3.3D,F). Second, although ECs lacking *Apc* appear to have large, polyploid nuclei and express molecular markers such as Pdm1, their nuclei are often detectably smaller than those of wild-type ECs (Fig. 3.4B,C). Furthermore, ECs lacking *Apc* often exhibit a restricted basal profile, failing to develop the tiled morphology that is characteristic of wild-type ECs (Fig. 3.4B,C). Finally, in the absence of *Apc*, ECs often display reduced cytoplasm, suggesting a requirement for cellular growth, a requirement that is not observed in either *Axin* mutant or arm^{S10}-expressing ICS lineages (Fig. 3.7; see also Supplemental Fig. S3.5).

The discovery that Apc is somatically mutated in cells of the smallest human adenomas (Miyoshi et al., 1992; Powell et al., 1992) and that the frequency of *Apc* mutations detected among early adenomas is roughly the same as the frequency of *Apc* mutations in more advanced carcinomas (Powell et al., 1992) were among the seminal observations that established Apc as the rate-limiting step for gastrointestinal tumor initiation (reviewed in (Clevers, 2006; Kinzler and Vogelstein, 1996)). Subsequently, a number of *Apc* models have been established in both mouse and zebrafish to study gastrointestinal tumorigenesis (Fodde et al., 1994; Haramis et al., 2006; Oshima et al., 1995; Su et al., 1992). Yet, the precise cell(s) in which Apc is required remained unknown. Recently, through the use of refined genetic cell lineage tracing methodologies in the mouse, specific subpopulations of cells in the intestinal mucosa have been identified (e.g. $Lgr5^{+}$ and $Bmi1^{+}$), which display the ability to self-renew and undergo multi-lineage differentiation (Barker et al., 2007; Sangiorgi and Capecchi, 2008).

Subsequent studies have demonstrated that deletion of *Apc* specifically within the $Lgr5^+$ cell population leads to the formation of rapidly proliferating cells in both the large and small intestine (Barker et al., 2009). Thus, in the case of both *Drosophila* ISCs and mouse $Lgr5^+$ cells, loss of *Apc* leads to a disruption of homeostasis in the intestinal stem cell lineage. The remarkable parallels that exist between the dipteran and mammalian gastrointestinal tract suggest that the *Drosophila* midgut will continue to be a powerful genetic model system with which to dissect the molecular mechanisms underlying tumor initiation.

3.6 Figures

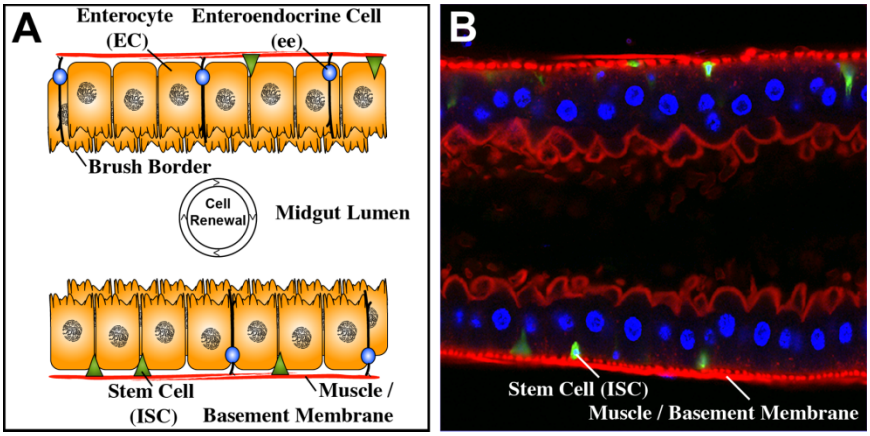

Figure 3.1: The adult *Drosophila* midgut is maintained by a population of multi-potent intestinal stem cells (ISCs). (A) Diagram of the adult midgut in cross section. ISCs (green) occupy a basal position in a niche adjacent to the basement membrane and the visceral muscle (red). ISCs give rise to two types of differentiated daughters, enteroendocrine (ee) cells (blue) and enterocytes (ECs; orange). (B) A cross section of the adult midgut showing ISCs marked by *esg-Gal4, UAS-GFP* (green). ECs have large polyploid nuclei (blue, DAPI) and form a polarized cellular monolayer with an actin-rich (red, phalloidin) brush border on their luminal surface; EE cells are not marked.

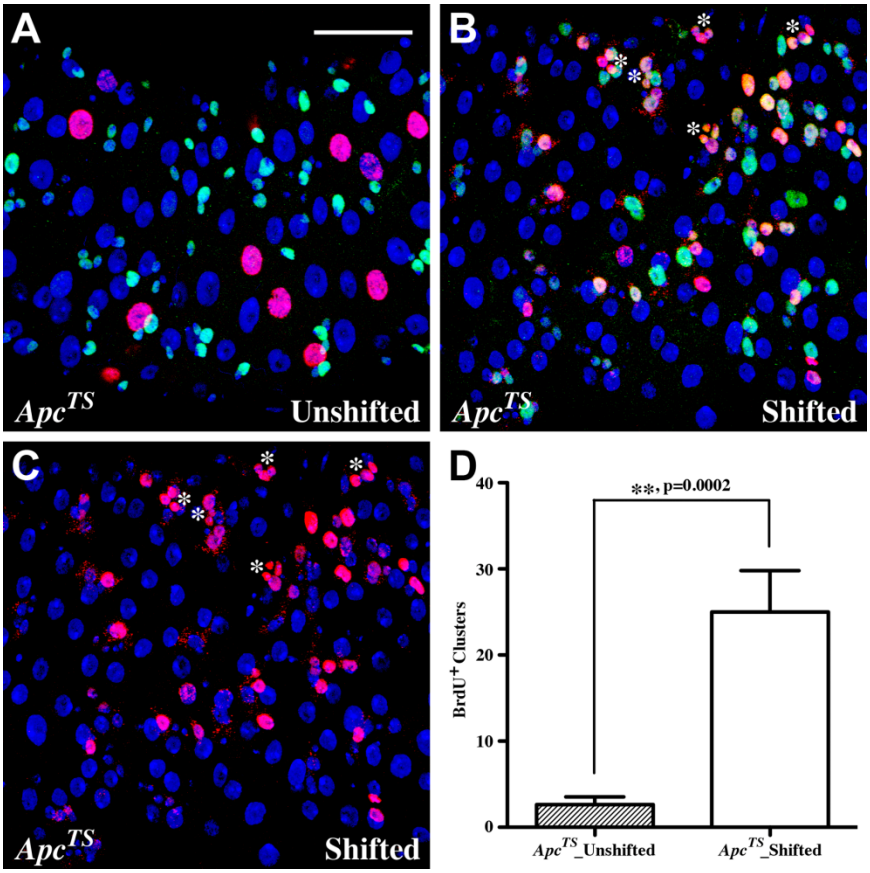

Figure 3.2: *Apc* is required to maintain adult midgut homeostasis. (A-D) Global reduction of *Apc* family genes leads to an increase in BrdU incorporation in *esg-lacZ* cells (anti-BrdU, red; anti-βgal, green; DAPI, blue). Superficial views of midgut. (A) Apc^{TS} unshifted. Note that large polyploid EC nuclei incorporate BrdU. (B,C) Apc^{TS} shifted. Asterisks indicate esg^{+} $BrdU^{+}$ cells. (D) Quantitation of $BrdU^{+}$ cells (unshifted, *n*=11; shifted, *n*=11). Error bars denote s.e.m. ***P*=0.0002. Scale bar: 50 μm.

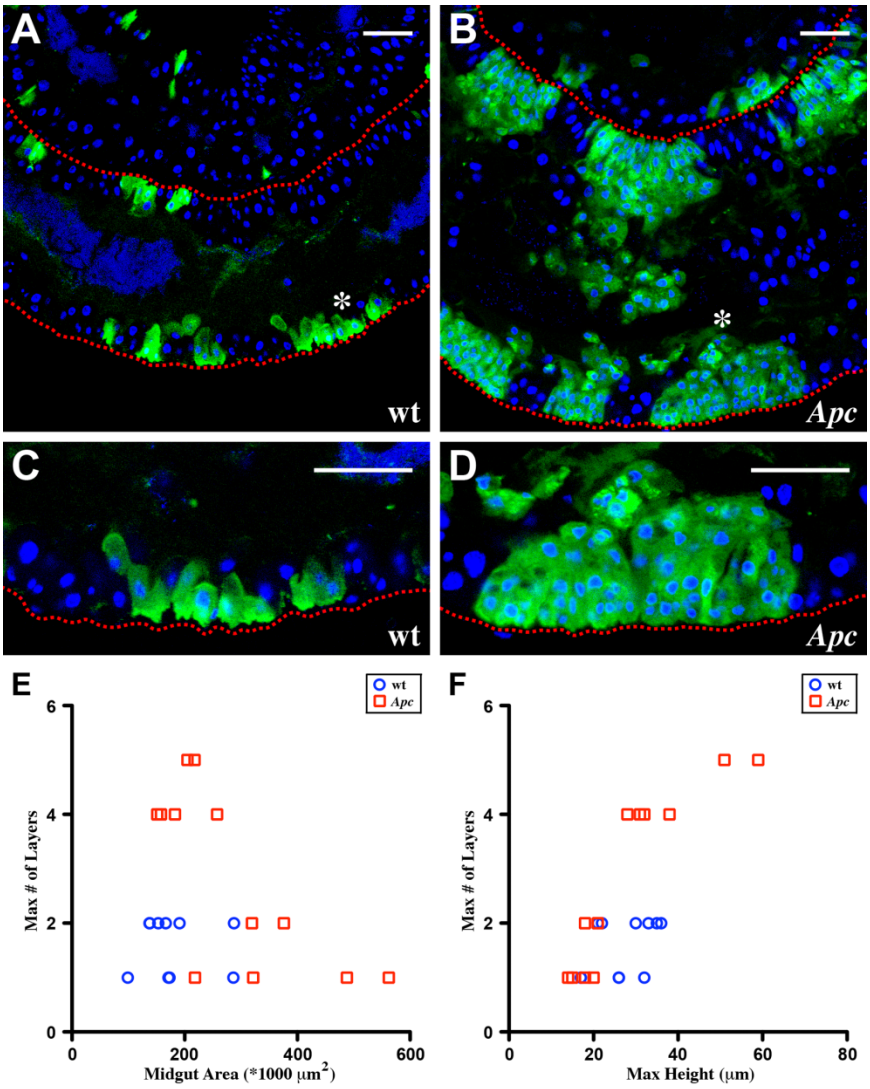

Figure 3.3: Loss of *Apc* in the midgut leads to hyperplasia and multi-layering. (A-D) The MARCM system was used to positively identify ISC lineages with GFP 20 days after induction (anti-GFP, green; DAPI, blue). Midgut viewed in cross section; dashed red line indicates midgut outline. (A) Wild-type ISC lineages. Marked cells define a single cellular layer. (B) ISC lineages lacking *Apc*. Loss of *Apc* leads to midgut hyperplasia and extensive multi-layering. (C) High magnification view of A. Frame corresponds to the region on the outer face of the midgut indicated by the asterisk (A). (D) High magnification view of B. Frame corresponds to the region on the outer face of the midgut indicated by the asterisk (B). (E) Maximal number of midgut layers plotted as a function of midgut area in wild-type and *Apc* mosaic midguts. Note the multi-layering and increased area in *Apc* mosaic midguts. (F) Maximal number of

midgut layers plotted as a function of maximal epithelial height in wild-type and *Apc* mosaic midguts. Scale bars: 50 μm.

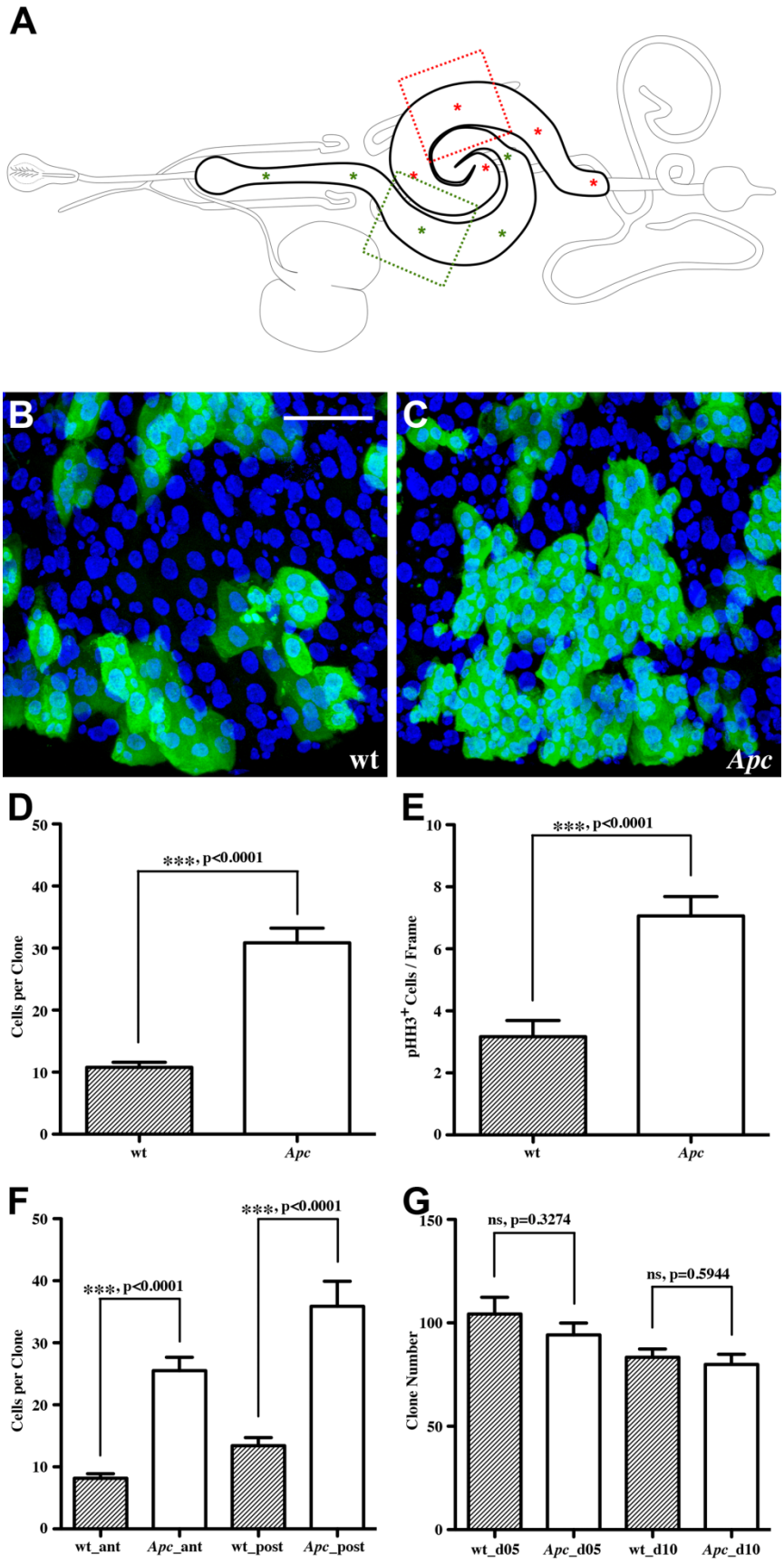
A
B
wt
C
Apc
D
***, p<0.0001
Cells per Clone
0
10
20
30
40
50
wt
Apc
E
***, p<0.0001
pHH3+ Cells / Frame
0
2
4
6
8
10
wt
Apc
F
***, p<0.0001
***, p<0.0001
Cells per Clone
0
10
20
30
40
50
wt_ant
Apc_ant
wt_post
Apc_post
G
ns, p=0.3274
ns, p=0.5944
Clone Number
0
50
100
150
wt_d05
Apc_d05
wt_d10
Apc_d10

Figure 3.4: Loss of *Apc* in ISCs leads to an increase in clone size. (A) Diagram of the adult *Drosophila* gastrointestinal tract (see Miller, 1950); midgut in heavy black outline. Data were collected from two morphologically defined regions: one in the middle of the anterior midgut (green frame) and one in the middle of the posterior midgut (red frame). (B-G) The MARCM system was used to positively identify ISC lineages with GFP (anti-GFP, green; DAPI, blue). (B) Wild-type ISC lineages in posterior midgut 5 days after induction, superficial view. (C) ISC lineages lacking *Apc* in posterior midgut 5 days after induction, superficial view. (D) *Apc* loss leads to an increase in the number of cells per clone (wild-type, *n*=76; *Apc*, *n*=76). (E) Mosaic midguts lacking *Apc* display an increase in the number of pHH3+ cells (wild-type, *n*=18; *Apc*, *n*=17). (F) Analysis of *Apc* clones along the anteroposterior axis of the midgut. Compared with wild-type, *Apc* clones are larger in both the anterior (wild-type, *n*=38; *Apc*, *n*=37) and posterior (wild-type, *n*=38; *Apc*, *n*=39) regions. (G) Self-renewal is not detectably altered in ISCs lacking *Apc* at 5 days (wild-type, *n*=6; *Apc*, *n*=6) or 10 days (wild-type, *n*=8; *Apc*, *n*=9) after induction. Error bars denote s.e.m. Scale bar: 50 μm.

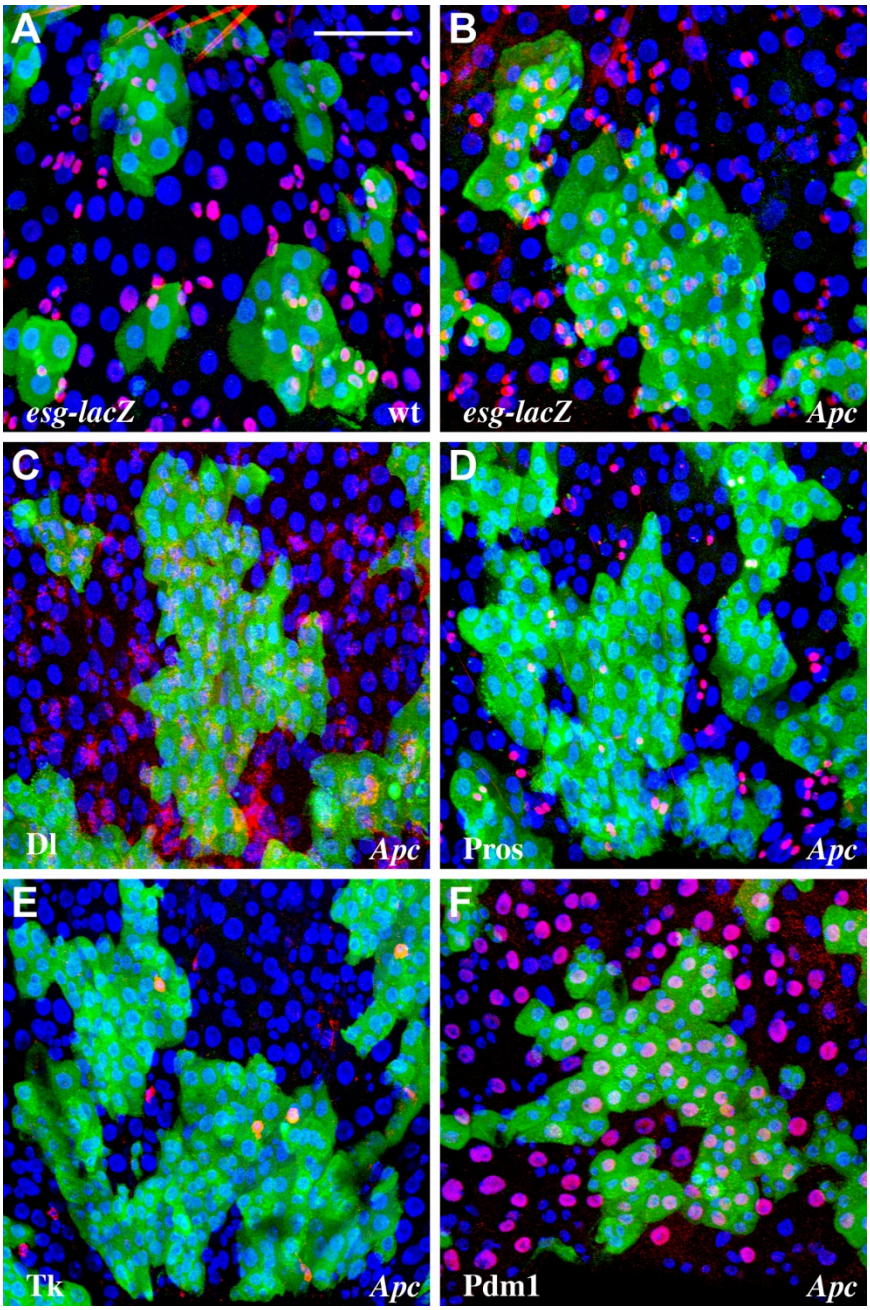

Figure 3.5: Cell fate in the ISC lineage is correctly specified in the absence of *Apc*. (A-F) The MARCM system was used to positively identify ISC cell lineages with GFP 5 days after induction (anti-GFP, green; DAPI, blue). (A) Wild-type ISC lineages. *esg-lacZ* (red) marks the undifferentiated cells in the ISC lineage: stem cells and their undifferentiated EB daughters. (B) ISC lineages lacking *Apc*; *esg-lacZ* shown in red. Note the presence of both esg^{+} and esg^{-} cells in marked *Apc* lineages. (C) ISC lineages lacking *Apc* (anti-Dl, red). (D) ISC lineages lacking *Apc*. Anti-Pros (red) marks EE cells in the clone. (E)

ISC lineages lacking *Apc*. Anti-Tachykinin (red) marks a subset of EE cells in the clone. (F) ISC lineages lacking *Apc*. Anti-Pdm1 (red) marks ECs. Scale bar: 50 μm.

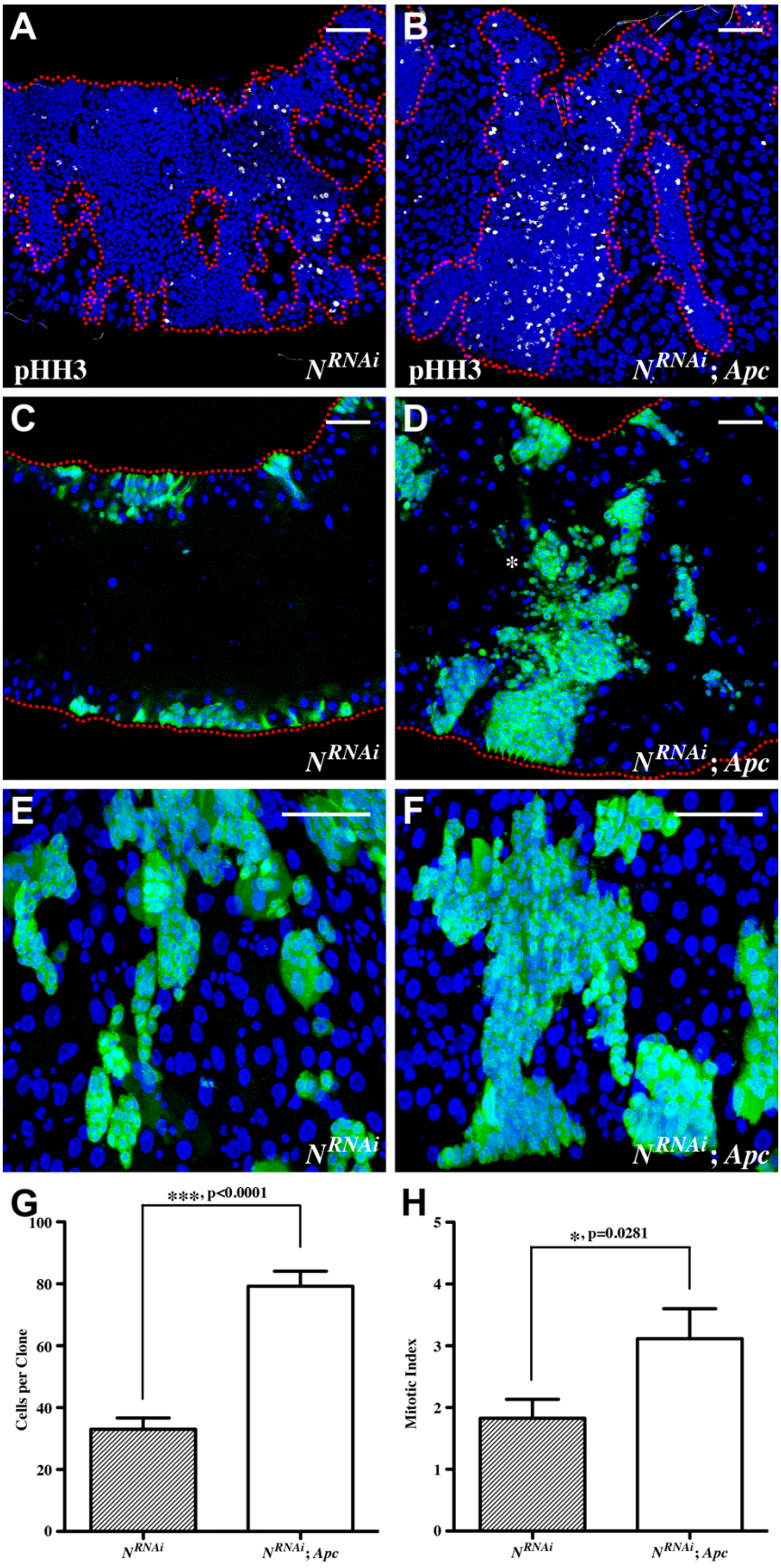
A
pHH3
N^RNAi
B
pHH3
N^RNAi; Apc
C
N^RNAi
D
*
N^RNAi; Apc
E
N^RNAi
F
N^RNAi; Apc
G
***, p<0.0001
Cells per Clone
100
80
60
40
20
0
N^RNAi
N^RNAi; Apc
H
*, p=0.0281
Mitotic Index
5
4
3
2
1
0
N^RNAi
N^RNAi; Apc

Figure 3.6: *Apc* is required in ISCs to regulate proliferation. (A-F) The MARCM system was used to positively identify ISC lineages with GFP. (A,B) Clone outlines indicated in red, nuclei in blue (DAPI), and dividing cells in white (phospho-histone H3). (A) ISC clones expressing N^{RNAi} 10 days after induction. (B) ISC clones expressing N^{RNAi} and lacking *Apc*, 10 days after induction. (C,D) ISC lineages marked with GFP (anti-GFP, green; DAPI, blue); dashed red line indicates midgut outline. (C) ISC clones expressing N^{RNAi} 10 days after induction. (D) ISC clones expressing N^{RNAi} and lacking *Apc*, 10 days after induction. Extensive multi-layering is evident in cross section. Asterisk indicates hyperplalastic cells in lower focal planes extending up into the luminal space. (E-H) Quantitation of ISC proliferation phenotype. (E) ISC clones expressing N^{RNAi} 5 days after induction. (F) ISC clones expressing N^{RNAi} and lacking *Apc*, 5 days after induction. (G) Comparison of N^{RNAi} and N^{RNAi}, *Apc* clone size 5 days after induction. N^{RNAi}, *Apc* loss leads to an increase in number of cells per clone (N^{RNAi}, n=116; N^{RNAi}, *Apc*, n=110). (H) Comparison of N^{RNAi} and N^{RNAi}, *Apc* mitotic index 5 days after induction. *Apc* loss leads to an increase in the ISC mitotic index (N^{RNAi}, n=18; N^{RNAi}, *Apc*, n=16). Error bars denote s.e.m. Scale bars: 50 μm.

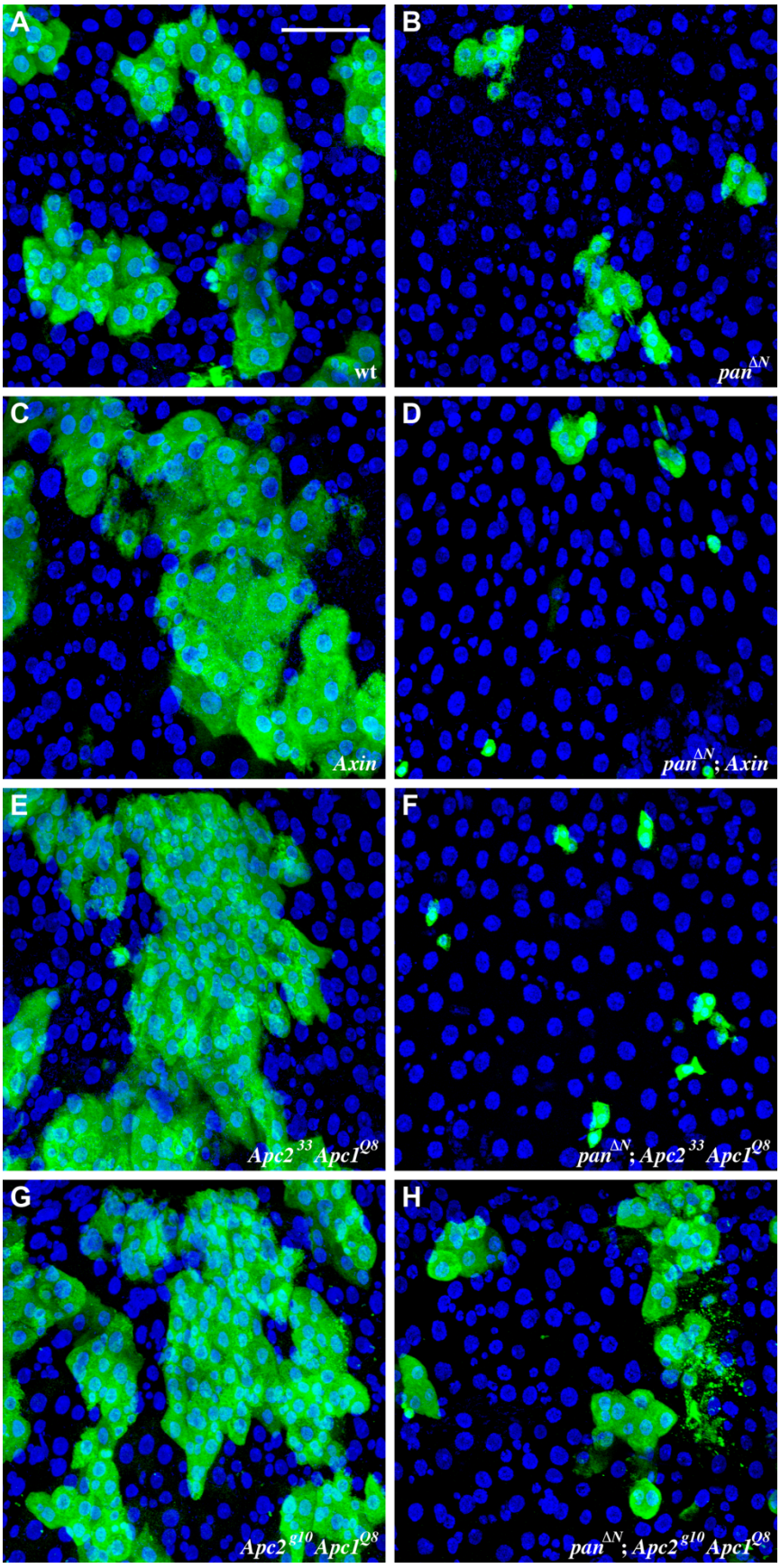
A
wt
B
pan^ΔN
C
Axin
D
pan^ΔN; Axin
E
Apc2^33 Apc1^Q8
F
pan^ΔN; Apc2^33 Apc1^Q8
G
Apc2^g10 Apc1^Q8
H
pan^ΔN; Apc2^g10 Apc1^Q8

Figure 3.7: *Apc* hyperplasia is suppressed by reducing Wnt signaling. (A-H) The MARCM system was used to positively identify posterior ISC cell lineages with GFP 5 days after induction (anti-GFP, green; DAPI, blue). (A) Wild-type ISC lineages. (B) ISC lineages expressing *pan*Δ*N* (dominant negative). (C) ISC lineages lacking *Axin.* (D) ISC lineages lacking *Axin* and expressing *pan*Δ*N*. (E) ISC lineages lacking $Apc2^{33}$ and $Apc1^{Q8}$. (F) ISC lineages lacking $Apc2^{33}$ and $Apc1^{Q8}$, and expressing *pan*Δ*N*. Note that hyperplasia is suppressed. (G) ISC lineages lacking $Apc2^{g10}$ and $Apc1^{Q8}$. (H) ISC lineages lacking $Apc2^{g10}$ and $Apc1^{Q8}$, and expressing *pan*Δ*N*. Scale bar: 50 μm.

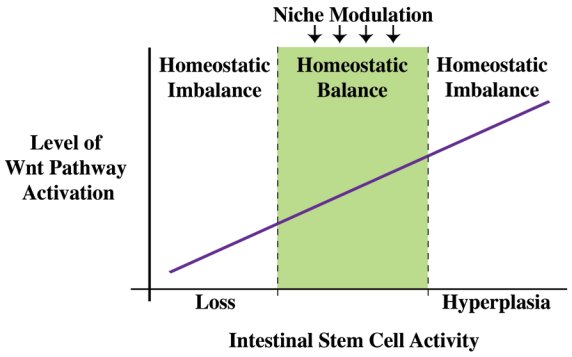

Figure 3.8: Wnt regulation of midgut ISCs. Wnt functions as a permissive signal, and at intermediate levels of signal transduction defines an adaptive homeostatic range for ISCs activity (green). In this model, niche modulation fine-tunes ISC activity within this adaptive homeostatic range.

3.7 Supplementary material

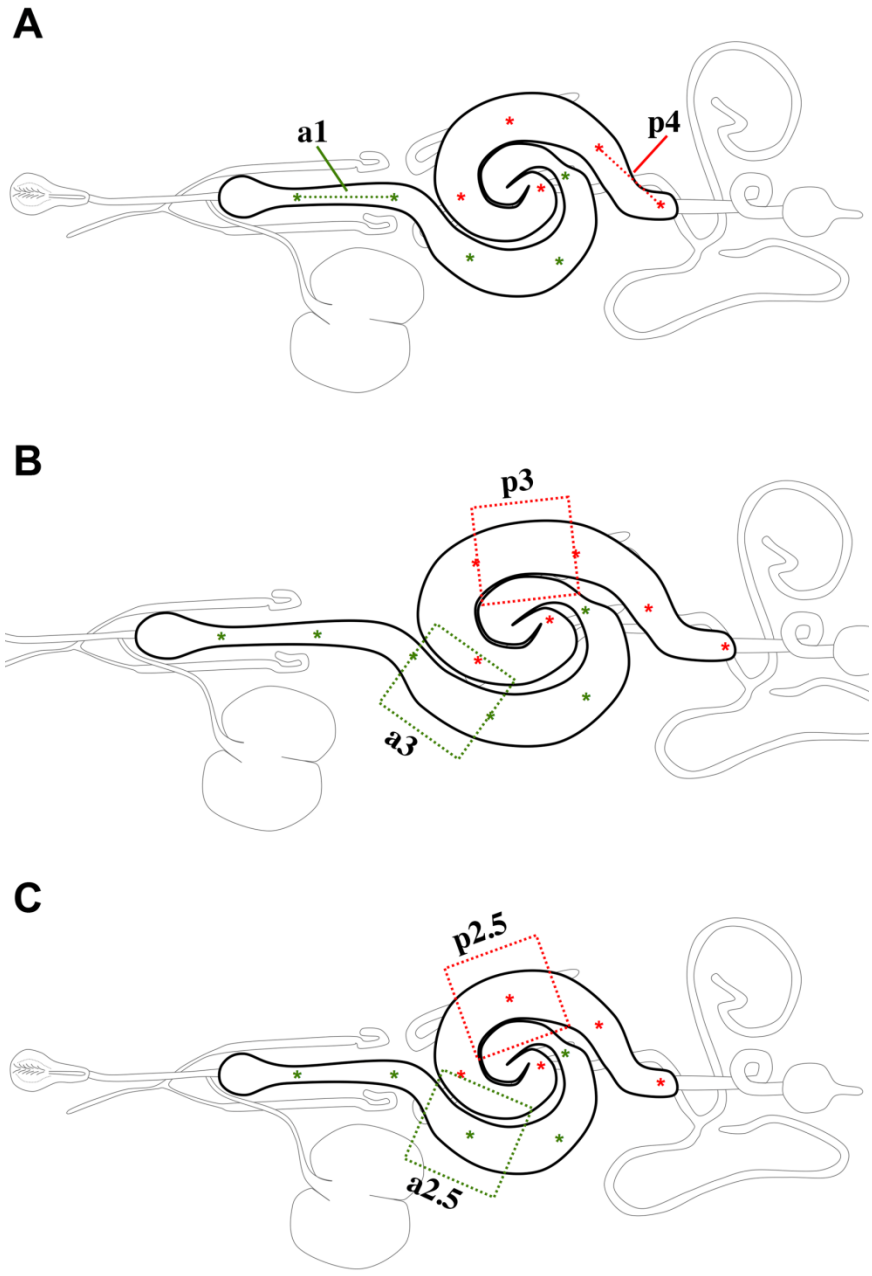

Supplemental Figure S3.1: The standard quantitative method used in analyzing mosaic midguts. (A) Diagram of the adult *Drosophila* gastrointestinal tract (see (Miller, 1994)). The adult midgut extends the length between the cardia and the pylorus (heavy black outline). Data were collected from two defined regions of each midgut analyzed: the middle of the anterior midgut and the middle of the posterior midgut. To reproducibly determine the middle of both the anterior and posterior midgut, each segment was first

independently divided into a series of non-overlapping 40x fields of view or frames using the confocal microscope (green and red asterisks, respectively). The anterior segment extends from the narrowest region following the cardia to the anterior limit of the copper cells; the anterior-most frame we designated a1. The posterior segment extends from the posterior limit of the copper cells to the anterior limit of the pylorus where the malpighian tubules enter the tract; the anterior-most frame of the posterior midgut we designated p1. Under our experimental conditions, we found that the anterior and posterior segments of the midgut can each be covered in the span of 5 (or 4) frames (e.g. a1-a5, p1-p4). (B) In a 10-frame midgut, the middle of the anterior is therefore centered at a3 (green frame), and the middle of the posterior is centered at p3 (red frame). (C) In an 8-frame midgut the middle of the anterior is centered at a2.5, and the middle of the posterior is centered at p2.5. Midguts were measured twice before selecting the final frames used for analysis.

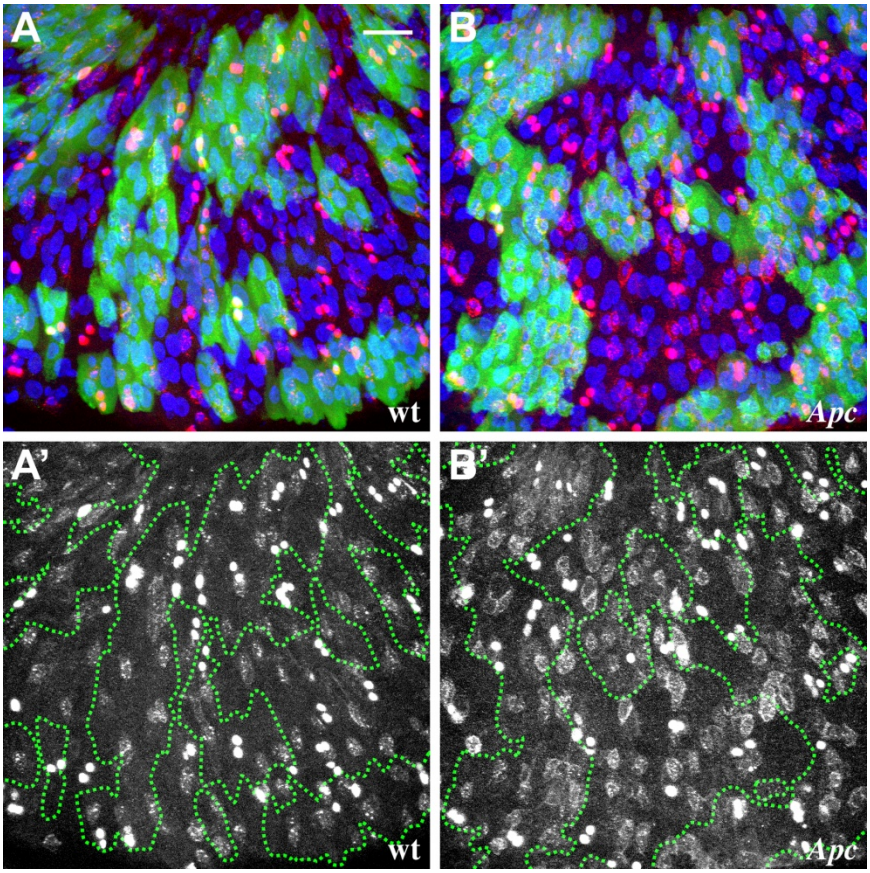

Supplemental Figure S3.2: *Apc* loss leads to increased Dl levels. (A,B) The MARCM system was used to positively identify ISC lineages with GFP 5 days after induction (anti-GFP, green; anti-Pros and anti-Dl, red; DAPI, blue). Note that anti-Dl and anti-Pros are both shown in red; Dl staining appears punctate and membrane localized, whereas Pros expression is saturated and nuclear. (A' ,B') Clone boundary indicated by green outline, anti-Dl and anti-Pros are both shown in white. (A, A') Wild-type ISC lineages. (B, B') ISC lineages lacking *Apc*. Note that, compared with wild type, Dl appears at higher levels in some ISC/EB pairs both within and outside of marked *Apc* lineages. Scale bar: 50 μm.

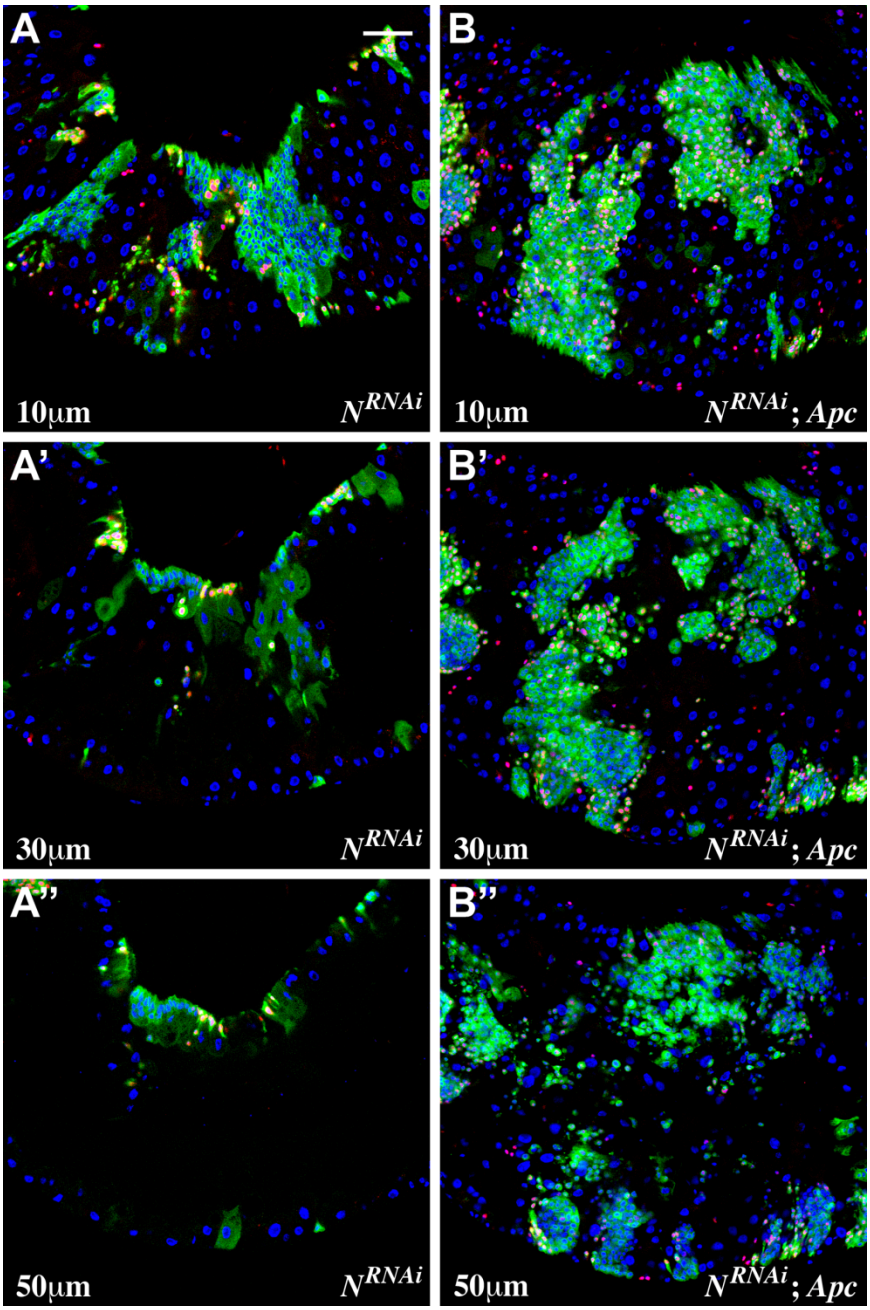

Supplemental Figure S3.3: Loss of Apc in ISCs enhances hyperplasia and multi-layering of the N^{RNAi} phenotype. (A, B) The MARCM system was used to positively identify ISC lineages with GFP 10 days after induction (anti-GFP, green; anti-Pros, red; DAPI, blue). A series of progressively deeper optical sections from the surface of the midgut is shown at 10 μm, 30 μm and 50 μm from the basement membrane. (A-A") ISC lineages expressing N^{RNAi}. (B-B") ISC lineages expressing N^{RNAi} but lacking *Apc*. Hyperplasia, multi-layering and disruption of midgut organization are evident. Scale bar: 50 μm.

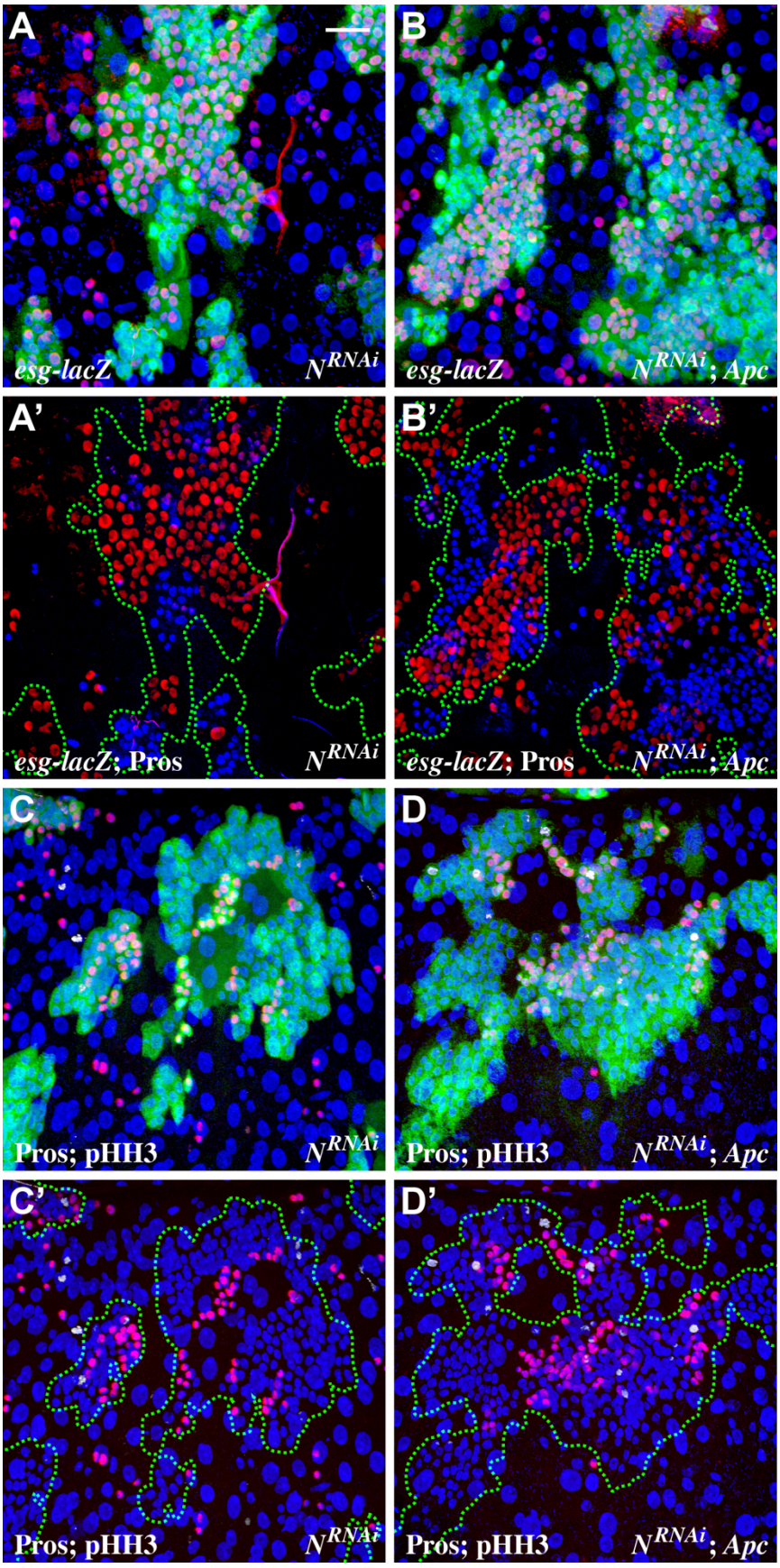
A
esg-lacZ
N^RNAi
B
esg-lacZ
N^RNAi; Apc
A'
esg-lacZ; Pros
N^RNAi
B'
esg-lacZ; Pros
N^RNAi; Apc
C
Pros; pHH3
N^RNAi
D
Pros; pHH3
N^RNAi; Apc
C'
Pros; pHH3
N^RNAi
D'
Pros; pHH3
N^RNAi; Apc

Supplemental Figure S3.4: Quantification of clone size and mitotic index in N^{RNAi}, *Apc* lineages. (A-D) The MARCM system was used to positively identify ISC lineages with GFP 5 days after induction (anti-GFP, green; DAPI, blue). (A'-D') Clone boundary indicated by green outline. (A', B') Quantification of the number of cells per clone. To quantify the phenotype only esg^+ $pros^-$ cells were scored (*esg-lacZ*, red; anti-Pros; blue). (A') N^{RNAi}; (B') N^{RNAi}, *Apc*. (C',D') Quantification of mitotic index. To quantify the phenotype, only small $pHH3^+$ $pros^-$ cells were scored (anti-Pros, red; anti-phospho-histone H3, white; DAPI, blue). (C') N^{RNAi}; (D') N^{RNAi}, *Apc*. Scale bar: 50 μm.

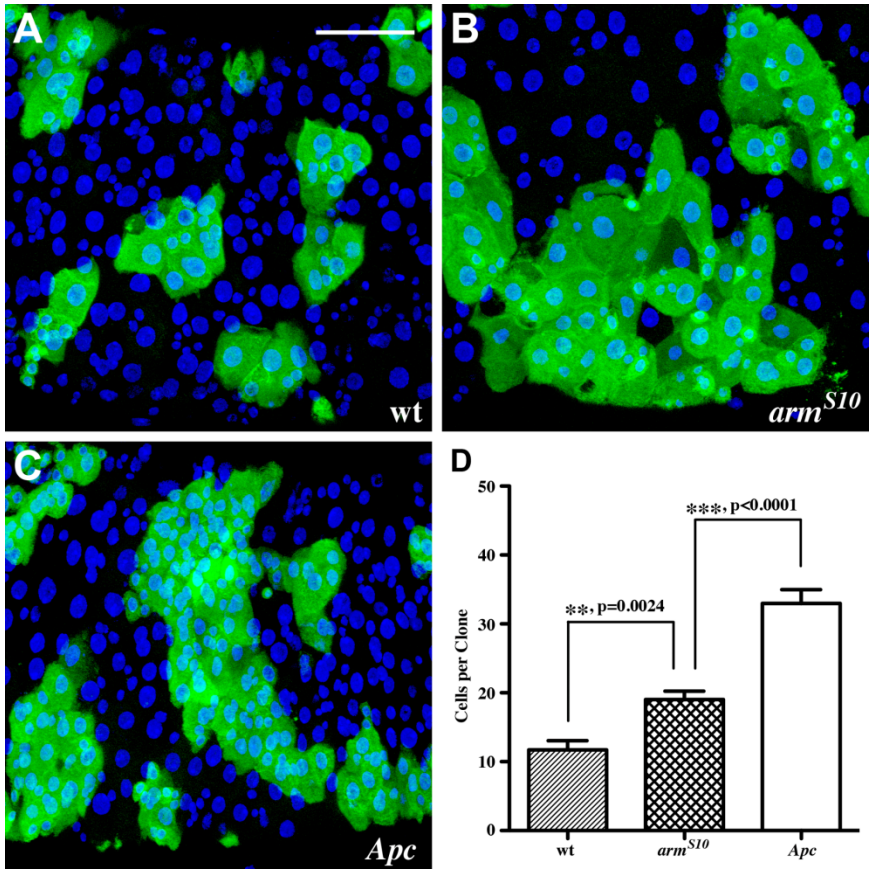

Supplemental Figure S3.5: Wnt activation in the ISC lineage leads to an increase in clone size. (A-D) The MARCM system was used to positively identify posterior ISC lineages with GFP 5 days after induction (anti-GFP, green; DAPI, blue). (A) Wild-type ISC lineages. (B) ISC lineages expressing arm^{S10}. (C) ISC lineages lacking *Apc*. (D) Quantitation of the number of cells per clone in arm^{S10} and *Apc* mutant lineages. arm^{S10} expression leads to a significant increase in clone size compared with wild type, although not as great as that caused by *Apc* loss. (wild-type, n=41; arm^{S10}, *n*=144; *Apc*, *n*=157). Error bars denote s.e.m. Scale bar: 50 μm.

3.8 References

Ahmed, Y., Hayashi, S., Levine, A., and Wieschaus, E. (1998). Regulation of Armadillo by a *Drosophila APC* Inhibits Apoptosis during Retinal Development. *Cell* 93, 1171-1182.

Ahmed, Y., Nouri, A. and Wieschaus, E. (2002). *Drosophila Apc*1 and *Apc*2 regulate Wingless transduction throughout development. *Development* 129, 1751-1762.

Akong, K., Grevengoed, E. E., Price, M. H., McCartney, B. M., Hayden, M. A., DeNofrio J. C. and Peifer, M. (2002a). *Drosophila APC2* and *APC1* Play Overlapping Roles in Wingless Signaling in the Embryo and Imaginal Discs. *Dev Biol.* 250, 91-100.

Akong, K., McCartney, B. M. and Peifer, M. (2002b). *Drosophila APC*2 and *APC*1 Have Overlapping Roles in the Larval Brain Despite Their Distinct Intracellular Localizations. *Dev Biol.* 250, 71-90.

Albuquerque, C., Breukel, C., van der Luijt, R., Fidalgo, P., Lage, P., Slors, F.J.M., Leitao, C.N., Fodde, R., and Smits, R. (2002). The 'just-right signalling model: APC somatic mutations are selected based on a specific level of activation of the β-catenin signalling cascade. *Hum. Mol. Genet.* 11, 1549-1560.

Axelrod, J. D., Matsuno, K., Artavanas-Tsakonas, S. and Perrimon, N. (1996). Interaction between Wingless and Notch signaling pathways mediated by dishevelled. *Science* 271, 1826-1832.

Barker, N., Ridgway, R. A., van Es, J. H., van de Wetering, M., Begthel, H., van den Born, M., Danenberg, E., Clarke, A. R., Sansom, O. J. and Clevers, H. (2009). Crypt stem cells as the cells-of-origin of intestinal cancer. *Nature* 457*, 608-611*.

Barker, N., van Es, J. H., Kuipers, J., Kujala, P., van den Born, M., Cozijnsen, M., Haegebarth, A., Korving, J., Begthel, H., Peters, P. J. and Clevers, H. (2007). Identification of stem cells in small intestine and colon by marker gene Lgr5. *Nature* 449, 1003-1007.

Brunner, E., Peter, O., Schweizer, L., and Basler, K. (1997). pangolin encodes a Lef-1 homolog that acts downstream of Armadillo to transduce the Wingless signal in Drosophila. *Nature* 385, 829-833.

Cheadele, J.P., Krawczak, M., Thomas, M.W., Kodges, A.K., Al-Tassan, N., Pleming, N., and Sampson, J.R. (2002). Different Combinations of Biallelic APC Mutation Confer Different Growth Advantages in Colorectal Tumors. *Cancer Res.* 62, 363-366.

Clevers, H. (2006). Wnt/beta-catenin signaling in development and disease. *Cell* 127, 469-480.
Fodde, R., Edelmann, W., Yang, K., van Leeuwen, C., Carlson, C., Renault, B., Breukel, C., Alt, E., Lipkin, M., Khan, P. M., et al. (1994). A targeted chain termination mutation in the mouse *Apc* gene results in multiple intestinal tumors. *Proc. Natl. Acad. Sci. USA* 91, 8969-8973.

Groden, J., Thliveris, A., Samowitz, W., Carlson, M., Gelbert, L., Albertsen, H., Joslyn, G., Stevens, J., Spirio, L. and Robertson, M., et al., (1991). Identification and characterization of the familial adenomatous polyposis coli gene. *Cell* 66, 589-600.

Hamada, F., Murata, Y., Nishida, A., Fujita, F., Tomoyasu, Y., Nakamura, M., Toyoshima, K., Tabata, T., Ueno, N. and Akiyama, T. (1999a). Identification and characterization of E-*APC*, a novel *Drosophila* homologue of the tumor suppressor *APC*. *Genes to Cells* 4, 465-474.

Hamada, F., Tomoyasu, Y., Takatsu, Y., Nakamura, M., Nagai, S., Suzuki, A., Fujita, F., Shibuya, H., Toyoshima, K., Ueno, N. and Akiyama, T. (1999b). Negative regulation of Wingless signalling by Daxin, a Drosophila homolog of axin. *Science* 283, 1739-1942.

Haramis, A. P., Hurlstone, A., van der Velden, Y., Begthel, H., van den Born, M., Offerhaus, G.J. and Clevers, H. C. (2006). Adenomatous polyposis coli-deficient zebrafish are susceptible to digestive tract neoplasia. *Embo Rep.* 7, 444-449.

Hayashi, S., Rubinfeld, B., Souza, B., Polakis, P. Wieschaus, E. and Levine, A.J. (1997). A *Drosophila* homolog of the tumor suppressor gene *adenomatous polyposis coli* down-regulates β-catenin but its zygotic expression is not essential for the regulation of Armadillo. *Proc. Natl. Acad. Sci. USA* 94, 242-247.

Hayden, M. A., Akong, K. and Peifer, M. (2007). Novel roles for *APC* family members and Wingless/Wnt signaling during *Drosophila* brain development. *Dev Biol.* 305, 358-376.

Ichii, S., Horii, A., Nakatsuru, S., Furuyama, J., Utsunomiya, J., Nakamura, Y. (1992). Inactivaton of both *APC* alleles in an early stage of colon adenoma in a patient with familial adenomatous polyposis (FAP). *Hum Mol Genet.* 1, 387-390.

Jones, D. L. and Wagers, A. J. (2008). No place like home: anatomy and function of the stem cell niche. *Nature Reviews* 9, 11-21.

Kinzler, K. W., Nilbert, M. C., Su, L. K., Vogelstein, B., Bryan, T. M., Levy, D. B., Smith, K. J., Preisinger, A. C., Hedge, P., McKechnie, D., et al. (1991). Identification of FAP locus genes from chromosome 5q21. *Science* 253, 661-665.

Kinzler, K. W. and Vogelstein, B. (1996). Lessons from hereditary colorectal cancer. *Cell* 87, 159-170.

Lamlum, H., Ilyas, M., Rowan, A., Clark, S., Johnson, V., Bell, J., Frayling, I., Efstathiou, J., Pack, K., Payne, S., Roylance, R., Gorman, P., Sheer, D., Neale, K., Phillips, R., Talbot, I., Bodmer, W., and Tomlinson, I. (1999). The type of somatic mutation at APC in familial adenomatous polyposis is determined by the site of the germline mutation: a new facet to Knudson's 'two-hit' hypothesis. *Nat. Med.* 5, 1071-1075.

Lee, T. and Luo, L. (1999). Mosaic analysis with a repressible cell marker for studies of gene function in neural morphogenesis. *Neuron* 22, 451-461.

Lin, G., Xu, N. and Xi, R. (2008). Paracrine Wingless signaling controls self-renewal of *Drosophila* intestinal stem cells. *Nature* 455, 310-312.

Margolis, J. and Spradling, A. (1995). Identification and behavior of epithelial stem cells in the *Drosophila* ovary. *Development* 121, 3797-3807.

McCartney, B.M., Dierick, H.A., Kirkpatrick, C., Moline, M.M. Baas, A., Peifer, M. and Bejsovec, A. (1999). *Drosophila APC*2 Is a Cytoskeletally-associated Protein that Regulates Wingless Signaling in the Embryonic Epidermis. *J. Cell Biol.* 146, 1303-1318.

McCartney, B.M., Price, M.H., Webb, R.L., Hayden, M.A., Holot, L.M., Zhou, M., Bejsovec, A. and Peifer, M. (2006). Testing hypothesis for the functions of *APC* family proteins using null and truncation alleles in *Drosophila*. *Development* 133, 2407-2418.

Micchelli, C. A. and Perrimon, N. (2006). Evidence that stem cells reside in the adult *Drosophila* midgut epithelium. *Nature* 439, 475-479.

Micchelli, C. A., Rulifson, E. J. and Blair, S. S. (1997). The function and regulation of cut on the wing margin of *Drosophila*: Notch, Wingless and a dominant negative role for Delta and Serrate. *Development* 124, 1485-1495.

Miller, A. (1950). The Internal Anatomy and Histology of the Imago of Drosophila Melanogaster. In *Biology of Drosophila* (ed. M. Demerec), pp. 420-534. NewYork: John Wiley & Sons, Inc.

Miyoshi, Y., Nagase, H., Ando, H., Horii, A., Ichii, S., Nakatsuru, S., Aoki, T., Miki, Y., Mori, T., and Makamura, Y. (1992). Somatic mutations of the *APC* gene in colorectal tumors: mutation cluster region in the *APC* gene. *Hum. Mol. Genet.* 1, 229-233.

Morrison, S. J. and Spradling, A. C. (2008). Stem Cells and Niches: Mechanisms that Promote Stem Cell Maintenance throughout Life. *Cell* 132, 598-611.

Ohlstein, B. and Spradling, A. (2006). The adult *Drosophila* posterior midgut is maintained by pluripotent stem cells. Nature 439, 470-474.

Ohlstein, B. and Spradling, A. (2007). Multipotent *Drosophila* Intestinal Stem Cells Specify Daughter Cell Fates by Differential Notch Signaling. *Science* 315, 988-992.

Oshima M, Oshima H, Kitagawa K, Kobayashi M, Itakura C, Taketo M. (1995).
Loss of *Apc* heterozygosity and abnormal tissue building in nascent intestinal polyps in mice carrying a truncated *Apc* gene. *Proc. Natl. Acad. Sci. USA* 92, 4482-4486.

Pai, L. M., Orsulic, S., Bejsovec, A. and Peifer, M. (1997). Negative regulation of Armadillo, a Wingless effector in *Drosophila*. *Development* 124, 2255-2266.

Powell, S. M., Zilz, N., Beazer-Barclay, Y., Bryan, T. M., Hamilton, S. R., Thibodeau, S. N., Vogelstein, B. and Kinzler, K. W. (1992). *APC* mutations occur early during colorectal tumorigenesis. *Nature* 359, 235-237.

Presente, A., Shaw, S., Nye, J. S., and Andres, A. J. (2002). Transgene-mediated RNA interference defines a novel role for Notch in chemosensory startle behavior. *genesis* 34, 165-169.

Rowan, A. J., Lamlum, H., Ilyas, M., Wheeler, J., Straub, J., Papadopoulou, A., Bicknell, D., Bodmer, W. F, and Tomlinson, I. P. (2000). APC mutations in sporadic colorectal tumors: A mutational 'hotspot' and interdependence of the 'two hits'. *Proc. Natl Acad. Sci.* USA, 97, 3352-3357.

Rubinfeld, B., Albert, I., Porfiri, E., Munemitsu, S. and Polakis, P. (1997). Loss of beta-catenin regulation by the *APC* tumor suppressor protein correlates with loss of structure due to common somatic mutations of the gene. *Cancer Res.* 57, 4624-4630.

Rulifson, E. J., Micchelli, C. A., Axelrod, J. D., Perrimon, N. and Blair, S. S. (1996). wingless refines its own expression domain on the *Drosophila* wing margin. *Nature* 384, 72-74.

Sangiorgi, E. and Capecchi, M. R. (2008). *Bmi1* is expressed in vivo in intestinal stem cells. *Nat. Genet.* 40, 915-920.

Siviter R. J., Coast, G. M., Winther, A. M., Nachman, R. J., Taylor, C. A., Shirras, A. D., Coates, D., Isaac, R. E. and Nässel D. R. (2000). Expression and functional characterization of a *Drosophila* neuropeptide precursor with homology to mammalian preprotachykinin A. *J. Biol. Chem.* 275, 23273-23280.

Su, L. K., Kinzler, K. W. and Vogelstein, B., Preisinger, A. C., Moser, A. R., Luongo, C., Gould, K. A. and Dove, W. F. (1992). Multiple intestinal neoplasia caused by a mutation in the murine homolog of the *APC* gene. *Science* 256, 668-670.

Su, L. K., Vogelstein, B., Kinzler, K. W. (1993). Association of the APC tumor suppressor protein with catenins. *Science* 262, 1734-1737.

Takacs, C. M., Baird, J. R., Hughes, E. G., Kent, S. S., Benchabane, H. Paik, R. and Ahmed, Y. (2008). Dual Positive and Negative Regulation of Wingless Signaling by Adenomatous Polyposis Coli. *Science* 319, 333-336.

van de Wetering, M., Cavallo, R., Dooijes, D., van Beest, M., van Es, J., Loureiro, J., Ypma, A., Hursh, D., Jones, T., Bejovec, A., Peifer, M., Mortin, M., and Clevers, H. (1997). Armadillo coactivates transcription driven by the product of the Drosophila segment polarity gene dTCF. *Cell* 88, 789-799.

Willert, K., Logan, C.Y., Arora, A., Fish, M., and Nusse, R. (1999). A Drosophila Axin homolog, Daxin, inhibits Wnt signalling. *Development* 126, 4165-4173.

Yeo, S. L., Lloyd, A., Kozak., K., Dinh, A., Dick, T., Yang, X., Sakonju, S. and Chia, W. (1995). On the functional overlap between two *Drosophila* POU homeo domain genes and the cell fate specification of a CNS neural precursor. *Genes Dev.* 15, 1223-1236.

Chapter 4

Enteroendocrine cells dynamically regulate the pro-secretory transcription factor Dimmed in response to the enteric pathogen *Pseudomonas entomophila*

The research work in Chapter 4 is currently under review at PNAS as of August 2014.
Katherine Beebe is the first author of this publication.

4.1 Summary

The endocrine system employs peptide hormone signaling to translate environmental changes into physiological responses in the organism. The diffuse endocrine system embedded in the gastrointestinal (GI) barrier epithelium is one of the largest and most diverse endocrine tissues. Furthermore, it is the only endocrine tissue in direct physical contact with the ever-changing microbial environment of the gut lumen. However, it remains unclear how this sensory epithelium responds to a broad spectrum of stimuli in a dynamic and regulated manner. We demonstrate that the enteroendocrine cells of the adult *Drosophila* midgut display a transient, systemic and highly sensitive induction of the pro-secretory factor Dimmed (Dimm) in response to the pathogenic bacteria *Pseudomonas entomophila (Pe)*. In enteroendocrine cells, *dimm* controls the expression of the targets *phm, dCAT4* and the peptide hormone, AstA. Finally, we identify *dimm* as a host factor that protects against infection by the Gram-negative pathogen *Pe*. We propose that *dimm* functions as a core component of the enteroendocrine pathogen sensor, which allows the barrier epithelium to dynamically shape endocrine output in response to the changing microbial composition of the gut lumen.

4.2 Introduction

The endocrine system mediates long-range peptide hormone signaling to broadcast environmental changes to distant target tissues via the circulatory system. Endocrine cells must therefore function as biological sensors that detect physiochemical stimuli and translate them into changes in peptide and amine signals. The diffuse enteroendocrine system of the gastrointestinal tract is notable for both its size and the diversity of its secretory products (Ahlman and Nilsson, 2001; Rehfeld, 2004). Because it is embedded within the barrier epithelium of the GI tract, enteroendocrine cells are uniquely situated with respect to the complex microbial communities of the gut lumen. Secreted enteroendocrine peptide hormones regulate local processes such as peristalsis and intestinal secretion, as well as broader systemic functions in host metabolism, immune response, and nervous system behavioral responses (Evans et al., 2013; Furness et al., 2013; Gunawardene et al., 2011). Thus, by dynamically responding to stimuli presented at the luminal interface, enteroendocrine cells coordinate essential aspects of organismal physiology.

Our understanding of the mechanism by which enteroendocrine cells respond to the complex environment of the lumen is incomplete. Studies in mammals have demonstrated the ability of enteroendocrine cells to respond to bacteria with secretion of peptides and changes in gene expression (Beales and Calam, 2000; Furness et al., 2013; Selleri et al., 2008). However, these studies were performed in vitro and are focused on isolated enteroendocrine cell types. Precisely how pathogenic challenges are sensed in the diffuse endocrine system under physiological conditions in vivo and how a coordinated adaptive response is mounted remains unknown.

Drosophila is a useful model organism to investigate the diffuse endocrine system. This population of cells can be readily detected along the entire anterior-posterior axis of the GI tract by the pan-enteroendocrine marker Prospero. The adult *Drosophila* midgut, like its mammalian counterpart, also expresses a diverse array of secretory peptides that exhibit regionalized distribution along the GI tract (Veenstra, 2009). Many of these peptides are functionally conserved across species (Dockray, 1977; Johnsen, 1998; Zitnan et al., 1993). Importantly, *Drosophila* has also proven to be a useful model system to study microbial effects on the cells of the GI tract. For example, *Pseudomonas entomophila* (*Pe*), a pathogenic Gram-negative bacteria isolated from the GI tract of wild *Drosophila*, is a potent stimulus to the midgut epithelium (Vodovar et al., 2005). *Pe* exposure stimulates a dramatic stem cell based renewal in many regions of the adult midgut epithelium (Buchon et al., 2009; Jiang et al., 2009; Strand and Micchelli, 2011). However, a response of the mature enteroendocrine population to *Pe* has not been characterized. Here we characterize the response of the adult diffuse endocrine system to the pathogenic bacteria *Pseudomonas entomophila* (*Pe*).

4.3 Results

4.3.1 Mature enteroendocrine cells induce Dimm in response to *Pe* infection

Dimm encodes a NeuroD-related bHLH transcription factor that functions as a 'master' regulator capable of conferring secretory properties to cells that do not otherwise display them; the ability to produce large dense core vesicles (LDCV) that store peptides and the enzymatic machinery necessary to post-translationally process pro-forms into biologically active signals (Hamanaka et al., 2010). We hypothesized that cells of the diffuse endocrine system in the adult gastrointestinal tract might display

high levels of Dimm in response to acute enteric infection. The pan-enteroendocrine marker Prospero (Pros) was used to visualize cells of the diffuse endocrine system along the length of the adult midgut. $Pros^{+}$ staining is readily detected in individual endocrine cells, as are secretory neuropeptides, such as Allatostatin A (AstA) (Figure 4.1A,B). To test if Dimm is normally expressed in wild type adult enteroendocrine cells under baseline conditions, we examined the co-localization of anti-Dimm in $Pros^{+}$ cells. Dimm protein was not detected in any cells of the adult midgut (Figure 4.1C), despite the fact that identical antiserum has been used to detect Dimm in other tissues (Hewes et al., 2003; Park et al., 2008). By contrast, exposure to the Gram-negative bacteria *Pseudomonas entomophila* (*Pe*) was sufficient to induce anti-Dimm staining in $Pros^{+}$ endocrine cells (Fig 4.1D). Upon induction, Dimm colocalized with nuclear DAPI, consistent with its characterized role as a transcription factor (Park et al., 2008) and with markers of specific enteroendocrine cell subtypes (Figure 4.1D inset). Dimm induction was highly reproducible across independent trials using two different wild type genotypes (Figure 4.2A, $p < 0.0001$). However, adult midguts from *dimm* mutants did not display $Dimm^{+}$ staining following *Pe* exposure, despite the presence of $Pros^{+}$ enteroendocrine cells (Figure 4.2A and S4.1). These results indicate that the immuno-reactivity observed in wild type enteroendocrine cells following bacterial challenge reflects changes in Dimm protein.

Pe exposure leads to rapid production of new epithelial cells in the gut through a stem cell mediated regenerative response (Jiang et al., 2009). It is therefore possible that the increase in Dimm signal reflects a part of the differentiation program for regenerating endocrine cells. Alternatively or additionally, Dimm induction following *Pe* exposure occurs homeostatically in extant enteroendocrine cells. To distinguish these possibilities, we examined the induction of Dimm in the context of an adult midgut epithelium depleted of its progenitor cells. We performed a conditional genetic ablation by shifting *UAS-rpr, UAS-hid; esgGal4, UAS-GFP; tubGal80^{TS}* adults to permit transgene expression. Ablation of progenitor cells was confirmed using GFP and this manipulation was not associated with accumulation of Dimm (Figure S4.2). Nevertheless, midguts depleted of progenitor cells were capable of robust Dimm induction in $Pros^{+}$ cells following exposure to *Pe* (Figure 4.1E-F'). Taken together, we conclude that Dimm protein is relatively low under baseline conditions, but is induced in mature enteroendocrine cells following exposure to *Pe*.

4.3.2 Dimm induction in enteroendocrine cells is transient and systemic

To determine if Dimm induction in enteroendocrine cells is dynamic, we next performed a time course analysis that ranges from 0-48 hrs following *Pe* exposure. Three parameters of Dimm induction were measured in the adult: the percentage of midguts with anti-Dimm staining; the percentage of enteroendocrine cells displaying Dimm per midgut; and anti-Dimm staining fluorescence of individual enteroendocrine cells (Figure 4.2). The percentage of midguts induced was quantified as a measure of the frequency of Dimm induction in a population of experimental organisms (Figure 4.2B). Midguts displayed $Dimm^{+}$ endocrine cells between 6 and 24h. Specifically, the percentage of midguts with $Dimm^{+}$ endocrine cells was 50%, 100%, and 88% at 6, 12, and 24h respectively. No Dimm positive cells were detected in midguts analyzed at times 0, 3, or 48h. We conclude that Dimm protein is induced in the majority of experimental organisms by 12 and 24h following *Pe* exposure, and is subsequently down regulated.

We independently examined anterior, middle, and posterior midgut data sets to identify any potential regional differences in either the timing or extent of Dimm induction (Figure 4.2D-D''). Midguts displayed variation in the percentage of $Dimm^{+}$ enteroendocrine cells, however all regions had the capacity for a high percentage of the endocrine population to be induced. Standard deviation in the percentage of enteroendocrine cell induction was higher at 6h than other time points. Regions did not significantly differ from each other within time points with the exception of the 12h time point, where the percentage of $Dimm^{+}$ endocrine cells was significantly higher in the middle region than either anterior or posterior regions (ANOVA). There were no significant differences between regions at the 6h or 24h time points. Finally, the intensity of anti-Dimm staining was also observed to change over time, showing significantly increased values at 6, 12, and 24h in all three regions (Figure 4.2E-E''). Similar to measurements of percentage induction, we observed maximum fluorescence intensities at the 12h time point in all three regions (Figure 4.2E-E''). Taken together, we conclude that enteroendocrine cells within all three major midgut regions can induce Dimm in response to bacterial challenge, and that Dimm levels subsequently decline.

4.3.3 Dimm induction in enteroendocrine cells is sensitive

We next asked whether Dimm induction varies with *Pe* dose. To test the dose response of Dimm induction, we exposed flies to doses ranging from OD 0.001 to OD 5 and quantified the percentage of guts induced, the percentage of $Dimm^+$ endocrine cells, and anti-Dimm fluorescence of individual enteroendocrine cells (Figure 4.2C). All doses below OD 1 were sublethal in the wild type *Canton-S* genotype (Figure S4.3). Each of the sublethal doses produced Dimm induction at 24h following exposure. The percentage of midguts with positive staining was 100% at all doses with the exception of OD 5, which displayed 88% Dimm positive midguts. We conclude that the percentage of midguts displaying induction did not vary between OD 0.001 and 1.

We next examined the effect of *Pe* dose on the percentage of $Dimm^+$ enteroendocrine cells in responding midguts (Figure 4.2F). In the anterior midgut, the percentage of $Dimm^+$ enteroendocrine cells was consistently above 50%, however variation was generally high. In the middle midgut region the mean percentage of $Dimm^+$ enteroendocrine cells was lower from OD 0.001 to 0.5 than OD 1 or 5 (Figure 4.2F'). The posterior midgut did not show a clear trend of an effect of dose and was the most variable across doses. Taken together, we conclude that the percentage of $Dimm^+$ enteroendocrine cells can reach high values at sublethal doses of *Pe*. Our data also suggest that the anterior region is most consistently responsive across a range of *Pe* doses. We also quantified the mean fluorescence of anti-Dimm staining in individual $Pros^+$ cells as an additional measure of Dimm induction across doses (Figure 4.2G-G''). Anti-Dimm staining varied between doses in the anterior, middle, and posterior regions; however even low doses were capable of intense anti-Dimm staining. This observation suggests that Dimm induction is robust in individual enteroendocrine cells independent of dose.

4.3.4 Enteroendocrine cells express Dimm target genes in a *dimm*-dependent manner

Transcriptional targets of Dimm have been identified in the developing CNS (Park et al., 2011; Park et al., 2008). We examined two such targets for their expression in adult midgut enteroendocrine cells: *phm*, which encodes the neuropeptide biosynthetic enzyme peptidylglycine alpha-monooxygenase, and *dCAT4*, which encodes a putative amino acid transporter. Under baseline conditions, wild type flies express *phm* in the midgut despite a lack of baseline Dimm staining (Figure 4.3A). Phm was also

detectible in enteroendocrine cells following *Pe* exposure (Figure 4.3B). We next asked whether *dimm* was required for normal Phm expression in enteroendocrine cells. Phm was not detectable in enteroendocrine cells of *dimm* mutants under mock or *Pe* infected conditions, despite the presence of $Pros^+$ cells in mutant midguts (Figure 4.3C,D). To test if Phm is induced in midguts exposed to *Pe* we quantified the percentage of Phm^+ / $Pros^+$ cells and anti-Phm staining levels under mock and *Pe* infected conditions. The percentage of Phm^+ enteroendocrine cells was not significantly changed in response to *Pe* exposure (Figure 4.3I). However, Phm staining intensity was significantly increased (Figure 4.3J). Similar results were observed with dCAT4, which was expressed at low levels under baseline conditions but was induced following *Pe* exposure (Figure 4.3J). Taken together, we conclude that two previously characterized Dimm transcriptional targets in the CNS show both *dimm* dependent expression and induction in midgut enteroendocrine cells.

4.3.5 *dimm* is required for changes in AstA expression following *Pe* infection

We hypothesized that Dimm induction by enteroendocrine cells could help support changes in peptide expression following *Pe.* To test this possibility, we examined the protein levels of Allatostatin A (AstA) in midguts of wild type and *dimm* mutant flies under mock and *Pe*-challenged conditions. In contrast to the target gene *phm*, AstA was detectable in both wild type and *dimm* mutants under baseline conditions (Figure 4.3E,G). AstA was also detectable in both genotypes following *Pe* exposure (Figure 4.3F,H). We noted a visual increase in the number and intensity of $AstA^+$ cells in the posterior midgut of samples exposed to *Pe*, and therefore quantified the percentage of $AstA^+$/ $Pros^+$ cells as well as AstA antibody staining levels. We observed that wild type midguts significantly increased the percentage and levels of AstA following exposure to *Pe* (Figure 4.3K,L). *dimm* mutants displayed a similar trend, but both percentage and levels responses were reduced (Figure 4.3K,L). We conclude that AstA is a regulated peptide during the midgut response to *Pe* and that *dimm* is not necessary for AstA expression *per se,* but is necessary for the changes in AstA following *Pe* exposure.

4.3.6 Dimm is a host factor that protects adult *Drosophila* against *Pe* infection

To test the functional requirement for Dimm, we examined the survival of flies with reduced *dimm* following *Pe* challenge. Flies of a strong loss of function *dimm* allelic combination were compared to heterozygotes and controls for survival following *Pe* exposure. Following infection, median survival of *dimm* mutants was significantly decreased compared to either wild type or *dimm* heterozygotes ($dimm^{-/-}$, 1.7 days; $dimm^{+/-}$, 2.5, and >7 days; $dimm^{+/+}$, >7 days) (Figure 4.4A). Whole animal mutant susceptibility may reflect a requirement for *dimm* during development. Therefore, we next tested the requirement for Dimm and Phm in the adult using the conditional *tubulinGal4-tubulinGal80*^{TS} system to express $dimm^{RNAi}$ or phm^{RNAi}. Each RNAi line was effective in knocking down the respective protein in the adult midgut following *Pe* challenge (data not shown). Median survival following infection was significantly shorter in $dimm^{RNAi}$ or phm^{RNAi} conditions in comparison to controls ($dimm^{RNAi}$, 2.5, 2.5, and >7 days; phm^{RNAi}, 1 day; control (*GFP*), >7 days) (Figure 4.3B). We conclude that *dimm* is a critical host factor that protects adults against infection by the Gram-negative pathogen *Pe*.

4.4 Discussion

4.4.1 Dynamic sensing of lumenal pathogens

The gut lumen presents a changing microbial stimulus to the host and the diffuse endocrine system functions to sense and signal these changes. We utilized the experimental system of the adult *Drosophila* midgut to investigate how the diffuse endocrine system senses acute pathogenic infection by a Gram-negative bacterium. Our studies indicate that the enteroendocrine response is gated by a transcription factor that also controls the level of secretory activity. In addition, we show that this essential factor protects the organism against pathogenic challenge. These studies suggest a molecular model explaining how changes to the luminal environment might result in a dynamically altered organismal physiology (Figure 4.4C). We have shown that mature enteroendocrine cells respond to the pathogenic bacterium *Pe* with induction of Dimm, a pro-secretory bHLH transcription factor. We measured cardinal parameters of this induction and found that infection results in a defined signature in these variables, including transience, sensitivity and systemic induction. Luminal sensing mediated by Dimm thus imparts the diffuse endocrine system with a repertoire of adaptive features for host defense.

4.4.2 Scaling-up transcriptional output in the diffuse endocrine system

Enteroendocrine cells respond to pathogens by becoming more active. We hypothesize that Dimm supports this response as a 'scaling factor' that controls a specific cellular domain or resource. Scaling factors control transcription and determine the size of sub-cellular compartments in specialized cells (Mills and Taghert, 2012). A Dimm-dependent pro-secretory program is triggered in response to enteric pathogens, as bona fide components of the regulated secretory pathway are elevated in response *Pe* challenge, including vesicular proteins like the Phm alpha-monooxygenase, *dCAT4* amino acid transporter and the AstA peptide hormone. Yet, despite this clear requirement, *dimm* homozygotes are recovered as adults. This suggests that Dimm is not likely to be absolutely required for secretion in general, but rather for the increased secretory capacity necessitated by episodic pathogenic challenge.

In the developing *Drosophila* CNS, genome-profiling studies show that both *phm* and *dCat4* are direct transcriptional targets of Dimm. However, peptide hormone-encoding genes were not among the putative targets found in this tissue (Park et al., 2011). Our genetic experiments in enteroendocrine cells demonstrate a requirement of *dimm* for AstA peptide. It remains unclear if secretory peptides such as AstA are direct or indirect targets of Dimm in enteroendocrine cells. Comparative studies between different endocrine cell types will be useful in distinguishing potential differences in the extent to which scaling factors such as Dimm directly control secretory capacity, as opposed to secretory peptides *per se*.

Dimm function and regulation in the *Drosophila* diffuse endocrine system may be analogous to other animals. For example, mammalian endocrine cells express at least three pro-endocrine bHLH regulators, Math1, neurogenin3, and NeuroD (Li et al., 2011). These factors could have unique or overlapping functions in the mammalian gut, issues which remain to be fully explored. However, on the basis of both loss and gain-of-function phenotypes NeuroD may be most similar to Dimm (Naya et al., 1997; Neptune et al., 2008). Thus, the principles of Dimm induction and pathogen induced scaling of enteroendocrine output established here may also extend to other organisms including mammals.

4.4.3 Targeting the diffuse endocrine system

The diffuse endocrine system represents a key homeostatic node that couples luminal stimuli with physiological responses. In principal, disruption of either upstream (microbial communities, nutrient excess) or downstream (hormones) elements of this pathway could lead to potentially pathogenic conditions in which an organism becomes uncoupled from the changes in the luminal environment. Increasingly the role of gut hormones in diabetes, obesity and response to surgically induced injury is gaining attention (Bradley et al., 2011; Holst, 2013). Furthermore, efforts to direct differentiation or design replacement cells from progenitors with defined characteristics are currently being refined (Borowiak and Melton, 2009). The diffuse endocrine system and the molecular control of secretion become salient targets for directed molecular, pharmacological or pro-biotic interventions. Insight into how gut hormones are regulated in response to external stimuli, as well as the endocrine sensing mechanism that initiates changes in secretion may therefore be of broad significance to managing health and disease. The lumen of the gut is a unique environment that presents varied physical and chemical signals to the host organism. Embedded in the epithelium of the GI tract, the diffuse enteroendocrine system functions as both sensor and communicator to the organism about this ever-changing environment. We utilized the experimental system of the adult *Drosophila* midgut to examine how the EE population responds to pathogenic infection. Various cell types of the adult *Drosophila* midgut have previously been shown to respond to infection, including intestinal stem cells, surrounding visceral muscle cells, and mature enterocytes (for example, (Buchon et al., 2009; Jiang et al., 2009). A response of the adult EE cell to pathogenic insults has to our knowledge not previously been demonstrated. The results presented here show that EEs respond to the pathogenic bacteria *Pe* with induction of the prosecretory bHLH transcription factor Dimmed. As an initial characterization of this response, we measured 4 parameters of induction, namely, the timing, dose sensitivity, regional differences, and induction of target genes. We found that *Pe* results in a defined Dimm expression signature in these 4 variables.

4.5 Experimental Procedures

4.5.1 Fly stocks and culturing

Wild type: *w^{1118}* and *Canton-S;*

w; pros-LacZ, *ry* / TM3 *ry, Sb, Ser;*

w, UAS-dcr2; NPFGal4 / CyO; tubGal80^{TS}, UAS-GFP / TM6C;

w; esgGal4, UAS-GFP, tubGal80^{TS} (esg^{TS});

w, UAS-dcr2; sp / CyO; tubGal4, tubGal80^{TS} (tub^{TS});

w, UAS-rpr, UAS-hid (X);

y w; P[EPgy2] dimm^{EY14636} (BL#21432, designated "dimm^{P3}");

y w; dimm^{Rev4} / CyO;

w; phm^{p29} / CyO, GFP

y v; P[TRiP.JF02093] attP2 (BL#26976, designated "dimm^{RNAi}")

P[KK112513]VIE-260B (BL#v104028, designated "phm^{RNAi}").

w; P[w[+mC]=UAS-2xEGFP]AH2 (BL#6874)

See FlyBase for additional information, http:flybase.org.

Mated female flies 3-10 days of age were analyzed in all experiments, with the exception of lethality experiments where flies were aged up to 21 days. Flies were maintained on standard food media (i.e. RF; (Lee and Micchelli, 2013)) and supplemented with yeast paste every 2-3 days in all RF conditions. Flies were cultured at 25°C with the exception of transfer to 29°C during infection, which is further described below.

4.5.2 Antisera

Primary antibodies. Primary antibodies included mouse anti-AstA (1:20, DSHB); anti-dCat4 (1:500), (Park et al., 2011); guinea pig anti-Dimm (1:250), (Allan et al., 2005); chicken anti-GFP (1:10,000, Abcam); mouse rabbit anti-Phm (1:750), (Kolhekar et al., 1997); anti-Pros (1:100, DSHB); rabbit anti-pH3 (1:2,000, Upstate); mouse anti-βGal (1:100, DSHB); rabbit anti-βGal (1:2,000, Cappel).

Secondary antibodies. Secondary antibodies used were goat anti-chicken Alexa Flour 488 (1:2,000, Molecular Probes); goat anti-mouse Alexa Flour 488 (1:2,000, Molecular Probes); goat anti-mouse Alexa Flour 568 (1:2,000, Molecular Probes); goat anti-rabbit Alexa Flour 568 (1:2,000, Molecular Probes); goat anti-guinea pig Alexa Flour 568 (1:2,000, Molecular Probes).

Mounting media and dyes. Vectashield+ DAPI mounting media (Vector) was used.

4.5.3 Histology

Isolation and whole mount immunostaining of adult midguts was performed as previously described in detail (Micchelli, 2014). Briefly, adult female flies were dissected in 1x PBS (Sigma). The midgut was removed and fixed in 0.5x PBS and 4% electron microscopy-grade formaldehyde (Polysciences) overnight at 4^{o}C or 1XPBS and 4% paraformaldehyde / 7% picric acid for 1hr at room temperature. Samples were washed in 1x PBS, 0.1~0.3% Triton X-100 (PBST) for a minimum of 2 hours, and then incubated in primary antibodies overnight. Samples were then washed for 2 hours in PBST, incubated in secondary antibodies for 3 hours, and washed again overnight in PBST. DAPI containing Vectashield mounting media (Vector) was used for mounting. AstA and Phm antibody staining were performed as described above with the exception that midguts were dissected directly in 4% formaldehyde.

4.5.7 Bacterial Infection

Flies were infected *ad libitum* with *Pseudomonas entomophila* (*Pe*). Infected flies were fed on Tegosept^{TM} free food supplemented with 0.5mL of *Pe.* *Pe* was concentrated and resuspended in 5% sucrose at OD_{20} and subsequently diluted to the specified OD. Mock-infected flied were placed on Tegosept^{TM} free food supplemented with 0.5mL 5% sucrose. Flies were maintained at 29°C throughout the course of infection. Exposure to *Pe* laced food was 24h in all experiments unless otherwise indicated. Flies were returned to regular food (RF) following mock or *Pe* treatment.

For the lethality assay, adult female flies were collected in the first 48h of eclosion and aged 3-12 days. Fly were cultured at 25°C at the ratio of 3 males + 20 females per vial. Survival of males was not included in the analysis. Flies were transferred to *Pe* laced food of designated OD and transferred to

29°C. Lethality was assayed daily for 7 days. Flies were transferred back to RF supplemented with yeast paste after 24h or 48h of *Pe* exposure.

4.5.8 Imaging acquisition and quantification

Confocal images were collected using a Leica TCS SP5 or Olympus FV500 FluoView confocal microscope. Photoshop CS (Adobe) and ImageJ (NIH) were used to process images for brightness and contrast.

Data was analyzed from confocal images collected using the same confocal settings and from samples processed in parallel. To analyze the percentage of Dimm+ midguts, samples were classified as positive when they displayed >2 anti-Dimm+ cells in the superficial side of the entire A-P length. $Dimm^{+}/Pros^{+}$ values were obtained by analyzing micrographs collected at 40X magnification from the entire A-P axis of each gut analyzed. Regional boundaries were defined by morphological constrictions present in the medial portion. ImageJ software (NIH) was used to measure mean intensity values. Specifically, using ImageJ, we defined particle areas using the anti-Pros channel and then measured mean intensity of the anti-Dimm channel in that area. Dimm levels were normalized for each micrograph. Levels were normalized using the following equation (R-B) / B where R = mean intensity in the particle area and B = mean intensity in a midgut region outside particle areas. Graphs and statistical analysis were generated using Prism GraphPad Software.

4.6 Acknowledgements

We would like to thank Dr. Lemaitre for *Pseudomonas entomophila* strains; the *Drosophila* Bloomington stock center; the VDRC sock center; the Developmental Studies Hybridoma Bank; Drs. Ross Cagan, Jan Veenstra, and Ping Shen for reagents; and members of the Micchelli and Taghert laboratories for helpful discussions. KBB is an Olin Fellow. CAM is an American Cancer Society Research Scholar. Additional funding for this research was provided by the National Institute of Health; P30-NS045713 supporting the Bakewell NeuroImaging Labs, R01 NS021749 (PHT) and RO1 DK095871 (CAM).

4.7 Figures

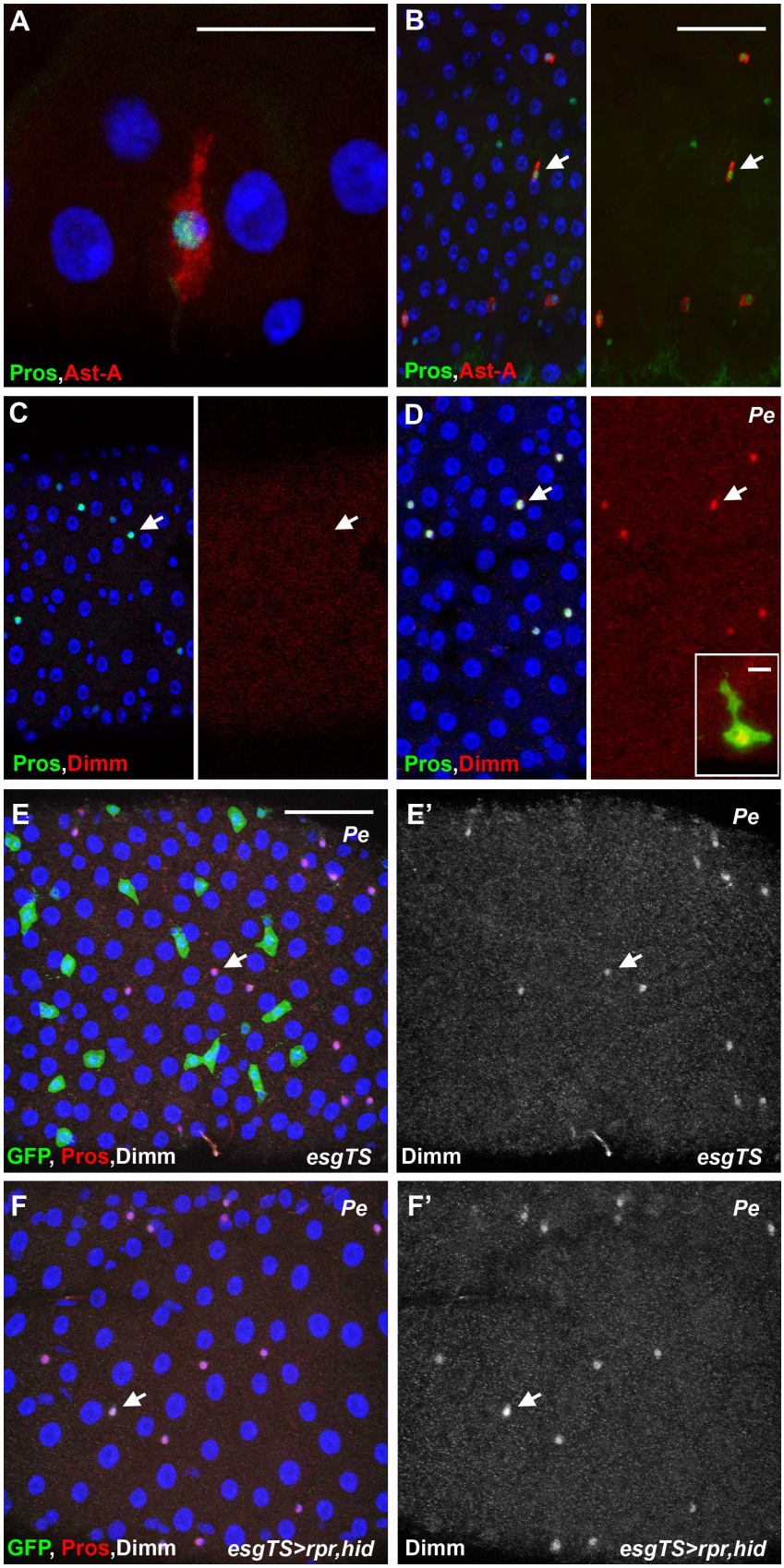
A
Pros,Ast-A
B
Pros,Ast-A
C
Pros,Dimm
D
Pros,Dimm
Pe
E
Pe
GFP, Pros,Dimm
esgTS
E'
Pe
Dimm
esgTS
F
Pe
GFP, Pros,Dimm
esgTS>rpr,hid
F'
Pe
Dimm
esgTS>rpr,hid

Figure 4.1 Adult enteroendocrine cells induce Dimm in response to the bacterial pathogen *Pe*. GI epithelium under baseline and infected conditions. (A,B) Confocal micrographs of the adult midgut epithelium stained for *pros*-LacZ and the peptide Allatostatin A (AstA) (DAPI, blue; anti-AstA, red; anti-βgal, green). (C,D) Confocal micrographs of the adult midgut epithelium stained for Pros and Dimm after exposure to mock (C) or *Pe* (D) food (DAPI, blue; anti-Dimm, red; anti-Pros, green). Inset: representative cell from a *Pe* treatment midgut expressing *npf*>GFP (anti-Dimm, red; anti-GFP, green). (E,E') Confocal micrographs of adult midguts temperature shifted to drive expression of GFP (F,F') or the pro-apoptotic genes *rpr* and *hid* (G,G') in esg^{TS} expressing progenitor cells and subsequently exposed to *Pe* food (DAPI, blue; anti-Pros, red; anti-GFP, green; anti-Dimm, white). Temperature shift to drive transgene expression was performed 3 days prior to *Pe* exposure. Control midguts exposed to regular food are displayed in Figure S2. Arrows provide a reference to example enteroendocrine cells. Scale bars: 10 μm (A), 50 μm (B,E), and 5 μm (D, inset).

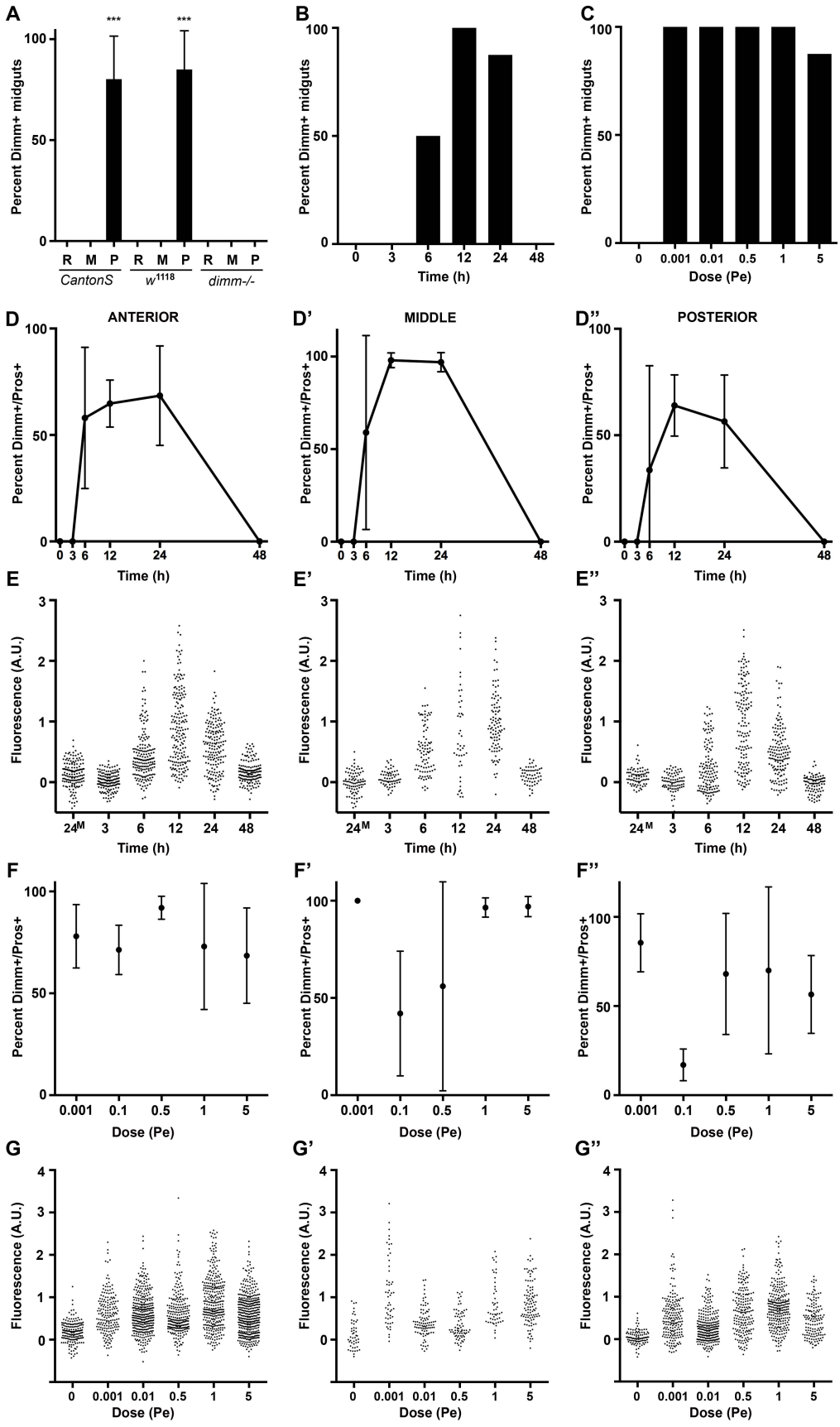
A
B
C
D
ANTERIOR
D'
MIDDLE
D''
POSTERIOR
E
E'
E''
F
F'
F''
G
G'
G''
Percent Dimm+ midguts
Percent Dimm+/Pros+
Fluorescence (A.U.)
Time (h)
Dose (Pe)
R M P R M P R M P
CantonS
w1118
dimm-/-
***
***
0 3 6 12 24 48
0 0.001 0.01 0.5 1 5
24M 3 6 12 24 48
0 0.1 0.5 1 5

Figure 4.2 Dimm is transiently induced and is sensitive to sublethal doses of *Pe*. Parameters of Dimm induction. (A-C) Quantification of the percentage of midguts that displayed at least two positive anti-Dimm cells. Bars indicate mean values ± SD. (A) Percent analysis of two independent control genotypes and *dimm* mutants (P3/Rev4) 24h following treatment (R, regular lab food; M, mock infection food; P, *Pseudomonas entomophila* laced food), (N = 4 independent trials, n = 6 midguts per trial), ANOVA, $p < 0.0001$, pairwise comparison by Tukey post-hoc test. (B) Percent analysis over time (N = 1 infection trial, n = 6 midguts). (C) Percent analysis over varying *Pe* dose (N = 1 infection trial, n = 6 midguts). (D-E'') Regional analyses of Dimm induction over time. (D-D'') Quantification of the percentage of Dimm+ EEs (N = 1 infection trial, n=6 midguts). Points indicate mean values ± SD. (E-E'') Quantification of mean florescence of anti-Dimm staining in individual Pros + cells over time (n = 4 midguts, n = 18-60 EEs per midgut). 24^{M} designates the mock infected control data set at time 24h. (F-G'') Regional analyses of Dimm induction over varying *Pe* dose. (F-F'') Quantification of the percentage of Dimm+ EEs (N = 1 infection trial, n=6 midguts). Points indicate mean values ± SD. (G-G'') Quantification of mean florescence of anti-Dimm staining in individual Pros + cells across *Pe* doses (n = 4 midguts, n = 20-60 EEs per midgut). See Experimental Procedures for details regarding collection and normalization.

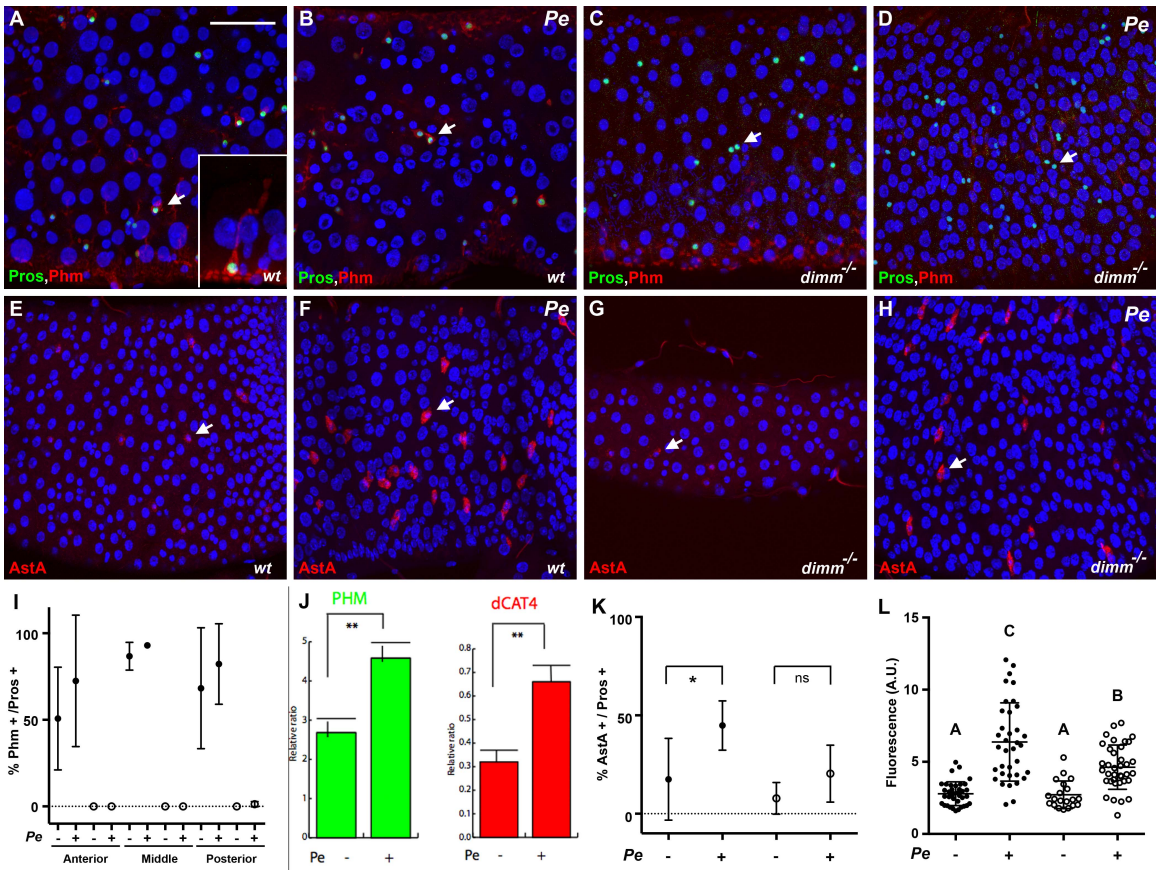

Figure 4.3 *dimm* is necessary for target gene expression and peptide regulation in enteroendocrine cells. Analysis of *dimm* target genes. (A-D) Confocal micrographs of adult midguts (DAPI, blue; anti-Phm, red; anti-Pros, green). (A-B) Representative wild type midguts exposed to mock (A) or *Pe* (B) food. Inset: high magnification of a Phm^{+},Pros^{+} cell displaying EE morphology. (C-D) Representative *dimm* mutant midguts following exposure to mock (C) or *Pe* (D) food. (E-H) Confocal micrographs of the final 40X frame of the adult posterior midgut in the AstA positive region (DAPI, blue; anti-AstA, red). (I-L) Quantitative analyses of Phm and AstA staining. Closed circles designate the wild type *Canton-S* genotype and open circles designate *dimm* mutants. (I) Quantification of the percentage of Phm^{+}/Pros^{+} cells in wild type and *dimm* mutant midguts following exposure to mock (-) or *Pe* (+) food. Points indicate mean values ± SD (N = 1 infection trial, n = 8 midguts). (J) Quantification of relative Phm and dCAT4 staining levels of wild type cells from mock (-) or *Pe* (+) treatments. (K) Quantification of the percentage of AstA^{+}/Pros^{+} cells. Points indicate mean values ± SD (N = 1 infection trial, n = 8 midguts), ANOVA, p = 0.0042, pairwise comparisons by Tukey post-hoc test. (L) Quantification of the mean

fluorescence of individual anti-AstA positive cells (n = 4 midguts, n = 5-10 cells per midgut), ANOVA, $p < 0.0001$, pairwise comparisons by Tukey post-hoc test revealed three groups (A,B,C) that differed significantly from one another. All confocal and quantitative analyses were performed from samples collected after a 24h exposure to mock or *Pe* OD 5 food, with the exception of panel J in which *Pe* dose was OD 20. Arrows provide a reference to example enteroendocrine cells. Scale bar: 50 μm.

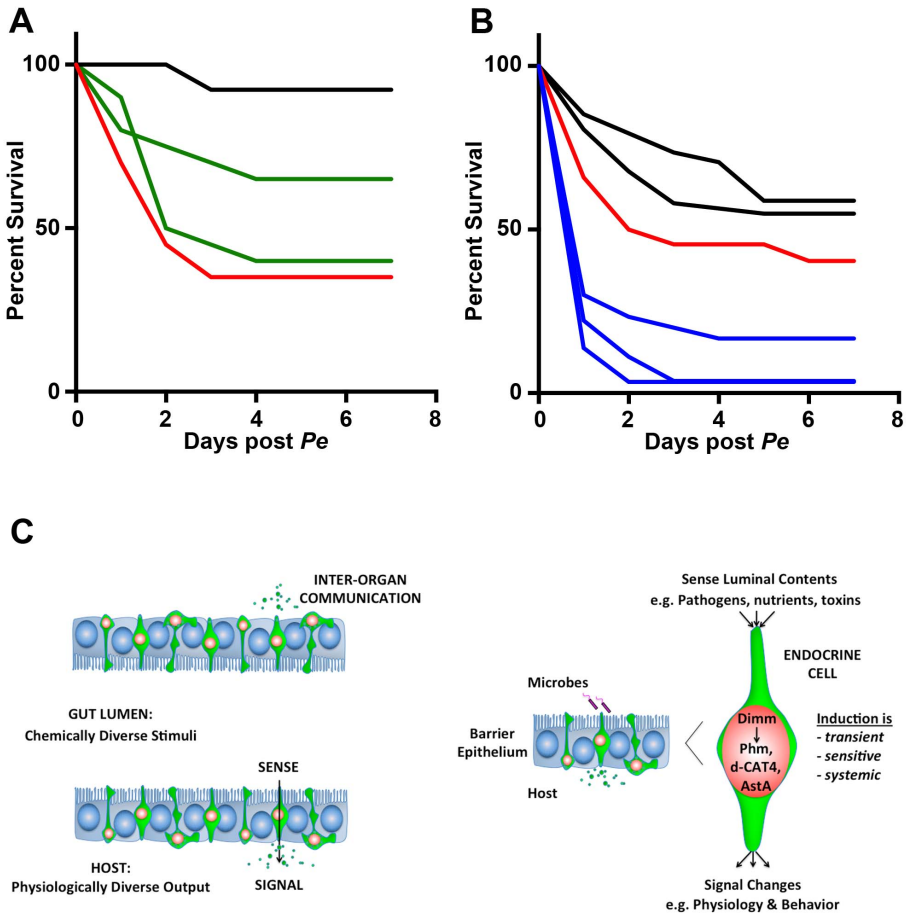

Figure 4.4 Dimm is a host factor that protects against *Pe* infection. Survival of *dimm* mutants following Gram-negative infection. (A) A representative survival plot of wild type (*CS / w*, black), *dimm* heterozygotes (*P3 / w*, green), and *dimm* hypomorphs (*P3 / Rev4*, red) following exposure to *Pe*. Flies were exposed to *Pe* at OD 15 for 24h. (B) A representative survival plot of flies expressing GFP (black), $Dimm^{RNAi}$ (red), or Phm^{RNAi} (blue), using a conditional *tubulin* driver system (tub^{TS}). Temperature shift to drive transgene expression was performed 3 days prior to *Pe* exposure. Flies were exposed to *Pe* at OD 20 for 48h. (C) A model of the midgut epithelial context and the principle findings of this study.

4.8 Supplementary material

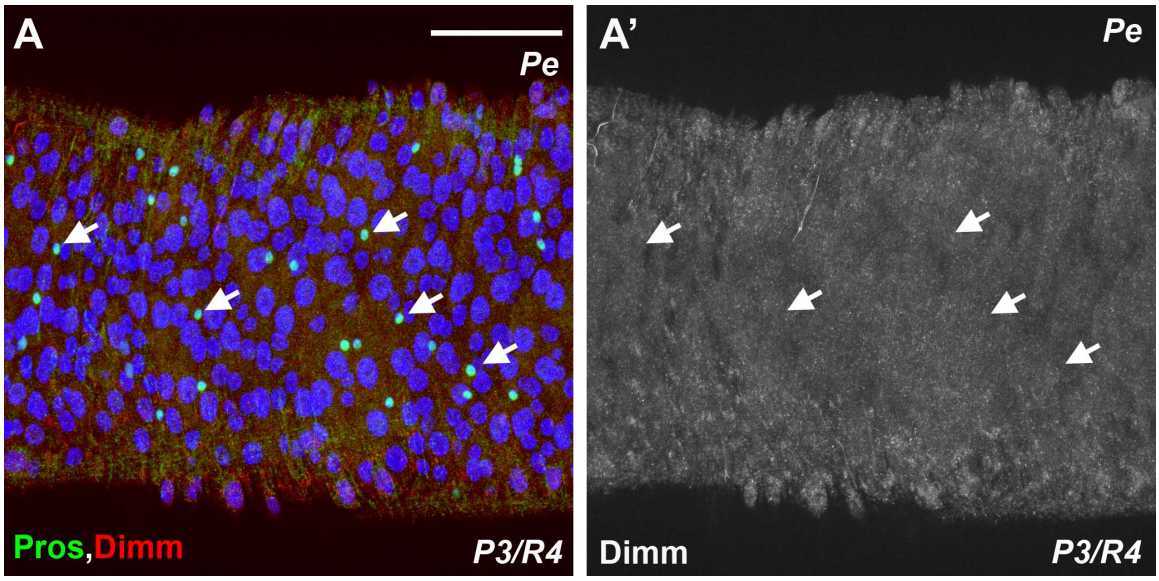

Supplementary Figure S4.1 Anti-Dimm staining is absent in *dimm* mutants. Confocal micrograph of the adult midgut epithelium of a *dimm* mutant midgut exposed to *Pe* OD5 for 24h (DAPI, blue; anti-Dimm, red; anti-Pros, green). *dimm* mutants display Pros+ cells but lack anti-Dimm staining following *Pe* exposure. Arrows provide a reference to example enteroendocrine cells. Scale bar: 50 μm.

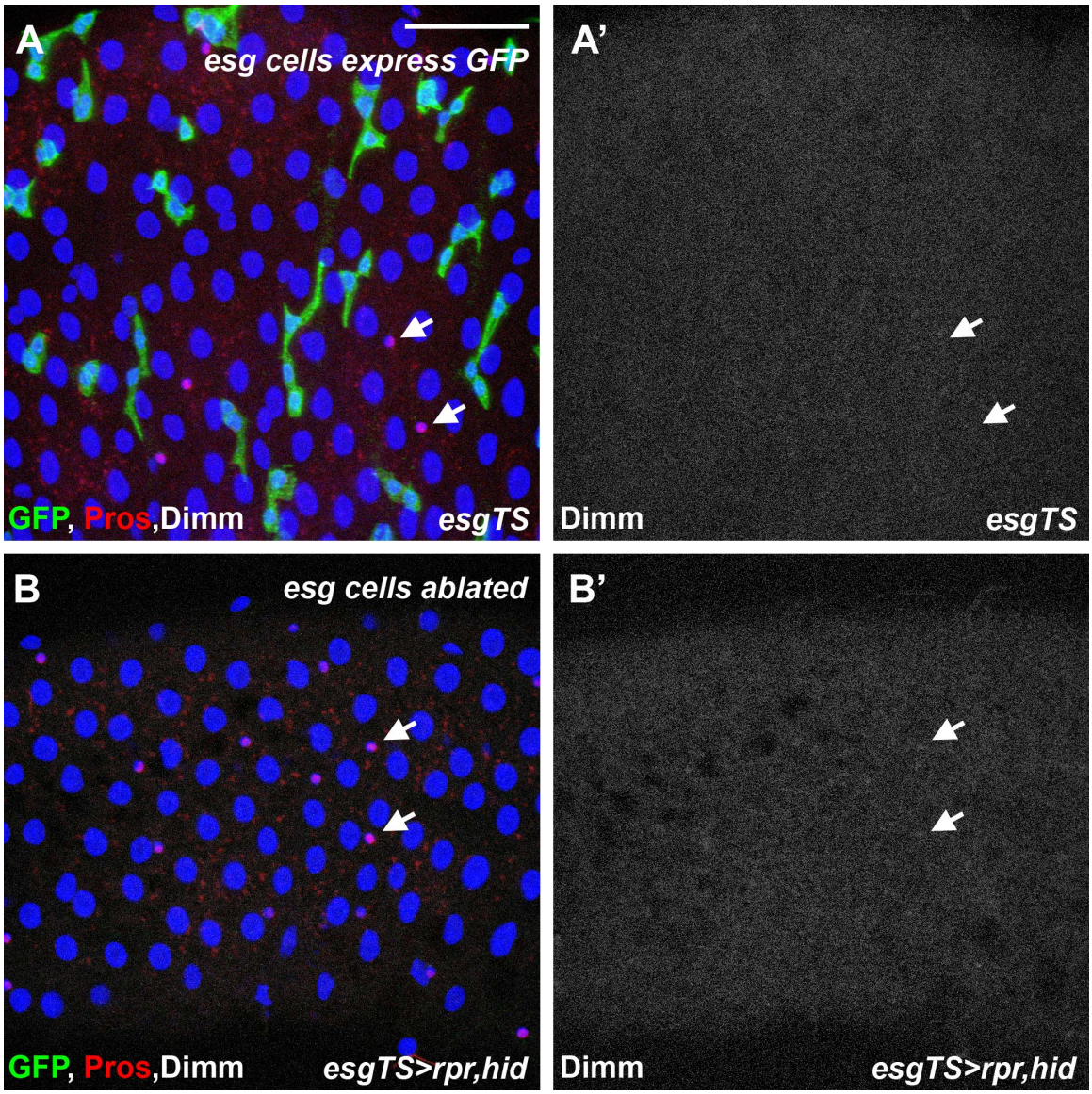

Supplementary Figure S4.2 Ablation of *esg* cells does not induce Dimm under baseline conditions. Confocal micrographs of adult midguts expressing either GFP or the pro-apoptotic genes *rpr* and *hid* using the esg^{TS} conditional system, (DAPI, blue; anti-Pros, red; anti-GFP, green; anti-Dimm, white). (A-A') The esg^{TS} genotype expresses GFP in adult midgut progenitor cells but does not express Dimm under baseline conditions. (B-B') Expression of the pro-apoptotic genes *rpr* and *hid* using esg^{TS} effectively ablates the esg^{TS} progenitor population and likewise does not induce Dimm under baseline conditions. Arrows provide a reference to example enteroendocrine cells. Scale bar: 50 μm.

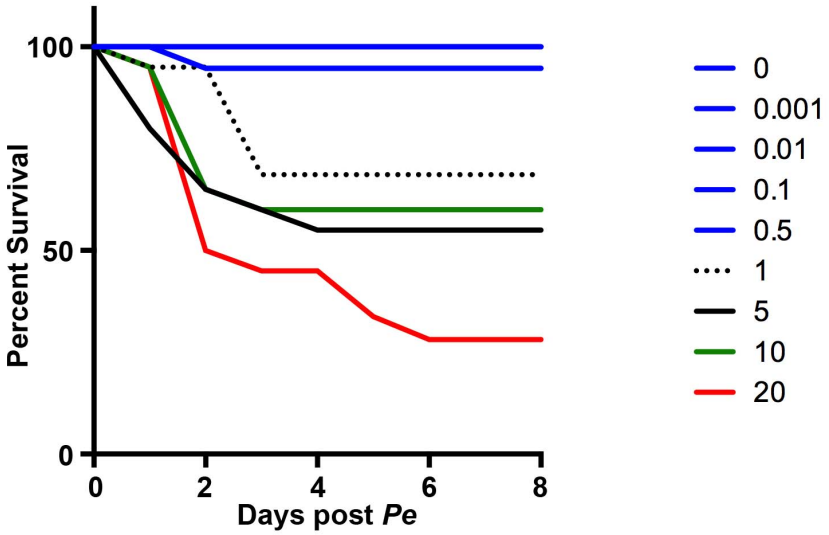

Supplementary Figure S4.3 Dose sensitivity of wild type *Canton-S* survival following exposure to *Pe*. A representative survival plot of adult *Canton-S* females in response to increased *Pe* dose. Flies were exposed to the respective dose of *Pe* for 48h and subsequently transferred to regular food.

4.9 References

Ahlman, H., and Nilsson (2001). The gut as the largest endocrine organ in the body. Annals of oncology : official journal of the European Society for Medical Oncology / ESMO *12 Suppl 2*, S63-68.

Allan, D.W., Park, D., St Pierre, S.E., Taghert, P.H., and Thor, S. (2005). Regulators acting in combinatorial codes also act independently in single differentiating neurons. Neuron *45*, 689-700.

Beales, I.L., and Calam, J. (2000). Helicobacter pylori increases gastrin release from cultured canine antral G-cells. European journal of gastroenterology & hepatology *12*, 641-644.

Borowiak, M., and Melton, D.A. (2009). How to make beta cells? Current opinion in cell biology *21*, 727-732.

Bradley, W.D., Zwingelstein, C., and Rondinone, C.M. (2011). The emerging role of the intestine in metabolic diseases. Archives of physiology and biochemistry *117*, 165-176.

Buchon, N., Broderick, N.A., Chakrabarti, S., and Lemaitre, B. (2009). Invasive and indigenous microbiota impact intestinal stem cell activity through multiple pathways in Drosophila. Genes & development *23*, 2333-2344.

Dockray, G.J. (1977). Molecular evolution of gut hormones: application of comparative studies on the regulation of digestion. Gastroenterology *72*, 344-358.

Evans, J.M., Morris, L.S., and Marchesi, J.R. (2013). The gut microbiome: the role of a virtual organ in the endocrinology of the host. The Journal of endocrinology *218*, R37-47.

Furness, J.B., Rivera, L.R., Cho, H.J., Bravo, D.M., and Callaghan, B. (2013). The gut as a sensory organ. Nature reviews Gastroenterology & hepatology *10*, 729-740.

Gunawardene, A.R., Corfe, B.M., and Staton, C.A. (2011). Classification and functions of enteroendocrine cells of the lower gastrointestinal tract. International journal of experimental pathology *92*, 219-231.

Hamanaka, Y., Park, D., Yin, P., Annangudi, S.P., Edwards, T.N., Sweedler, J., Meinertzhagen, I.A., and Taghert, P.H. (2010). Transcriptional orchestration of the regulated secretory pathway in neurons by the bHLH protein DIMM. Current biology : CB *20*, 9-18.

Hewes, R.S., Park, D., Gauthier, S.A., Schaefer, A.M., and Taghert, P.H. (2003). The bHLH protein Dimmed controls neuroendocrine cell differentiation in Drosophila. Development *130*, 1771-1781.

Holst, J.J. (2013). Enteroendocrine secretion of gut hormones in diabetes, obesity and after bariatric surgery. Current opinion in pharmacology *13*, 983-988.

Jiang, H., Patel, P.H., Kohlmaier, A., Grenley, M.O., McEwen, D.G., and Edgar, B.A. (2009). Cytokine/Jak/Stat signaling mediates regeneration and homeostasis in the Drosophila midgut. Cell *137*, 1343-1355.

Johnsen, A.H. (1998). Phylogeny of the cholecystokinin/gastrin family. Frontiers in neuroendocrinology *19*, 73-99.

Kolhekar, A.S., Roberts, M.S., Jiang, N., Johnson, R.C., Mains, R.E., Eipper, B.A., and Taghert, P.H. (1997). Neuropeptide amidation in Drosophila: separate genes encode the two enzymes catalyzing amidation. The Journal of neuroscience : the official journal of the Society for Neuroscience *17*, 1363-1376.

Lee, W.C., and Micchelli, C.A. (2013). Development and characterization of a chemically defined food for Drosophila. PloS one *8*, e67308.

Li, H.J., Ray, S.K., Singh, N.K., Johnston, B., and Leiter, A.B. (2011). Basic helix-loop-helix transcription factors and enteroendocrine cell differentiation. Diabetes, obesity & metabolism *13 Suppl 1*, 5-12.

Micchelli, C.A. (2014). Whole-mount immunostaining of the adult Drosophila gastrointestinal tract. Methods.

Mills, J.C., and Taghert, P.H. (2012). Scaling factors: transcription factors regulating subcellular domains. BioEssays : news and reviews in molecular, cellular and developmental biology *34*, 10-16.

Naya, F.J., Huang, H.P., Qiu, Y., Mutoh, H., DeMayo, F.J., Leiter, A.B., and Tsai, M.J. (1997). Diabetes, defective pancreatic morphogenesis, and abnormal enteroendocrine differentiation in BETA2/neuroD-deficient mice. Genes & development *11*, 2323-2334.

Neptune, E.R., Podowski, M., Calvi, C., Cho, J.H., Garcia, J.G., Tuder, R., Linnoila, R.I., Tsai, M.J., and Dietz, H.C. (2008). Targeted disruption of NeuroD, a proneural basic helix-loop-helix factor, impairs distal lung formation and neuroendocrine morphology in the neonatal lung. The Journal of biological chemistry *283*, 21160-21169.

Park, D., Hadzic, T., Yin, P., Rusch, J., Abruzzi, K., Rosbash, M., Skeath, J.B., Panda, S., Sweedler, J.V., and Taghert, P.H. (2011). Molecular organization of Drosophila neuroendocrine cells by Dimmed. Current biology : CB *21*, 1515-1524.

Park, D., Shafer, O.T., Shepherd, S.P., Suh, H., Trigg, J.S., and Taghert, P.H. (2008). The Drosophila basic helix-loop-helix protein DIMMED directly activates PHM, a gene encoding a neuropeptide-amidating enzyme. Molecular and cellular biology *28*, 410-421.

Rehfeld, J.F. (2004). A centenary of gastrointestinal endocrinology. Hormone and metabolic research = Hormon- und Stoffwechselforschung = Hormones et metabolisme *36*, 735-741.

Selleri, S., Palazzo, M., Deola, S., Wang, E., Balsari, A., Marincola, F.M., and Rumio, C. (2008). Induction of pro-inflammatory programs in enteroendocrine cells by the Toll-like receptor agonists flagellin and bacterial LPS. International immunology *20*, 961-970.

Strand, M., and Micchelli, C.A. (2011). Quiescent gastric stem cells maintain the adult Drosophila stomach. Proceedings of the National Academy of Sciences of the United States of America *108*, 17696-17701.

Veenstra, J.A. (2009). Peptidergic paracrine and endocrine cells in the midgut of the fruit fly maggot. Cell and tissue research *336*, 309-323.

Vodovar, N., Vinals, M., Liehl, P., Basset, A., Degrouard, J., Spellman, P., Boccard, F., and Lemaitre, B. (2005). Drosophila host defense after oral infection by an entomopathogenic Pseudomonas species. Proceedings of the National Academy of Sciences of the United States of America *102*, 11414-11419.

Zitnan, D., Sauman, I., and Sehnal, F. (1993). Peptidergic Innervation and Endocrine-Cells of Insect Midgut. Archives of insect biochemistry and physiology *22*, 113-132.

Chapter 5

Summary and future directions

The work presented in this dissertation contributes to our understanding of intestinal stem cell and enteroendocrine biology. Specifically, the studies in Chapters 2 and 3 make a contribution to the establishment of the adult *Drosophila* intestinal stem cell system as a model system relevant to human health and disease. The findings in Chapter 4 represent a novel discovery in the response of the mature enteroendocrine system to pathogenic bacterial challenge. There are many possible areas of future investigation within each of these projects. Below I have outlined hypotheses and experiments of a subset that I see as having high potential for further discovery and contribution to the field.

5.1 A screen to identify novel regulators of ISC proliferation

A number of published studies have characterized roles for conserved signaling pathways, such as N, Wnt, JAK/STAT, EGF, InR and Hippo in regulating the ISC lineage (For example, Beebe et al., 2010; Jiang et al., 2011; Micchelli and Perrimon, 2006). Although this characterization provides an important fundamental understanding the system, one of the strengths of *Drosophila* research is the ability to perform forward genetic screens and identify novel regulators of a biological process. Because baseline proliferation in the adult midgut is relatively low, over-proliferatiive phenotypes are easily identified with GFP expression in progenitor cells (Figure 5.1A). Furthermore, a screen to identify repressors of proliferation is theoretically more likely to have specific functional roles than a screen to identify under-proliferative phenotypes, which might be due to more general disruption of cellular processes. I undertook a small-scale RNAi based screen to identify novel regulators of ISC proliferation. Specifically, this approach used temporally regulated RNAi knockdown in adult midgut progenitor cells to identify repressors of proliferation under baseline conditions (Figure 5.1B). 48 chromatin modification gene transcripts were targeted by RNAi. These genes were chosen from Filion et al., 2010 based on their coverage of a variety of different chromatin modification processes and availability as UAS-RNAi lines (Filion et al., 2010). Of these, 9/48 (19%) displayed increased proliferation in the primary screen of *esg*>GFP expansion (one example in Figure 5.1C). I performed a secondary screen measuring pH3 levels as a more specific measure of increased mitotic events in *esg* expressing cells (Figure 5.1D). 1 of 9 hits from the primary screen displayed a highly significant phenotype at the level of pH3 counts following RNAi expression in *esg* cells. Follow-up experimentation from this screen showed that the initial

proliferation phenotype was reproducible with an independent RNAi line and loss of function allele (Figure 5.2A-C). Overexpression of the gene of interest was also sufficient to suppress proliferation following *Pe* infection (data not shown).

These experiments provide an example of the potential for screens using the adult *Drosophila* midgut system to identify novel regulators of ISC biology. This screen design can be modified to different cell-type drivers and can be used to examine suppression and enhancement of UAS overexpression based phenotypes.

5.2 Characterization of the prosecretory response of enteroendocrine cells

There are a number of interesting and important directions for further work in the enteroendocrine project presented in Chapter 4. Outlined below are hypotheses and experiments aimed at understanding (1) the upstream mechanism of Dimm induction and (2) the downstream physiological consequences of Dimm induction.

5.2.1 Transcriptional induction of Dimm

The work presented in Chapter 4 provides evidence for Dimm induction at the level of protein detection by antibody staining. I hypothesize that *dimm* transcript is also induced acutely following *Pe* exposure. To test this hypothesis, I will use RT-PCR methodology to compare uninfected and infected midguts for *dimm* mRNA levels during the first 24 hours following *Pe* exposure.

5.2.2 Specificity of Dimm induction

Pe is a potent inducer of Dimm protein in mature EEs. This finding raises the question of the specificity of this EE response to the *Pe* stimulus. There are a variety of other stimuli that cause changes in midgut biology. These include dietary stimuli, chemical, thermal, and other species of bacteria with varying degrees of pathogenicity. To test the question of specificity of Dimm induction, I plan to measure changes in *dimm* by antibody staining and RT-PCR following exposure to various stressors. I hypothesize that Dimm induction will show specificity in mature EEs. Preliminary analysis suggests that the induction of Dimm displays specificity in response to bacterial versus nutritional cues (Figure 5.3).

Current experiments are aimed at testing the induction of Dimm in response to a Gram-negative bacteria also isolated from the Drosophila midgut, *Erwinia carotovora* (*Ecc*15) (Basset et al., 2000). These experiments will compare the induction of Dimm following exposure to two distinct Gram-negative bacterial pathogens.

5.2.3 Identification of the upstream mechanism of Dimm induction

Both candidate and screening based approaches can be used to identify the upstream mechanism of Dimmed induction in EEs. One set of likely candidates to regulate Dimm induction are the EGF ligands and Upd cytokines produced by non-enteroendocrine cells following infection. In order to test this possibility, Upd and EGF ligands can be ectopically expressed and tested for their sufficiency to induce Dimm. In addition, the necessity for JAK/STAT and EGF signal transduction autonomously in the EE can be tested. I have performed preliminary experiments to test these possibilities. In this work, I found that ectopic expression of Upd1 in *esg* cells under baseline conditions was sufficient to induce proliferation of the progenitor cell population but did not induce Dimm in EEs at 24 or 48 time points. Similarly, I found that expression of RNAi lines activating and repressing JAK/STAT signaling in a subset of *npf* expressing EE cells was not sufficient to induce dimm under baseline conditions, and was not necessary for dimm induction following *Pe* challenge. These hypotheses suggest that JAK/STAT and EGFR signaling are not sufficient or necessary for EE induction of Dimm.

Screening based approaches can be used similar to those outlined above for JAK/STAT to identify genes regulating the induction of Dimm. Specifically, using an EE specific Gal4 line (*npf*-Gal4) in conjunction with *tub*Gal80^{TS} allows temporally regulated knockdown of transcripts in a subset of EE cells. This screen can be used to identify genes that repress Dimm levels under baseline conditions as well as genes that are necessary for Dimm induction following challenge. Preliminary results from this screen are presented in Table 5.1. Manipulation of EGFR signaling and Phm levels revealed mild phenotypes that can be further investigated. Although a signaling pathway based screen has not yet revealed any strong phenotypes beyond the positive controls (Dimm RNAi and UAS-Dimm), it does establish this method as a viable method for screening RNAi libraries.

5.2.4 Identification of downstream physiological consequences of Dimm induction

In order to identify downstream phenotypes of Dimm induction in EEs, it will be important to develop an EE specific Gal4 line through which to manipulate Dimm levels with cellular and temporal resolution. *npf*-Gal4 is one possible line, however it targets only a subset of EE cells. One approach will be to combine multiple peptide promoter Gal4 lines to provide more complete coverage of the adult EE population. Available peptide promoter-Gal4 lines will be cross-examined for adult neuroendocrine expression as well to determine the extent to which they are EE specific.

The potential phenotypes of EE manipulation are varied. EEs express numerous peptides, and furthermore receptors to these peptides are present in cells of various different tissues (Helander and Fandriks, 2012). Thus, one place in which to begin is examination of physiological processes characterized as EE regulated processes. As one example, AstA is shown to repress feeding behavior in adult *Drosophila* (Hergarden et al., 2012). Furthermore, our studies demonstrate that AstA levels are increased following exposure to *Pe* in a *dimm* dependent fashion (Figure 4.3). Therefore, one example of a candidate physiology approach would be to use feeding assays, such as a blue food assay, to examine behavior following *Pe* infection in the presence and absence of *dimm.* RNAi lines targeting the peptides themselves, in this case *allatostatin* RNAi, can be used as positive controls.

5.3 Figures

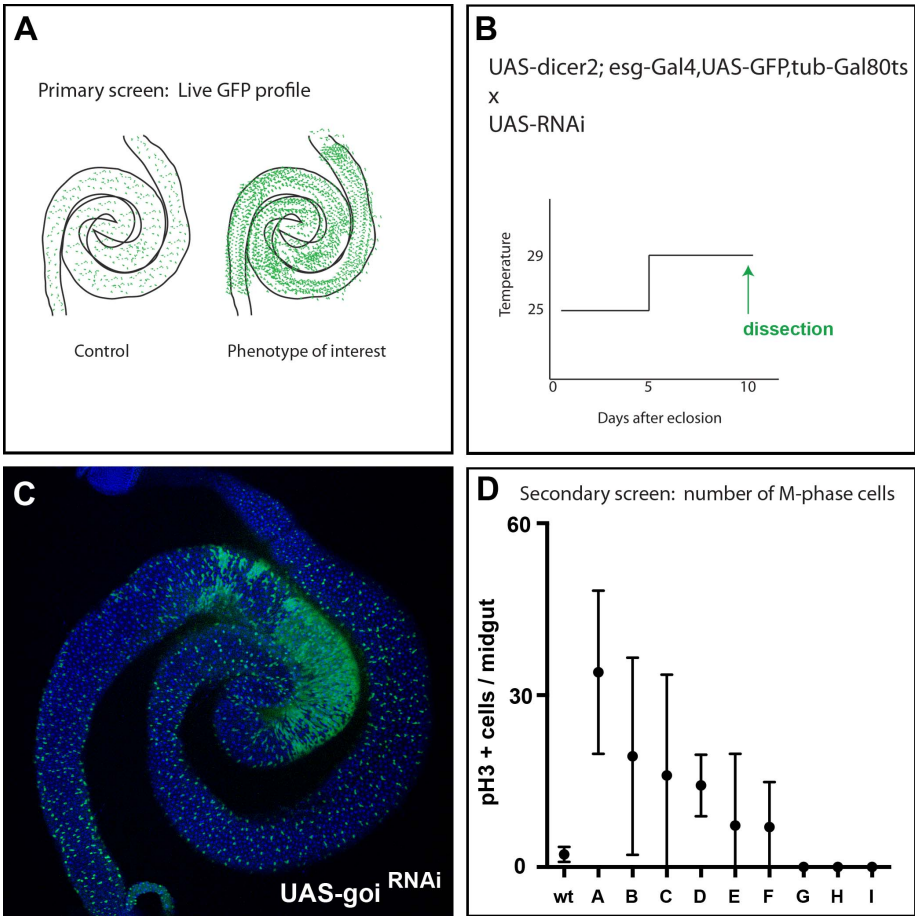

Figure 5.1 An RNAi based genetic screen to identify repressors of ISC proliferation. (A) A primary screen used live GFP from the driven using the *esg*^{TS} system to identify expansion of the progenitor cell population. (B) Methodology of the timing of RNAi expression and sample analysis. (C) One example of an RNAi line of identified that results in regional expansion of *esg*>GFP expressing progeniors. "goi" denotes gene of interest. (D) A secondary screen examined pH3 numbers as a more direct measure of a proliferation phenotype. (n=3 midguts examined per RNAi line).

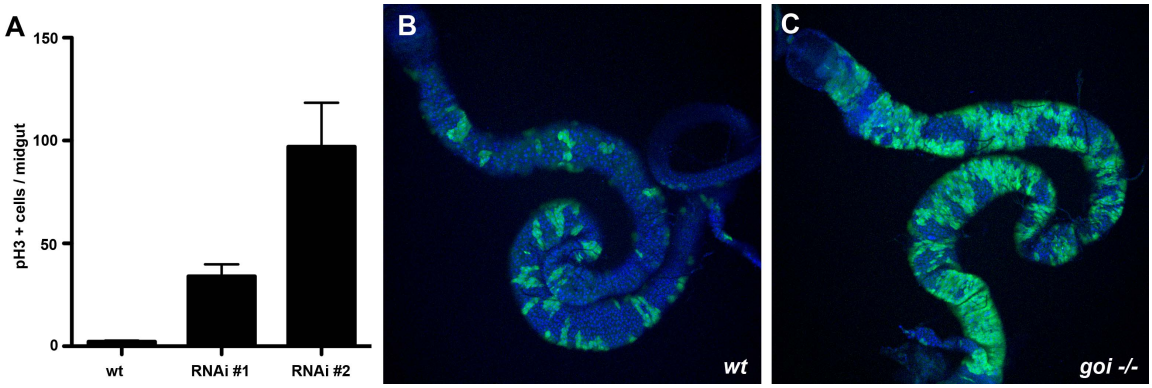

Figure 5.2 Validation of the RNAi phenotype and mutant analysis. (A) Two independent RNAi lines targeting the gene of interest (goi) resulted in increased pH3 numbers when expressed using the *esg*^{TS} system. Transgene expression was initiated 3 to 5 days before analysis. (B-C) Whole midgut images of positively marked MARCM lineages 14 days after induction. (B) Wild-type GFP expressing lineages. (C) Homozygous loss of function lineages.

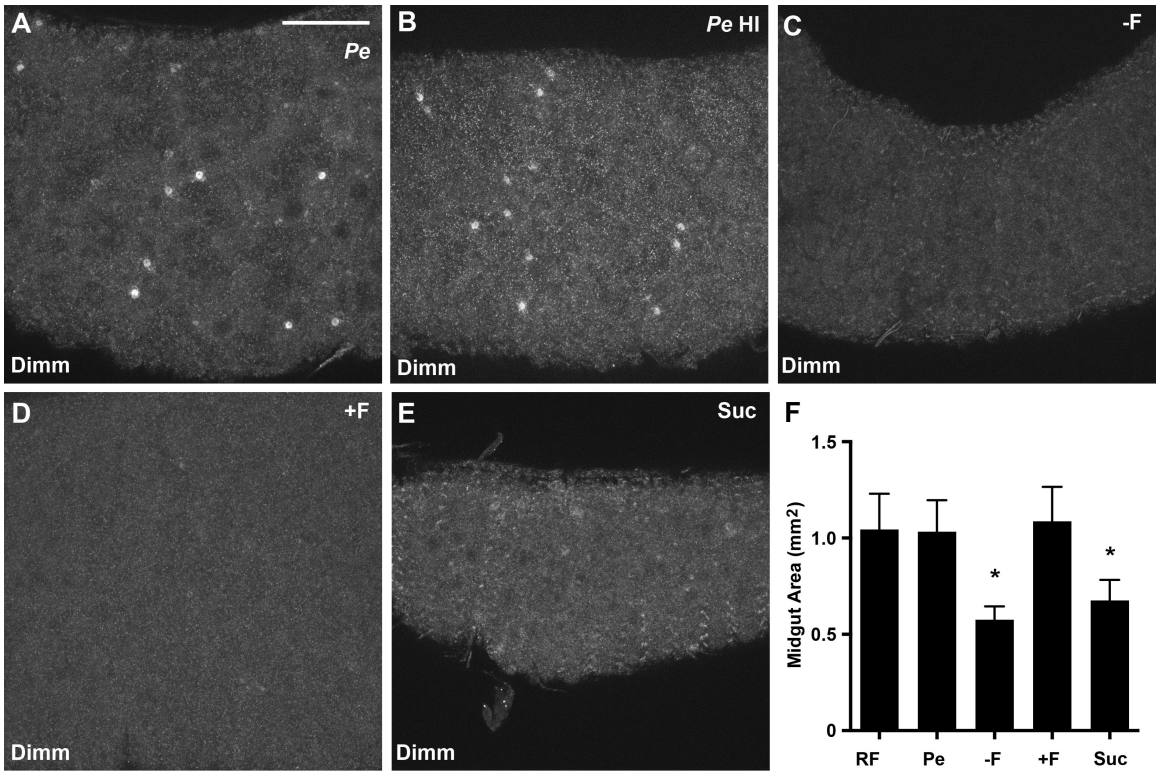

Figure 5.3 DIMM induction in EEs occurs in response to specific stimuli. (A-E) Confocal micrographs of adult midguts exposed to a various stimuli (anti-Dimm, white). Labels are as follows: *Pe, Pseudomonas entomophila*; *Pe* HI, heat inactivated *Pe* bacteria; -F, agar starvation; +F, refed following starvation; Suc, sucrose only in agar. Scale bar: 50 μm. (F) Quantification of midgut area 24h following various dietary treatments. Bars indicate mean values ± SD ($p < 0.0001$, $n = 6$ midguts). Heat inactivation of bacteria was performed by resuspending bacteria in 5% sucrose and subsequently incubating the solution in a 60°C water bath for 45 minutes. Bacteria were streaked on LB plates following each heat inactivation protocol to confirm lack of subsequent bacterial growth. Starvation was performed by transferring flies to vials containing 1.5% agarose in water. Refeeding was performed by returning flies to regular lab food supplemented with yeast paste following 24h starvation. Sucrose treatment consisted of 1.5% agarose, 5% sucrose in water. Midguts were analyzed for Dimm at 12, 24 and 48h post dietary challenge treatments. Representative micrographs are from 24h time points.

5.4 Tables

Pathway	UAS line	Ectopic Dimm?	Failure to induce Dimm?
control	rpr,hid	n/a	+
control	dimm RNAi	-	+
control	GFP	-	-
control	dimm	+	n/a
AMP expression	Caudal RNAi	-	-
AMP expression	Caudal	-	-
DUOX	MKP3 RNAi	-	-
DUOX	p38 RNAi	-	-
DUOX	MEKK RNAi	-	-
EGF	**EGFR1**	**+ (mild)**	-
EGF	**EGFR2**	**+ (mild)**	-
EGF	Ras85D	-	-
EGF	Ras N17	-	-
EGF	dRAS RNAi	-	-
EGF	**EGFR RNAi**	-	**+ (mild)**
Hh	Smo RNAi	-	-
IMD	PIMS RNAi	-	-
IMD	PGRP-SC1a RNAi	-	-
IMD	PGRP-SC1b RNAi	-	-
IMD	PGRP-SC2 RNAi	-	-
IMD	TAK1 RNAi	-	-
IMD	Relish RNAi	-	-
Insulin	InR act	-	-
Insulin	InR K10409A	-	-
JAK/STAT	UAS-socs RNAi	-	-
JAK/STAT	dom RNAi	-	-
JAK/STAT	stat RNAi	-	-
JAK/STAT	hop RNAi	-	-
JAK/STAT	hop RNAi	-	-
JNK	Puc RNAi	-	-
JNK	JNK RNAi	-	-
TGF-B	tkv QD	-	-
TGF-B	smad4 RNAi	-	-
TGF-B	tkv RNAi	-	-
TOLL	Dif RNAi	-	-
TOLL	Dorsal RNAi	-	-
TOR	TOR RNAi	-	-
VEGF	vegfR RNAi	-	-
Wnt	Pan	-	-
Wnt	arm s10	-	-
RSP	**phm RNAi**	**+ (mild)**	-

Table 5.1 A pathway based screen to identify upstream regulators of Dimm. The UAS lines displayed were expressed in adult *npf* expressing EEs using the *npf*^{TS} system. Midguts were examined using anti-pros and anti-Dimm staining for the ectopic expression of Dimm under baseline conditions, as well as the failure to induce Dimm *Pe* exposure. In the latter, midguts were exposed to *Pe* for 24h at OD 20. Blank cells represent normal Dimm level phenotypes similar to controls. n = 3 to 6 midguts examined per treatment.

5.5 References

Basset, A., Khush, R.S., Braun, A., Gardan, L., Boccard, F., Hoffmann, J.A., and Lemaitre, B. (2000). The phytopathogenic bacteria Erwinia carotovora infects Drosophila and activates an immune response. Proceedings of the National Academy of Sciences of the United States of America *97*, 3376-3381.

Beebe, K., Lee, W.C., and Micchelli, C.A. (2010). JAK/STAT signaling coordinates stem cell proliferation and multilineage differentiation in the Drosophila intestinal stem cell lineage. Developmental biology *338*, 28-37.

Filion, G.J., van Bemmel, J.G., Braunschweig, U., Talhout, W., Kind, J., Ward, L.D., Brugman, W., de Castro, I.J., Kerkhoven, R.M., Bussemaker, H.J.*, et al.* (2010). Systematic protein location mapping reveals five principal chromatin types in Drosophila cells. Cell *143*, 212-224.

Jiang, H., Grenley, M.O., Bravo, M.J., Blumhagen, R.Z., and Edgar, B.A. (2011). EGFR/Ras/MAPK signaling mediates adult midgut epithelial homeostasis and regeneration in Drosophila. Cell stem cell *8*, 84-95.

Micchelli, C.A., and Perrimon, N. (2006). Evidence that stem cells reside in the adult Drosophila midgut epithelium. Nature *439*, 475-479.

Katherine Beebe

Saint Louis, Missouri
katbeebe@gmail.com

EDUCATION

Ph.D. Developmental, Regenerative and Stem Cell Biology, 2014
Washington University, St. Louis, MO

B.A. Biology, Brown University, Providence, RI 2002

RESEARCH EXPERIENCE

Ph.D. Thesis. Washington University in St. Louis. 2006-present
"Dynamic Responses at the Barrier Epithelium." Mentor: Craig Micchelli.

- Discovered induction of prosecretory response in mature enteroendocrine cells in response to pathogenic challenge
- Characterized the role of JAK/STAT and Wnt pathways in regulating homeostasis of the intestinal stem cell lineage

Research Technician, 2004-2006
Fred Hutchinson Cancer Research Center, Seattle, WA

- Research experience in hematopoietic stem cell biology and gene therapy
- Developed a core service for retroviral production used by researchers at the Fred Hutchinson and University of Washington

Research Assistant, 2002-2003
Princeton University and The Smithsonian Tropical Research Institute

- Independently managed a field project in Panama investigating seasonal reproduction in an equatorial bird species

Research Assistant, University of Massachusetts, Amherst 2001

- Designed and performed experiments testing the role of Epidermal Growth Factor in cumulus cell proliferation and viability

NSF Research Intern, Geophysical Institute, University of Alaska Fairbanks 2000

- Deployed seismic stations throughout the Alaskan Range and collected original data on earth mantle movement to create core/mantle profiles

PUBLICATIONS

Hau M, **Beebe K**. *Plastic endocrine regulation of year-round territorial aggression in tropical male spotted antbirds.* Gen Comp Endocrinol. 2011 Jun;172(2):305-13.

Beebe K, Lee WC, Micchelli CA. *JAK/STAT signaling coordinates stem cell proliferation and multilineage differentiation in the Drosophila intestinal stem cell lineage.* Dev Biol. 2010 Feb 1;338(1):28-37.

Lee WC, **Beebe K**, Sudmeier L, Micchelli CA. Adenomatous polyposis coli regulates *Drosophila* intestinal stem cell proliferation. Development. 2009 Jul;136(13):2255-64.

Jung CW, Beard BC, Morris JC, Neff T, **Beebe K**, Storer BE, Kiem HP. *Hematopoietic stem cell engraftment: a direct comparison between intramarrow and intravenous injection in nonhuman primates.* Exp Hematol. 2007 Jul;35(7):1132-9.

Beard BC, Dickerson D, **Beebe K**, Gooch C, Fletcher J, Okbinoglu T, Miller DG, Jacobs MA, Kaul R, Kiem HP, Trobridge GD. *Comparison of HIV-derived Lentiviral and MLV-based Gammaretroviral Vector Integration Sites in Primate Repopulating Cells*. Mol Ther. 2007 Jul;15(7):1356-65.

Zhang XB, Beard BC, **Beebe K**, Storer B, Humphries RK, Kiem HP. *Differential effects of HOXB4 on nonhuman primate short- and long-term repopulating cells.* PLoS Med. 2006 May;3(5):e173.

Beebe K, Bentley GE, and Hau M. *A seasonally breeding tropical bird lacks absolute photorefractoriness in the wild, despite high photoperiodic sensitivity*. Functional Ecology. 2005 Jun;19(3):505-512.

SUBMITTED MANUSCRIPTS

Beebe K, Park D, Taghert PH, Micchelli CA. *Enteroendocrine cells dynamically regulate the pro-secretory transcription factor Dimmed in response to the enteric pathogen Pseudomonas entomophila.* Submitted to PNAS, August 2014.

HONORS AND AWARDS

Spencer T. Olin Fellowship for Women
NSF Graduate Research Fellowship Honorable Mention

ABSTRACTS

Direct Intramarrow Injection of CD34+ Cells May Improve Long-Term Engraftment in Nonhuman Primates. Jung CW, Morris JC, Beard BC, Neff T, **Beebe K**, and Kiem HP. American Society of Hematology annual meeting (2004).

EGF Receptor Activation in Bovine Cumulus Cells Induces [Ca2+]I Elevation and Cell Death. Zhao Z, Garbett D, **Beebe K**, Duby R, and Gross D. The American Society for Cell Biology annual meeting (2001).

Broadband Experiment Across the Alaska Range (BEAAR) and Crustal Structure Beneath Central Mainland Alaska. Meyers EV, Christensen DH, Abers GA, Stachnik JC, Holland AR, and **Beebe KB**. American Geophysical Union annual meeting (2000).